MSc thesis in Geomatics for the Built Environment

The influence of the visible views on cyclists' route choices

Gina Michailidou
2019

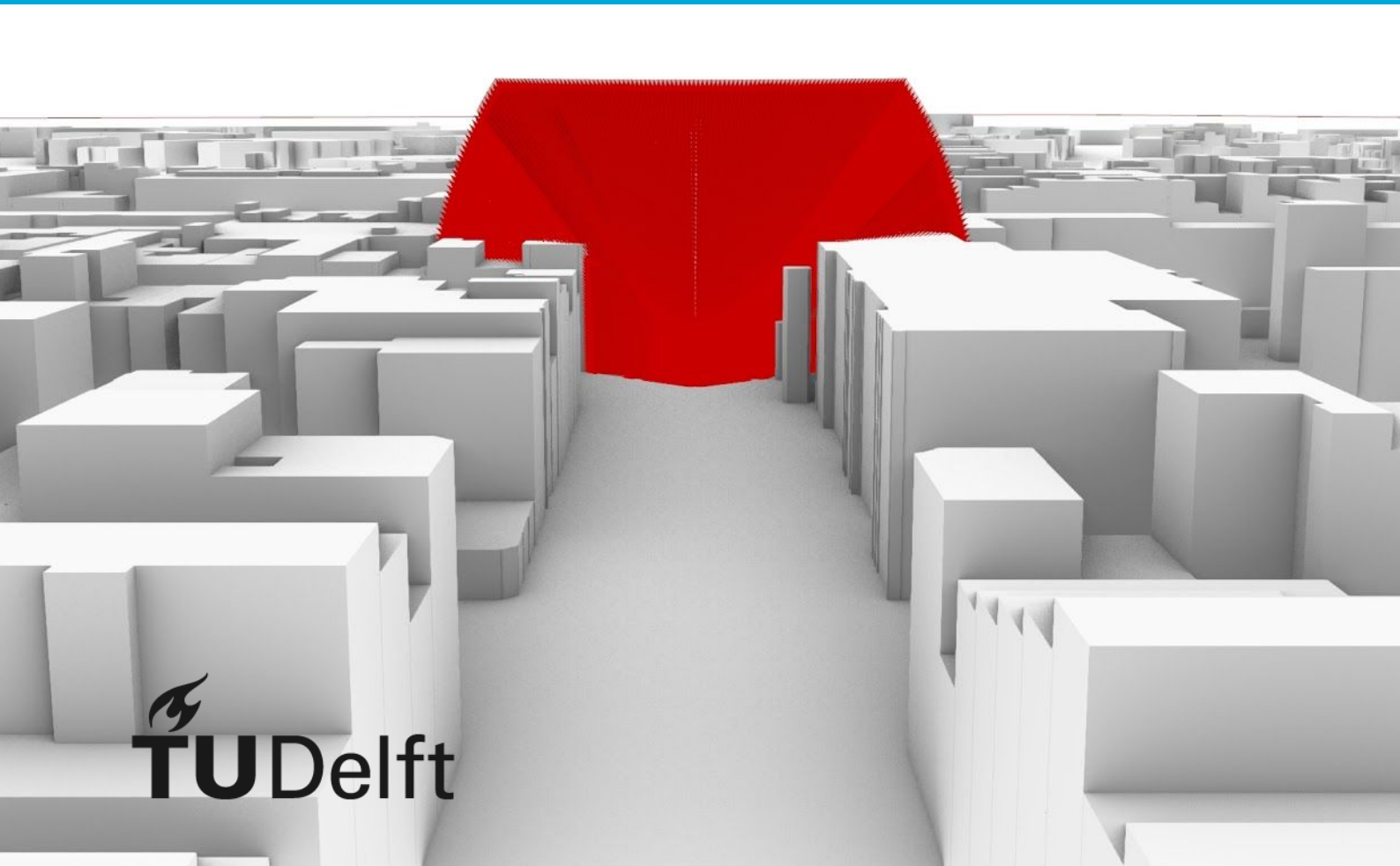

TU Delft

THE INFLUENCE OF THE VISIBLE VIEWS ON CYCLISTS ROUTE CHOICES.

A thesis submitted to the Delft University of Technology in partial fulfillment of the requirements for the degree of

Master of Science in Geomatics for the Built Environment

by

Gina Michailidou

18 April 2019

Gina Michailidou: *The influence of the visible views on cyclists route choices.* (2019)

ISBN 999–99–9999–999–9

The work in this thesis was made in the:

Urban Design group
Department of Urbanism
Faculty of Architecture & the Built Environment
Delft University of Technology

Supervisors:	Dr.ir. S.C. van der Spek
	Dr.ir. D.C. Duives
	PhD researcher Lara-Britt Zomer
Co-reader:	Dr. Giorgio Agugiaro

ABSTRACT

Route choice of cyclists recently became a hot topic of research for different disciplines such as transport and urban planning. Among other factors that influence these route choices, the urban environment has been identified as one in a network, road or aesthetic level. However, how the morphology of the built environment influences the cyclists remains rather unexplored. Considering that two routes are equally distant and safe, would a cyclist choose the most idyllic route in terms of its spatial openness?

This thesis aims to explore the extent that the visible views of the urban environment affect the route choosing of a cyclist while traveling in the center of Amsterdam, The Netherlands. It also For this purpose, 127 GPS trajectories of the Fietstelweek dataset of 2015 are compared with alternative routes suggested by OpenStreetMap (OSM) via the OpenRouteService Directions API. The suggested alternatives can be either the fastest routes, the longest routes or those recommended by OSM (in terms of travel distance, travel time or safety. Throughout this MSc thesis a methodology based on the visibility of the cyclist is proposed. The visibility analysis is based on the ray casting algorithm in a 3D environment and gives as an output 3D isovists. The 3D isovists are used in order to measure the spatial openness as the ratio of the amount of visible sky, visible buildings and visible ground, as well as the shape of the 3D isovist itself. Opposite to similar researches that are performing the visibility analysis on the actual GPS routes, this thesis project applies the visibility analysis to a simplified version of the OSM street network in the centre of Amsterdam. The simplified OSM street network consists of street segments, the nodes of which represent real road intersections. The output of the visibility analysis per street segment is later mapped to the GPS trajectories and the alternative routes as an aggregated value.

Finally, the routes are compared to each other with the ANOVA statistical method (N=127) and the Tukey's post hoc test, resulting to a quantification of the differences of the GPS routes in terms of spatial openness. The results of the statistical analysis indicate the importance of the distance in the cyclists route choices but also the importance of the ratio of buildings and visible sky, the ratio of buildings and ground as well as a significant preference of the cyclists towards non-homogeneous routes with variation on the street profiles. We consider the methodology as an interesting proposal of measuring attributes that are difficult to be interpreted by using the traditional space syntax methodology and as a new way to provide design guidelines of the city to urban planners and architects when a detailed 3D environment is provided.

Keywords: Bicycle route, Built Environment, Visibility analysis, 3D Isovists, Spatial Openness, GPS, OpenStreetMap, Fietstelweek, Qualitative analysis, ANOVA analysis.

ACKNOWLEDGEMENTS

I would like to thank everyone that contributed and supported me during this thesis!

CONTENTS

LIST OF FIGURES

LIST OF TABLES

ACRONYMS

AHN3 Actueel Hoogtebestand Nederland 3 3

ANOVA Analysis of the variance 44

API Application Programming Interface 17

BAG Basisregistratie Adressen en Gebouwen 62

BGT Basisregistratie Grootschalige Topografie 62

CRS Coordinate Reference System 16

DEM Digital Elevation Model 2

GPS Global Positioning System 1

GUID Globally Unique IDentifier 29

JSON JavaScript Object Notation 20

LOD Level of Detail 2

OD PAIR Origin-Destination pair of a route 19

OSM OpenStreetMap 16

RP Revealed Preference methods 1

RCL Road Center Line 18

SP Stated Preference methods 1

SPSS Statistical Package for the Social Sciences 44

TIN Triangular Irregular Network 2

DEFINITIONS

- **Street:** A public road that is part of a city or town and not of rural areas. A street has usually buildings along one or both sides, facilitating public interaction.
- **Street intersection:** An at-grade junction where two or more streets cross or meet. The number of street segments, the design of the lanes and the traffic controls may be used for the classification of intersections.
- **Street profile:** The profile of a street regarding the building forms, the amount of sky and the amount of ground that are visible to an observer.
- **Street network:** A system of interconnected lines and nodes that represent the streets and roads of a particular area. It is used as the basis of a network analysis and the investigation of the movements of various types of road users.
- **Street network (3D):** A street network with height information.
- **Route:** A path that is taken by the user in getting from an origin location (starting point) to a destination location. The path consists of a sequence of adjacent streets.
- **Alternative Route:** A route that connects the origin location to the destination location of the user but it is not followed by him.
- **Street segment (2D):** A line segment that connects two street intersections in the real street network. A street segment can has one or more different street names and a unique segmentID.
- **Street segment (3D):** Same characteristics as the 2D street segment with an additional elevation value (z value) inherited by the 3D ground points of the AHN3 Point Cloud dataset.
- **Street node (2D):** A 2D point with latitude and longitude that represents a street intersection. One node can belong to only one street segment in the case of a dead end or can be shared by two or more street segments. Street nodes have the same direction as the direction of the street segment, one or more segmentIDs and a unique nodeID value.
- **Street node (3D):** Same characteristics as the 2D street node with an additional elevation value (z value) inherited by the 3D ground points of the AHN3 Point Cloud.
- **Isovist:** "The set of all points that are visible from a specific vantage point in space and with respect to the (built) environment"
- **3D Isovist:** An isovist that is created in a 3D environment and so it considers height information.

- **Observer's point / Scene:** The vantage point of where the isovist is created.
- **Spatial Openness:** The amount of the open/free space that can be seen by an observer's point.
- **Urban Environment:** For the way Urban Environment is defined in this thesis see Section 2.1.2
- **Built Environment:** For the way Built Environment is defined in this thesis see Section 2.1.2
- **B-rep:** Method of computer-aided design for representing shapes using the boundaries of the solids and non-solids [1]. B-reps consist of faces, edges and vertices and have both geometry and topology.
- **LoD1 building:** "A generalized way of representing a 3D building as a prismatic block model with vertical walls and horizontal roofs" [Gröger and Plümer]. A LoD1 building does not contain semantics on the composed geometries.
- **Metric:** A determinant that is used to measure the output of the visibility analyses and perform the statistical analyses. It describes either the Spatial Openness or the shape of the 3D isovist.

USED DATASETS

	22+1 Areas - Amsterdam Maps Data
Description	The dataset contains the boundaries of the administrative areas in the city of Amsterdam. In total, 23 areas together with the water bodies are included.
Provider	City of Amsterdam, Gemeente Amsterdam - Onderzoek, Informatie en Statistiek
Website	https://maps.amsterdam.nl/open_geodata/
Geographic Coverage	Amsterdam
Temporal Extent	April, 2016
Format	Vector (ESRI: Polygon)
CRS	EPSG:4326 (WGS84)
Legal aspect	There is no warranty for using, re-using, distributing and modifying the dataset with respect to the terms specified by the city of Amsterdam.

	Actueel Hoogtebestand Nederland 3 Point Cloud (AHN3)
Description	The AHN3 Point Cloud dataset containes the measured heights of the Netherlands in the form of points. Each point in the dataset is classified into either water, artefact, ground, building or other.
Provider	Kadaster
Website	https://www.pdok.nl/introductie/-/article/actueel-hoogtebestand-nederland-ahn3-
Geographic Coverage	The Netherlands
Temporal Extent	September, 2015
Format	LAS
CRS	EPSG:28992 (Amersfoort / RD New)
Legal aspect	Access to the data and use of the data are free and without restrictions for users and companies.

	Basisregistraties adressen en gebouwen (BAG)
Description	The data consists of buildings and a partial selection of these buildings and the residential objects contained therein.
Provider	Kadaster
Website	https://www.pdok.nl/introductie/-/article/basisregistratie-adressen-en-gebouwen-ba-1
Geographic Coverage	The Netherlands
Temporal Extent	2019
Format	WFS
CRS	EPSG:28992 (Amersfoort / RD New)
Legal aspect	Access to the data and use of the data are free and without restrictions for users and companies.

	Basisregistratie Grootschalige Topografie (BGT)
Description	Detailed large-scale digital map that depicts location of physical objects such as buildings, water and roads.
Provider	Kadaster
Website	https://www.pdok.nl/introductie/-/article/basisregistratie-grootschalige-topografie-bgt-
Geographic Coverage	The Netherlands
Temporal Extent	2019
Format	GML
CRS	EPSG:28992 (Amersfoort / RD New)
Legal aspect	Access to the data and use of the data are free and without restrictions for users and companies.

	European Urban Atlas 2012
Description	Land-use and land-cover data.
Provider	European Environment Agency (EEA) under the framework of the Copernicus programme.
Website	http://land.copernicus.eu/local/urban-atlas/urban-atlas-2012/view
Geographic Coverage	Functional Urban Area (FUA) in EEA39 countries.
Temporal Extent	2011-2013
Format	Vector (ESRI Polygon)
CRS	EPSG:3035 (ETRS89, LAEA)
Legal aspect	Access to data is based on a principle of full, open and free access as established by the Copernicus data and information policy Regulation (EU) No 1159/2013 of 12 July 2013. In addition, any modification or adaptation of the data should be clearly stated by the user.

	Fietstelweek 2015
Description	The dataset provides an insight on the bicycle movements in the Netherlands. The bicycle rides of 50,000 participants were captured with GPS via the Fiets Tel-app within one week and were mapped on the OSM network. Apart from the GPS trajectories, the dataset includes valuable information on the trip itself such as the cycling speed, the day and time of the trip and the travel distance. The true origin and the destination locations of the trips are excluded from the dataset for privacy purposes.
Provider	Transport - Planning Department of the Faculty of Civil Engineering and Geosciences of TU Delft and the Municipality of Amsterdam.
Website	http://fietstelweek.nl
Geographic Coverage	The Netherlands
Temporal Extent	September, 2015
Format	Vector (ESRI: Point)
CRS	EPSG:4326 (WGS84)
Legal aspect	Part of the Fietstelweek dataset of 2015 and of 2016 is freely available for use. Access and use of the whole datasets requires confirmation from the providers.

	OpenStreetMap (OSM)
Description	Up-to-date road and cycling network.
Provider	Map data © OpenStreetMap contributors
Website	https://www.openstreetmap.org
Geographic Coverage	Based on the study area, the center of Amsterdam.
Temporal Extent	January, 2019
Format	Vector (ESRI Polyline)
CRS	EPSG:4623 (WGS84)
Legal aspect	OpenStreetMap is a collaborative project to create free editable map of the world. OpenStreetMap data is freely available for use, contribution, modification, distribution and transmission under the Open Database Licence (ODbL). Use of the data requires credit to OpenStreetMap and its contributors.

1 INTRODUCTION

The urban environment attracts social and economic activities leading to a continuous worldwide trend for cities to grow. By 2050, it is expected that more than 60% of the world's population will be living in cities [Gemeente Amsterdam]. This affects the transportation and mobility patterns of people and demands sustainable and smart mobility solutions. The bicycle is one of the most affordable, efficient, sustainable, and healthy means of transportation in urban environments [38]. As a consequence, national and local governments are eager to promote cycling in order to obtain the associated benefits [Mertens et al.].

Although the mobility patterns have a high degree of freedom and variation, they also exhibit structural patterns due to geographic, topographic and socio-economic constraints [Schwenker et al.]. This results to large variations in bicycle use in a national [1] or local scale [2][Pucher and Buehler]. In a local scale, variations between neighborhoods of a city are highly associated with the fact that two places, the origin and the destination, are connected to each other by more than one possible routes. This induces the need of making a route choice [Bovy and Stern; Casello and Usyukov]. In order to understand the preferences and the behavior of the cyclist, four choices need to be made, namely who, why, when and where an individual is cycling [Ton et al.]. The four choices are influenced by categories of factors ranging from measurable attributes (such as travel distance and travel time) to perceived attributes (such as enjoyment, feeling of safety, aesthetics) [Segadilha and Sanches]. One of the categories that is associated with the where individuals are cycling and why they choose to follow a specific route is the urban environment.

Studies from different disciplines, such as transport and urban planning, geography, computer science and behavioral studies have previously reported a lack of clarity on the way the urban environment influences the route choices of cyclists[Krenn et al.; Mertens et al.; Rybarczyk and Gallagher]. This conclusion extracted after studying the cyclists' behavior (in a group or individual level) or exploring the influence of specific attributes. In this context, survey methods such as Stated Preference methods (SP), Revealed Preference methods (RP), field observations (i.e. Global Positioning System (GPS) data) or a combination of them were used. In particular, field observations with GPS require the use of smartphones, embedded devices or specialized units for the collection of the data and may also be result of participatory sensing. In this way, it provides a generalized cost function that can reflect cyclist's evaluation of path alternatives [Yeboah; Casello and Usyukov] or enhances the understanding regarding

1 In North America and Australia bicycle is used in 1-2% of all trips; a percentage much lower than in northern Europe where the cycling modal sharing fluctuates between 26% in the Netherlands, 19% in Denmark and almost 10% in Germany and Belgium [Pucher and Buehler].

2 In Zwolle, Leiden and Groningen more than 45% of the movements are done by bicycle, whereas the bicycle use in Rotterdam and Heerlen accounts 22% and 11% respectively [CBS Netherlands].

the cyclists' preferences on the facility types, such as street paths, slope and traffic volumes [Broach et al.; Hood et al.; Izadpanahi et al.].

The collected data may further be combined with the Space Syntax methodology by performing a n-Dimensional visibility analysis [Mertens et al.; Schramka et al.; Tang and Wang]. However, most of the related studies stayed limited to 1- and 2-Dimensional analyses leading to a less realistic representation of the urban environment.

A 3-Dimensional analysis can be performed using 3-Dimensional data that were created by point cloud. The advantages of point cloud have been presented in literature and can be summarized as the high accuracy and the high density of the collected points, the provision of detailed information (compared to traditional raster or Triangular Irregular Network (TIN)/Digital Elevation Model (DEM) models) even for vegetation and the good way of working with different Level of Detail (LoD) [Grasso et al.; Díaz-Vilariño et al.].

1.1 OBJECTIVES AND RESEARCH QUESTIONS

The aim of the current MSc thesis project is to explore the relation between the urban environment and the route choices of the cyclists in the city of Amsterdam. A methodology supported by LiDAR Point Cloud, a visibility analysis and the creation of 3D isovists was formed for this purpose. The exploration of this relationship includes two different aspects, meaning that the final aim of the thesis is twofold. Firstly, pre-defined determinants of urban environment will be quantified with regards to their significance on the route choices of the cyclists. Secondly, a characterization of the cyclists' route will be performed based on the spatial openness of the route and the shape of the 3D isovists. Based on these requirements, the research question and the scope of the study were specified.

1.1.1 Research Question

The current MSc thesis aims to answer the following research question:

To what extent do the directly visible views of the urban environment influence the route choices of the cyclists and how these different views can be objectified?

In order to give an answer to the main research question, the following sub-questions were formed:

- Which determinants of the urban environment that have been identified in prior studies can be implemented in the current research?
- How the cyclists' route choices will be examined?
- What is the added value of the point cloud as a method for investigating the visibility of cyclists in an urban environment, compared to the use of other 3D and 2D data?
- What is the role of space syntax in the current research?
- Which cyclists' routes should be used for the current research and how they can be filtered?

- What is the proper number of scenes to be created for the visibility analysis?
- What are the differences between the routes of the cyclists and the alternate routes?
- What route characteristics are considered significant for the cyclists during the trip?

An extensive list of these determinants has been already identified in prior studies by using questionnaires, on-the-fly observations and empirical surveys. Therefore, the aim of this research is not to identify the elements of the urban environment but to examine their significance to the route choices of the cyclists in Amsterdam.
In this study we will define the effect of the environment to the cyclist focusing on what the cyclist views during the ride. For this, the notions of both 3-Dimensional (3D) isovists and Spatial Openness were used.

1.1.2 Scope

In order to shape a clear research scope, the following are pointed out:

- The current methodology is tested in a limited number of elements that form the urban environment. However the elements can be increased and a more complete view of the environment can be made.
- The Actueel Hoogtebestand Nederland 3 (AHN3) point cloud is used as the elevation dataset in order to create the 3D environment. This does not mean that another 3D datasets cannot be used directly. The main aim of this selection was to include a powerful dataset that in the future can be used extensively by self-driving cars.
- The GPS points of the Fietstelweek dataset were not map-matched to the existing road network. On the contrary a simplified graph of the road network itself was used to perform the visibility analysis.
- Demographics (i.e. age, genre etc.) are not provided in the Fietstelweek dataset and will not be taken into consideration on the results. The aim is to gain a general insight of the influences on cyclists as users of these active transportation modes. If more knowledge required on the specific groups of cyclists then a distinction should be performed based on the census data and the activity of the sample.

1.2 SOCIETAL AND SCIENTIFIC IMPACT

The current thesis aims to give find the significance of the visible views in the route chooses of the cyclists. In this way, the thesis investigates the role of the urban environment on the preferences of the cyclists by introducing a methodology based on ray-tracing and isovist creation in order to measure this significance. In this way, a characterization of the streets in Amsterdam Centrum will be provided based on the visible views of the cyclists.

1.3 THESIS OUTLINE

The present thesis report is organized as follows:

The report continues by introducing the METHODOLOGY and its distinct modules followed throughout this thesis. Each module consists of multiple steps in between and decisions that required critical thinking. The preparation of the data, the generation of the 3D environment as input for the implemented visibility analyses, and the computation of the metrics are the main aspects that the METHODOLOGY deals with. The CASE STUDY: AMSTERDAM, NL shows how this proposed methodology applied to real data and what possible adaptations required. The output of this chapter is qualitatively and statistically analyzed in the RESULTS. Furthermore, RESULTS presents a qualitative analysis on a network and route level and describes the statistical analyses of these results. A reflection of these results on the proposed methodology is given in the DISCUSSION. The final chapter includes the CONCLUSION AND FUTURE RESEARCH which summarizes the previously published knowledge on the route choices of the cyclists and the suggested methodology with respect to the research questions mentioned in 1.1. In the last chapter, existing gaps that require further research are also presented as future steps.

2 LITERATURE RESEARCH

2.1 DETERMINANTS ON ROUTE CHOICES OF CYCLISTS

Studies from different disciplines such as transport and urban planning, geography, computer science and behavioral studies tried to give an answer to the factors that affect route choices of cyclists. In this context, Stated Preference and Revealed Preference methods are two types of survey methods used in cycling route choice research. The result of the aforementioned survey methods is the identification of numerous determinants that influence the cyclists' route choices.

2.1.1 Categorization of determinants

Ton and colleagues proposed a conceptual framework that was based on the current state-of-the-art reviews and assigned these determinants to five categories; 1) the individual characteristics, 2) the trip characteristics, 3) the environmental conditions, 4) the social surroundings and 5) the urban environment [Ton et al.]. This conceptual framework will be the basis for the skeleton of the next paragraph.

Individual characteristics

The individual characteristics include both the demographic characteristics (gender, age, education level, income etc.) and the expectations and the cycling experience of an individual. The fact that this category includes personal characteristics leads to big differences between countries and even municipalities. Although this category gives little insight in the place where people are cycling, it can provide valuable information on cyclists' route preferences when it is combined with other data, such as safety, road and bicycle infrastructure.

Demographic characteristics such as *gender* and *age* appear to be cultural-dependent and, thus, belong to the non-linear factors. In general, males are inclined to cycle for commuting more frequently than women and cycling tends to be dominated by younger adults [Sallis et al.; Sener et al.; Garrard et al.]. In addition, men prefer fastest and more direct routes, whereas women are generally attracted by routes with maximum separation from motorized traffic, bicycle facilities and lanes, or high terrain grade / slope [Sener et al.; Dill and Gliebe; Garrard et al.]. These are may indications of gender difference in risk aversion and sensitivity to comfort and are more visible in low-cycling countries, such as UK [Garrard et al.; Tilahun et al.]. By contrast, no significant gender difference has been detected in the frequency and the travel patterns of commuting cycling in the Netherlands [Sallis et al.; Bovy and Bradley]. Similarly, in Denmark, only the age factor seems to affect travel patterns

since the elderly seek routes with comfort and lower traffic volumes [Bernhoft and Carstensen]. However, these differences might be a result of societal changing rather than aging.

Socioeconomic factors include the *ownership of a car*, the *educational level* and the *income of an individual*. These factors are all mainly connected to the mode choosing rather than the route choosing. Briefly, car owners, individuals with average educational level or higher personal income show less interest in cycling. This is mainly because they associate it with a lack of comfort and safety [Pucher and Buehler]. In the Netherlands, cycling appears equitable of all transport modes since groups with lower personal income and average educational level cycle only slightly more than high-income individuals [Pucher and Buehler; Fietsberaad Crow].

Finally, psychological factors such as the *history of an accident* can affect negatively the motivation of an individual to cycle, increasing odds of using a bicycle facility by 5% at the same time [Larsen and El-Geneidy]. A traumatic experience that happened in a street or during a trip can influence the routing preferences of a cyclist but no relative studies have been found to indicate its significance. Although psychological and social support can encourage cycling, *self-efficacy* seems to be the most consistent psychological factor of choosing a bike as a transport mode [Engbers and Hendriksen].

The level of *cycling experience* constitutes a major factor for route choosing [Sener et al.; Dill and Gliebe; Hunt and Abraham]. Cycling times on roadways tend to become less inconvenient as level of cycling experience increases, because cyclists tend to develop tactics of manoeuvring, positioning themselves safely and adjusting to the pace and rhythm of others road users [Hunt and Abraham; Van Duppen and Spierings]. Less experienced cyclists prefer factors that make a trip easier, such as less traffic and of routes that require less physical effort [Dill and Gliebe].

Trip characteristics

Every trip that is commuting by an individual is described by static or dynamic characteristics.

The *purpose of the trip* is described mainly from the trip's destination (work, recreation) and it can shape the cyclist group, its routing preferences and the cycling experience. For example, recreational cyclists pay more attention to scenery and roadway grade [Ehrgott et al.; Menghini et al.]. On the contrary, commuter cyclists, and especially those travelling long distances, are sensitive to heavy traffic volumes, possibly because of the safety concerns considering the longer exposure to traffic [Sener et al.; Bovy and Bradley]. At the same time, they are willing to follow the shortest route in order to reach their destination as fast as possible [Broach et al.].

This means that *travel time* and *travel distance* can become major barriers depending on the purpose of the trip [Kang and Fricker; Dill and Gliebe; Tilahun et al.; 87; Bovy and Bradley]. Very interestingly though, the actual time and distance differ from what the cyclist perceived as ones. A small field study between Utrecht Central Station and the Ravellaan showed that cyclists often choose a longer route because they considered it as more pleasant and they often perceived it as being shorter [Coffeng]. Similar findings, also from Utrecht, were reported by Van Duppen and Spierings [Van Duppen and Spierings]. According to Engbers et al. this fact should be targeted in cycling campaigns for non-cyclists living within cycling distance from work [Engbers and Hendriksen]. In literature, travel distance is

taken into consideration instead of travel time when a fixed cycling speed across the whole network is assumed [Beheshtitabar et al.].

Of great importance as factor influencing the route choices seems to be also the quality of the travel time. Furthermore, the time spent cycling in *mixed traffic* is awkward for the individual, even more than the time itself spent cycling on bike lanes or bike paths [Hunt and Abraham]. Even between the active mode individuals, a shared space between cyclists and pedestrians is considered as the least safe option [Si et al.; Lawson et al.]. The more the *time spent together with pedestrians*, the more likely for an accident to be caused [Lawson et al.].

The *time of the day* and the *day of the week* when a trip is commuting can also affect the cycling patterns [Ton et al.]. Although these characteristics are often less investigated, they can provide an explanation of the cyclists' route choosing when combined with factors such as the level of the traffic volumes, the safety, the weather conditions etc.

Environmental conditions

Numerous studies have investigated the effects of seasonal (long-term) and weather (short-term) conditions on the daily bicycle use. Most of them pointed out that the recreational demand is more sensitive than the utilitarian demand [Heinen et al.; Thomas et al.; Nankervis]. Surprisingly, literature is more focused on the effect of environmental characteristics on the use of bicycle as a transport mode, rather than on the route choices that are taken under different weather conditions.

Regarding the *seasonal conditions*, winter is generally considered negative to cycling partly because of the cold temperatures and partly because of the darkness [Spencer et al.; Winters et al.]. On the other hand, the warmer temperatures of the summer encourage cycling activity, especially commuting trips [Miranda-Moreno and Nosal; Winters et al.; Nankervis]. In addition, cycling season affects negatively bicycle facility choosing, meaning that people have lower odds of choosing a better facility during winter than during the summer [Tilahun et al.].

Among the *weather conditions*, the average temperature of the day, the duration of the sunshine, the duration of the precipitation and the average wind velocity are the most important weather factors influencing the cycling duration [Thomas et al.]. Both rain and wind, specifically stronger winds, reduce the frequency of trips, and in particular the longer trips [Corcoran et al.; Heinen et al.; Spencer et al.; Bergström and Magnusson]. A reason for that may be the fact that cyclists have limited capacity to protect themselves from the bad weather [Heinen et al.]. Weather conditions do not affect different countries on the same way. In the Netherlands, the average temperature of the day is considered as the most important factor, whereas the average wind velocity as the least important [Thomas et al.]. Dutch cyclists are rarely discouraged by showers, the effect of which will be a faster cycling speed and shorter travel distances [DUTCH].

Other environmental characteristics, such as *air pollution* and *noise* have been studied regarding their effects on cyclists' health after exposure [Apparicio et al.; Jarjour et al.]. Only a few though indicated the negative influence of a noisy environment, mainly on commuters who appear slightly more sensitive to higher noise levels [Winters and Cooper]. However, whether certain route choices are made because cyclists seek for quieter environments, remains unexplored.

Social surroundings

Social surroundings refer both to the safety inside a neighborhood and to the applied national and local policies. The former can be described by the traffic safety and the social safety of an individual.

The *safety* of a cyclist inside a neighborhood can be defined in different ways depending on both the context and the study area. In this section, traffic safety and the social safety of an individual are going to presented while design characteristics are not taken into consideration (see Section 5). The significance of *traffic safety* on route choosing has been already mentioned in previous paragraphs. In a nutshell, however, busy streets and neighborhoods with heavy traffic volumes, different road users and non-experienced cyclists are often avoided by a cyclist. Bicycle safety remains a point of attention even for high-cycling countries, since serious injuries and fatalities are still increasing. In the Netherlands, serious injuries while cycling constitute the 52% of all incidents, proving the high vulnerability of cyclists as a road user [for Transport Policy Analysis].

On the other hand, the exploration of *social safety* in the context of route choosing remained surprisingly limited. The few examples that already exist are coming from countries with high levels of criminality, indicating the lack of social safety is a negative factor for a cyclist [Segadilha and Sanches]. Even though the Netherlands is considered a relatively safe country, cycling in some locations can make people feel unsafe. This feeling is influenced by the time of the day that the trip is taken place. According to Safety monitor, 16% of all Dutch sometimes feel unsafe cycling outside their neighborhood during the evening [Netherlands]. From them, only 2% is changing their route whereas 10% stated that sometimes choose to detour because of safety issues [Netherlands]. Nevertheless, cyclists may choose to detour without being aware of the reason. What could characterize the detour is the population density, the existence of lightning, a main road, familiarity, but no relative study has been proven their influence.

Property crimes such as the risk of *bicycle theft* seems to be the most common crime in high-cycling countries. In the Netherlands, 558,000 victims of bicycle theft were reported only in 2015, with most of the incidents taken place close to the train stations [CBS Netherlands]. However, the relationship of bicycle theft and the route choosing has remained unexplored.

In addition to the safety aspect, governmental policies in a national and local level, play an important role in both mode and route choice. Countries and municipalities can influence a route choice by communicating the application of a policy as well as the consequences of this policy to the individuals, directly or indirectly. Furthermore, design guidelines and plans on the infrastructure and formation of policies for other competitive modes such as cars, can enhance the safety level and the degree of satisfaction of the cyclists [Rietveld and Daniel]. Policies towards car-free cities are followed by Copenhagen and in the Netherlands and are communicated to the public strategically. A great example of successful policies comes from the municipality of Houten which won the title of "Cycling City 2018". Some of the characteristics of Houten is that the main street from the center to the train station is dedicated only to active mode users (cyclists and pedestrians), the great number of straight streets, the presence of greenery and the removal of many bollards on the cycleways that provide cyclists with comfort and safety [DUTCH].

Urban environment

The built environment influences the route choices of the cyclists, as well as the safety perception for each kind of route [Song et al.]. According to Handy et al., the built environment can be defined as all the man-made and man-modified views in the physical environment that comprises the transportation system, the urban design and the land use [39]. These elements are used throughout this section as the subcategories which describe the factors of built environment that influence the cyclists' choices.

A *transportation system* is described by both the physical infrastructure such as roads and bike paths, and the level of service [39]. Road geometry as part of the physical infrastructure influences the cyclist's comfort and for that reason it is considered as important as the travel time [Li et al.; Hull and O'Holleran]. Regarding the *width of road*, cyclists tend to avoid one-way bicycle paths, and therefore, they are usually directing themselves towards roads with *several bicycle lanes*, *separated bicycle lanes* or *bicycle boulevards* [Hyodo et al.; Dill and Gliebe; Mertens et al.; Larsen and El-Geneidy; Winters and Teschke; Li et al.]. This may happens because wide bicycle lanes offer to cyclists a personal space away of traffic [Hyodo et al.; Snizek et al.]. *Directness* is a crucial factor in a sense that its absence can discourage a cyclist from selecting a certain route and contribute negatively to an otherwise positive cycling experience [Parkin et al.; Snizek et al.; Winters and Teschke]. *Connection* of bicycle lanes should be as direct as possible and avoid *detours*. The existence and design of cycling facilities [Sener et al.; Dill and Gliebe] are also important factors because they attract the cyclists, they make them feel safe and they contribute to a pleasant trip [Dill and Gliebe; Sener et al.; Snizek et al.].

However, in a road infrastructure level, the *frequency of turns*, either left or right, has a negative effect on route choosing because turns delay cyclists and add them the mental cost of having to remember the correct sequence of turns [Broach et al.]. However, limited research has been done to understand the exact relation between the number of turns and the cyclist's perceived travel distance. On a network infrastructure level, the *frequency of intersections, the signalized intersections* and the *junctions* also have a negative influence on cycling experience [Snizek et al.; Broach et al.; Soren]. The main reason for that is the lack of safety. For example, research on the behavior of cyclists at intersections in the city of Amsterdam revealed that, although the majority of the Dutch cyclists (83%) belong to the category of conformists (i.e. carefully follow all the formal rules and designed routes), a significant number of cyclists behave as momentumists (12%) or recklists (5%) [Institute]. However, junctions can be safe if the cyclists are given priority or if the road has separate bicycle lanes [Reynolds et al.]. Between the traffic calming elements, *traffic lights* and *stop signs* influence negatively the cyclists because they decrease route's utility and require more physical effort from the individual [Segadilha and Sanches; Hood et al.; Larsen and El-Geneidy; Sener et al.]. Exception on that are cases in which cyclists make turns across intersections or in which conflicting traffic volumes are high. There, traffic lights increase perceived safety and, thus, are considered attractive [Alexander]. On the other hand, *street lighting* has been cited as essential to increase the sense of security [Menghini et al.; Segadilha and Sanches]. The same effect is seen when the *number of bus stops* is limited. Regarding the *speed limit* factor, cyclists and specifically commuters, show a preference for roadways with moderate to low speed limit routes [Sener et al.]. However, it is still unclear

whether this is because the cyclists are seek for a health benefit or want to increase personal safety. The consideration of speed limits as a route choice influencing factor should be relevant to the study area and the routes that are compared. Inside city areas where speed limits are similar between routes, other factors are more important for the determination of a route. Terrain grade and slope play an important role in cyclist route choices; however this factor is less important for Dutch cyclists since the landscape in the Netherlands is generally flat [Sener et al.; Dill and Gliebe; Garrard et al.]. In principal, commuters opt for routes that are smooth and therefore, require minimum physical effort.

The urban design involves the design of the city and the physical elements within it. Here, the presence of greenery and water areas, the aesthetics of a neighborhood and the beauty of scenery seem to be the most significant factors. Studies on the role of greenery and water in route decision making have shown different results. More specifically, Mertens et al. showed that the presence of green and water areas did not affect the route choices of cyclists [Mertens et al.]. However, these factors were significantly influenced by the gender. On the contrary, other studies showed that streets with green and water bodies attract cyclists, creating positive experiences to them [Krenn et al.; Winters and Teschke; Snizek et al.]. The existence of *barriers*, such as bridges, railways and roads directly affects a cyclist's route choice because they tend to create a lot of discomfort [Emond and Handy; Ghekiere et al.]. However, no information is provided regarding the level of discomfort or the exact way how these factors influence the cyclists. On the other hand, other studies affirm that bridges, if they have cycling infrastructure, may be attractive because they decrease the trip length [Van Duppen and Spierings; 88; Aultman-Hall]. Furthermore, cyclists tend to dislike the neighborhoods close to train stations and choose for neighborhoods with *bicycle-friendliness* [Krenn et al.; Biernat et al.]. A bicycle-friendly neighborhood offers traffic calming features (trees, parked cars, presence of litter and streets with a maximum speed limit of 30km/h), comfort and safety and is described by high aesthetics from the side of an individual [Krenn et al.; Mertens et al.]. As expected, frequent cyclists are sightly more sensitive to the overall bicycle-friendliness of a neighborhood, but the difference compared with the recreational cyclists is not very significant. It has been reported that frequent cyclists thend to choose a bicycle-friendly neighborhood to live in or travel through [Biernat et al.]. Importantly, the impact of bicycle friendly neighborhood is high in cities like Paris but not so important within the Randstad region of the Netherlands [Mertens et al.]. In the Netherlands another factor which is the overall satisfaction of a cyclist's senses appears to be more important. For example, a very interesting study of van Duppen in the city of Utrecht revealed how the smell of coffee and the view of a canal can create a *fluid sensescape* to cyclists depending on the wind, while commuting their trips on a bridge [Van Duppen and Spierings]. In addition, the *population density, the number of shops and facilities and a mixture of land-use* were found to affect significantly a cyclist's choice [Krenn et al.; Winters and Teschke].

2.1.2 The role of Urban Environment

The classification of the previous paragraph makes a distinction between the urban environment and the built environment. Based on this classifi-

cation it is essential to specify the role of the urban environment and the corresponding role of the built environment.

Defining the urban environment

The Space syntax method was firstly by Hillier and Hanson in 1987 with the aim to measure the indoor and outdoor space. The method defines the urban environment as the natural form of the urban tissue for every settlement of city that can be considered as a single and continues spatial system [Hillier et al.]. Based on the before mentioned we define the urban environment as

a high level of city resolution that is created by combining elements of the built environment, the population density and the nature and is described by the urban morphology and the urban forms. The urban environment is always alive meaning that is dynamically changing based on the human activities, the environmental conditions and the interrelationships between the urban forms. It can be augmented by both the human senses and its aura, reaching in that way the highest level of resolution.

Furthermore, the built environment can be considered as a subset of the urban environment that however forms in a high level the image of a city. The built environment in contrast to the urban environment it is combined by alive (such as canals, trees and parks) and non alive elements (such as infrastructure, traffic elements and the buildings). Between these two categories of the built environment, the buildings are one of the most visible category together with the infrastructure and the one that remains consistent as a part of every urban area, satellite or other areas [Hillier et al.]. Winston Churchill points out twice "*We shape our buildings, and afterwards they shape us*" [2]. A relation between the behavior of the people and the buildings is well-known and have been examined extensively through the years.For example, Space Matrix is giving a high importance of the building forms by defining different indicators to measure the urban forms. The Floor Space Index, the Open Space Index and the Ground Space Index are some of the indicators used for this purpose.

2.2 VISIBILITY ANALYSIS

Visibility computations have an important role in computer graphics algorithms, and the used when the determination of objects visible from a vantage point is required. Outside of the computer gaming, serious gaming, a visibility analysis is performed as a key task in architectural and urban design that can give . In that context a visibility analysis belongs to the space syntax methodology in order to give the three major space syntax elements, namely the axial map, the isovist and the convex space.

A visibility analysis can be performed in environments of different dimensionality. A map-based approach for the network and route choice analyses was the most popular methodology among the studies. Furthermore, the use of desk-based rating of the urban environment using remote imaging sources such as Google Street View is become popular (Bethlehem et al., 2014; Charreire et al., 2014; Curtis, Curtis, Mapes, Szell, & Cinderich, 2013; Mertens et al., 2017).

2.2.1 1-Dimensional visibility analysis

For the 1-Dimensional analyses, the basis is the axial map, where the street and road network of built environment is represented by the longest and fewest sight lines. The global and local integration analyses (for the to-movement potential) and the angular integration analyses (for the through-movement potential), all belong to the same dimensionality of the environment and have be used extensively in literature studies. For example, Raford et.al analyzed the distribution of cycling trips in central London area, focusing on a sample of work-based commuting trips. This analysis of the relationship between street accessibility and cyclist route choice was performed by using segment based angular analysis and multiple regression statistical modeling. They concluded that the angular minimization is an important variable; especially compared to the usually used metric trip length. They also pointed out the difficulty to have results when the research is focused on each cyclist's choices since the motivations differ [Raford et al.]. Manum and Nordstorm compared the mapped route choices of individual cyclists with the results from space syntax analysis. Although the results matched for most of the routes, they highlighted that features such as the road slope, road segments and intersections are difficult to be captured (Manum & Nordstrom, 2013). McCahill et al tested space syntax measures to model the distribution of bicycle volumes in the road network of the city of Cambridge. They used a linear regression model and a space syntax measure to predict aggregated bicycle volumes [McCahil and Garrick].

2.2.2 2-Dimensional visibility analysis

The 2-Dimensional visibility analyses is connected to the isovists analyses, a useful method for analyzing the degree of visibility for the location of important urban artifacts and the degree that trees and vegetation affect or block the inter-visibility in urban areas. The concept of isovists was introduced from the first time in 1967 by Tandy referring to the landscape architecture. Although an innovative idea, isovists were outside of the context of the built environment until Benedikt, being heavily influenced by Gibson pushed the theoretical background of the isovists. Benedikt defines isovists as "the set of all points visible from a specific vantage point in space and with respect to the (built) environment" [Benedikt]. From that point no other definition was such complete and rich as the former one. An isovists field can be 180 (i.e. first view when an agent enters a location) or 360 degrees (i.e. the view when the agent is rotating in the standing point), meaning that the applicability of isovists is manifold (Figure 2.1). Since the shape and size of isovists change when moving in the built environment, it is possible to visualize the sequences of scenes from particular points along the movement routes. These properties augment the idea of using isovist fields for the calculation of what the cyclist perceives while traveling.

Figure 2.1: 2D Isovist representation created in Depthmapx.

2.2.3 3-Dimensional visibility analysis

On the other hand, the use of 3D environments was mainly focusing on modeling the cyclists' behavior in microsimulation systems despite the numerous advantages of its use [Schramka et al.; Tang and Wang]. Some of the advantages of a 3-Dimensional analysis -compared to a 2-Dimensional analysis- are 1) the consideration of the vertical dimension(heights of the buildings), 2) the possibilities for facade analysis (inter-visibility between facades regarding safety issues), 3) the consideration of the difference in heights in the walkable surface of the urban environment, 4) the performance of a more complete landmark analysis, 5) the possibilities for comparison of the perspectives regarding safety, 6) the possibility to relate the concept of urban design and planning, 7) a typology of space, 8) a connection to cognitive pattern recognition and 9) the discrimination of lighting and cover conditions during night and day, bad and good weather, for navigation and safety [Van Bilsen].

LiDAR-based 3D visibility analysis

The literature regarding the usage of point cloud for the performance of visibility analysis is rather limited. The majority of the studies were focusing on exploring the use of point cloud in indoor or outdoor environments by calculating the visibility after transforming the 3D data to 2D data.

A number of studies conducted a visibility analysis in a small scale directly using LiDAR-point cloud data (i.e. without prior transformation of the data). In this context, Peters et al. were used medial axis transform for visibility analysis in a built environment that included both trees and buildings. The medial balls were inside buildings. They concluded that the computation of a point's normal is the most important part of the research and that defining the normal of vegetation points is a difficult process [Peters et al.]. Bator et al. transformed LIDAR vegetation points into spherical multipatch objects for the creation of rapid and more accurate 3D visibility modeling in order to pick the most visible location for advertising exposure [Bator et al.]. Fisher-Gewirtzman et al. proposed

the Spatial-Openness Index in order to further develop the quantitative descriptions and evaluation of the buildings shapes. In addition, they aimed to explore the visibility and permeability of different spatial configurations that were related to the open space observed from inside the buildings [Fisher-Gewirtzman and Wagner]. An extension of this work comes from Morello and Ratti who created a 3-Dimensional model of buildings in the urban context, that were concerned with the properties of inter-building visibility and 'openness' or measures of the proportion of visible sky [Morello and Ratti]. The latest work comes from Schmid et al. who proposed an approach of generating highly accurate isovists from LiDAR scans in order to quantify a location's spatial configuration. They aimed to link the subjective risk perception (coming from opinion-based VGI) to the spatial configuration of a cyclist's vista space, with the reasoning that spatially complex or constantly changing situations are experienced by cyclists as more dangerous [Schmid and von Stülpnagel].

In an indoor environment, Grasso et al. improved the idea of isovists by proposing a method to evaluate in a quantitative way the complexity of a certain path within a 3D point cloud environment. The proposed method was taken into consideration the space visible from a certain point of view, depending on the moving agent [Grasso et al.]. This last research is a key point for the current study, which aims to extent the method to outdoor environments and measure the determinants by performing a visibility analysis on the LiDAR point cloud.

Another way to use the LiDAR point cloud when this is airborne is to transform them to an easily handled condition. This is important when a visibility analysis is performed in the eye-level of the observer and thus facades are required.

3 METHODOLOGY

The methodology used in this MSc thesis consists of six different modules: the preparation of the research, the data collection, the processing and simulation of the data, the metrics, the comparison of the GPS and alternative routes, and the conclusion and future research. A detailed description of each module is presented below as a separate section. A generic overview of the followed methodology is shown in Figure 3.1.

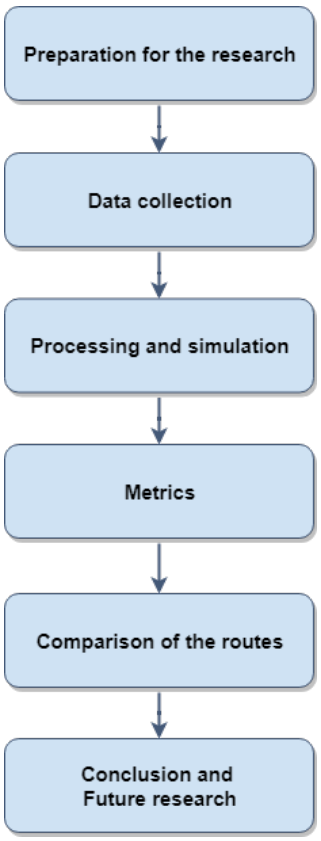

Figure 3.1: Generic overview of the suggested methodology.

3.1 PREPARATION OF THE RESEARCH

The preparation of this research study includes the formation of novel and solid research questions and sub-questions and the determination of the general scope of this study (Figure 3.2). State-of-the-art research regarding different trends in cyclists route choices is part of this phase and is presented in Chapter 2. Briefly, this research study investigates a. the factors affecting the cyclists' route choices, b. the visibility analysis methods and techniques

for the isovists creation in 2D or 3D environments and c. the way spatial openness is defined and measured.

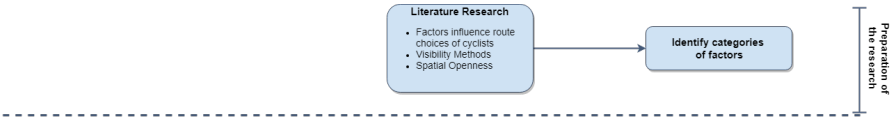

Figure 3.2: Generic overview of the module "Preparation of the research".

The majority of the tools used in this research study are freely available, whereas a few tools were only accessible via TU Delft. More specifically, I used the following open source software packages: QGIS, Python programming language, C, PostgreSQL and PostGIS. In addition, I used the following software packages requiring license includes: ArcGIS, Rhino3D, and SPSS.

3.2 DATA COLLECTION

The data collection phase involves the selection and/or confinement of the study area and the collection of the required datasets (Figure 3.3). The used datasets differ according to the study area, although popular datasets with worldwide coverage such as OpenStreetMap (OSM) can be used in any case. All datasets should be adjusted to a common Coordinate Reference System (CRS) and resolution.

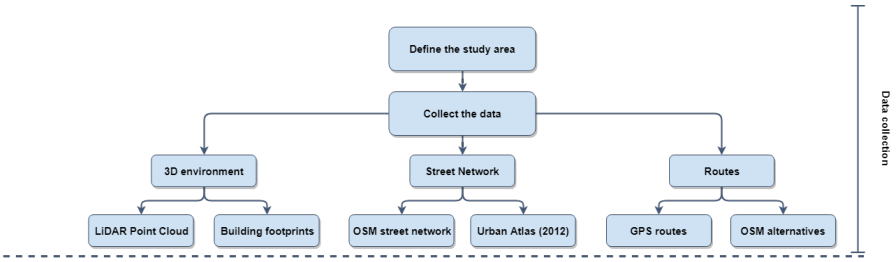

Figure 3.3: Generic overview of the module "Collection of the datasets".

3.2.1 Defining the study area

The study area determines the required datasets meaning that no further processing can be followed otherwise. What forms the decision regarding the study area is essentially the availability and accessibility of one or more datasets.

When the availability of datasets is not an issue, a flow mapping and further investigation of the cycling movements and patterns in the GPS dataset can convey valuable information with regards to the study area. Alternatively, it can lead to the restriction of the existing study area in smaller city blocks (such as neighbourhoods). The urban morphology and building forms of a city/town can be used as a guide to this decision as well.

3.2.2 Collecting the datasets

Routes: GPS routes and alternatives

For the comparison of the routes and the exploration of the influence of the urban environment on cyclists route choices, two different datasets are needed.

The first dataset contains the GPS routes, i.e. the actual route traversed by a cyclist. Depending on the source and the nature of the dataset, possible outliers produced due to the limitations of the GPS technology may be absent. In the opposite case, the dataset may require pre-processing and map matching.

The second dataset provides alternative routes. These alternatives can be gathered in different ways. They are computed by the user using pgRouting or Python or can be obtained by using an Application Programming Interface (API). The choice of the workflow depends on the aim of the study. The second choice is the one followed in the present methodology since we want to investigate alternative routes that can be accessed via a smartphone. Although Directions APIs can be provided by private companies and organizations such as Google (Google Directions API) or Microsoft (BING Routes API), one should consider possible billing for each request (Table 3.1). For example, in Google Directions API one response for alternative does not match to one request. Google Directions API seems to count as one request every lookup is performing in order to suggest a route. To avoid these uncertainties, the OpenServiceRoute Directions API for OSM is used. Openserviceroute API provides for free 2,500 requests per day and 50 requests per minute and can be used in Python [3]. Opposite to Google Directions API that provides the user with an alternative routes of possibly the same travel distance or travel time (up to 3 alternatives), the Openrouteservice gives as alternatives with a POST request either the shortest route, the fastest route or the recommended route by OSM. The recommended route by OSM can be chosen based on the travel time, travel distance and safety. The POST request returns a route between two or more locations and its settings as a JSON respond.

Table 3.1: Comparison between the Google Directions API, BING Routes API and Openrouteservice API.

API	Type of alternative	Requests	Pricing
Google Directions	Up to 3 routes of possibly similar travel times/travel distances	50 per second Based on the plan	2,500 per day free After that 5.00 USD per 1000 queries (Based on the plan)
Bing routes	Not suitable for cycling routes	-	Not published
Openrouteservice	Fastest, shortest or recommended routes	50 per minute 2,500 per day	Free

Street network: OSM and Urban Atlas

For the simplification of the street network, two datasets can be used, namely the OSM street network and the Urban Atlas dataset. Both datasets provide a European coverage and so one can specify them to the selected study area.

The OSM street network consists of line segments that are described by numerous attributes such as the wayID, the type and the characteristics of the lane (distance, color, material, etc.). Each line segment does not match a street in the real street network, meaning that the nodes of each line segment do not represent road intersections. In this context, in OSM street network

a line segment is created each time an attribute is changing. This induces the need for the filtration and simplification of the OSM street network. OSM street network is available for free, either by exporting it from the official website (see Used Datasets), by requesting it from PostGIS or QGIS, or by downloading it from data providers such as GEOFABRIK. The use of the OSM street network comes with advantages such as:

1. the provision of updated information, especially information about all transport modes,

2. the easiness of being accessed, and

3. the fact that the Road Center Line (RCL) can be found in most cases.

[34] On the other hand, when using the OSM street network, one has to deal with topological and geometrical issues, such as missing segments and nodes at intersections, duplicate and overlapping lines, disconnected segments, and orphans; they require cross-checking and, of course, too much information. These disadvantages are not enough to discourage the use of OSM street network, especially in cases where national datasets are less detailed or missing valuable information and data [Girres and Touya; 34].

Urban Altas (UA) 2012 dataset of the European Environment Agency - Copernicus is the second dataset used, as mentioned above. The Urban Atlas is "providing pan-European comparable land use and land cover data for Large Urban Zones with more than 100,000 inhabitants as defined by the Urban Audit". Between the 21 different land-use classes contained in the dataset, the "Road and the associated land use" was the one used in the phase of the street network simplification. This class contains the road network of the many European cities, as well as information regarding areas enclosed by roads, motorways or service roads, and bicycle lanes, etc. The "Road and associated land use" class is represented as a single polygon with the boundaries of the selected city. This dataset may be replaced by other polygon or polyline datasets when available.

3D Environment: Building footprints and PC

These datasets may be skipped when a 3D environment has already been created.

For the generation of the 3D environment (i.e. the creation of the 3D buildings) a 2D dataset with the building footprints and a Point Cloud dataset should be used. Both datasets should correspond to the determined study area.

Building footprints can be obtained either by a national dataset or from OSM, although differences on the attributes of the building footprints may be present.

The LiDAR Point Cloud dataset consists of 3D points (x,y,z) that describe the urban environment. It is used to assign the elevation information on the building footprints. The Point Cloud dataset is provided by a national or private provider and comes as a LAS/LAZ or PCL file. Because the size of the dataset is enormous, one should be sure that the study area is well specified.

This Point Cloud dataset is also used for the generation of the 3D street network.

Other helpful datasets

A 2D vector dataset that holds the administrative boundaries of the study area should be used in combination with the aforementioned datasets. Urban Atlas is one choice to get the administrative boundaries with pan-European coverage. A national dataset could be used alternatively.

3.3 PROCESSING AND SIMULATION

The Processing and simulation module uses the previously introduced datasets in order to prepare the 3D environment and perform the visibility analyses on the street network. Furthermore, the module presents the methodological steps required for a. the generation of the GPS and alternative routes, b. the simplification and correction of the street network, c. the generation of the 3D environment, d. the implementation of the visibility analysis, e. the preparation and run of the implementation. The generic methodology followed in this module is pictured in Figure 3.4.

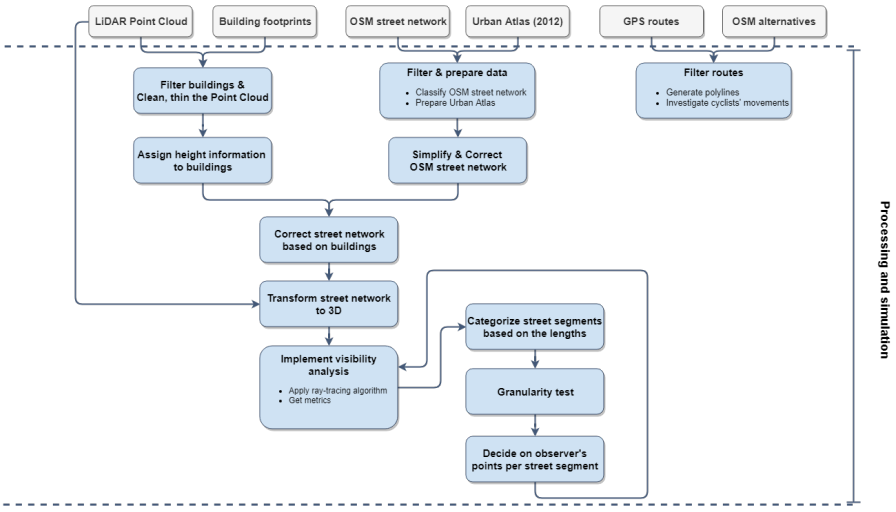

Figure 3.4: Generic overview of the module "Processing and simulation".

3.3.1 Routes generation

The processing and simulation module begins with the generation of GPS and alternative routes.

The process of generating GPS routes depends on the type of the entities contained in the dataset. In case the GPS routes come as polylines then no farther processing is required. However, if the GPS routes come as points then there is a need for transforming them to polylines based on the route the points belong to. The points can be transformed into polylines in QGIS by using the ReconstructLine plugin. Each GPS route has an origin location and destination location (Origin-Destination pair of a route (OD pair)) and depending on the dataset other important information. All this information is stored in the database as a new table after the data re-projected to the WGS84 CRS. This CRS is the one that OSM is using for the requests.

The origin and destination pairs of the GPS routes are used to request the OSM alternatives via the Openrouteservice Directions API. As mentioned

before the OSM alternatives can be the shortest route, the fastest route or the one OSM recommends considering the travel time, travel distance and safety. In this thesis, all three alternatives are requested. The response of the Openrouteservice Directions API is a decoded polyline in JavaScript Object Notation (JSON) format. The geometry of the alternate routes is stored in the database, together with other information on the trip that is included in the JSON response after requested by the user. Such information can be the distance of the route, the name of the streets that the route includes, the permitted speed limits and the detour factor. Between this information, the two first are important for the analysis.

This step was performed with a self-developed script in Python programming language.

3.3.2 Street Network simplification

Having determined the study area, the next step involves the filtration and simplification of the OSM street network. The output of this process (i.e. the street segments of the simplified OSM street network) is a street network that consists of segments and nodes that represent real intersections. This street network will be used as the input of the visibility analysis. This procedure is important in order to a. reduce the information given by OSM and b. eliminate geometry and topology issues, like those mentioned in the Collection of the datasets section. The methodology is a combination of the methodologies suggested by [34; Sileryte]. The process starts by introducing the rules for the simplification of the street network and continues with step-by-step instruction on the simplification and correction process.

Rules for the OSM street network simplification

The rules under which the OSM street network simplified are the following:

1. Streets of length smaller than 5 meters are excluded from the OSM street network. This rule ensures that small streets leading to buildings are not existing in the street network.

2. Parallel lanes: In an RCL map different lanes (typically found in motorways and highways) are represented by two parallel lines. These parallels will preserve if they are equal to or more than 10 meters apart.

3. Bicycle lanes and primary or secondary streets: Bicycle lanes within a maximum distance of 10 meters are merged with the street and are represented as a centreline of the whole street.

4. The complete street network is represented based on the computation of the centrelines. Although in reality, these centrelines could fall into a canal or pass through a tree, in this methodology these elements of the built environment are not taken into consideration.

5. Street segments crossing long tunnels should be modified, meaning that the street segments should end where the tunnel starts. If a street segment crosses a small tunnel, then the tunnel is excluded from the dataset. This is required because of the way the 3D buildings are modeled in this thesis (as LoD1s) and so tunnels are not represented in the 3D environment.

Procedure

The process of the simplification of the OSM street network begins by clipping the street network based on the administrative boundaries of the study area. At first glance, one can notice the disadvantages of the OSM network with regards to the existence of a. many short street segments, b. a large number of nodes and more importantly c. an enormous amount of information.

To reduce this information, filtration is required and this can be achieved by classifying the information provided by OSM. This classification of the OSM street segments can be done based on "highway" and "access" tags of the dataset and should always be in line with the purpose of the study. The "highway" tag indicates the importance of the highway within the street network. For a cyclist, street segments tagged as "construction", "platform" or "track" should be removed from the dataset as they are not relevant to this particular study. On the other hand, all street segments tagged as "unclassified" should be remained because they may represent a secondary street, path, etc. in the real street network. Filtration based on the "access" tag comes as the next step of the process. The values of this tag describe the legal access for highways and other transportation networks. Therefore, a private street or a street that does not permit the use of bicycles or access are considered irrelevant and should be removed from the dataset.

The second step of the process was the simplification of the OSM street network using the OSMnx package of Python. The package reduces the number of unnecessary nodes without taking into consideration overpasses or underpasses. In case that orphan segments and duplicates, and discontinued lines are contained to the resulted network, topology and geometry correction is required. Therefore, segments shorter than 5 meters length containing naked nodes should be removed because they can be indicative of small streets leading to houses (inrit). The topology and the geometry of the resulting network should be cleaned and built.

The street segments of the cleaned network are used to create buffers of a fixed distance of 10 meters. These polygon buffers represent the street segments of the OSM network and are used in the following steps together with the Urban Atlas polygon dataset.

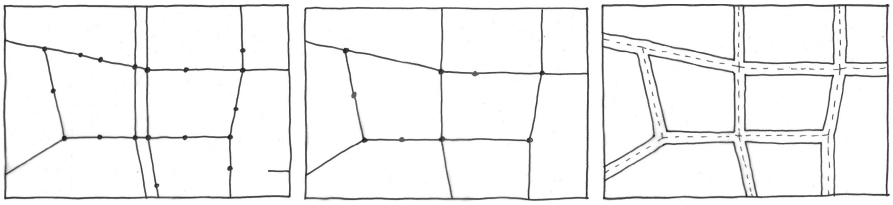

Figure 3.5: Simplification of the network by removing uneccessary nodes and creation of buffers.

In order to make use of the OSM polygons and the Urban Atlas, the two datasets were re-projected to the EPSG:102013 (European Conic projection) coordinate system. This step is necessary in order to ensure a same projection of the datasets and the transformation of the units from degrees to meters for the reduction of computations.

The polygons of the "Roads and associated land use" data of the Urban Atlas are dissolved in order to transform the initial polygons into one polygon with all the information. A check of the validity of the polygons and

possible duplicates in the dataset is also required in this step. The two polygon datasets (i.e. the UA and the OSM network) are now merged and dissolved based on their geometry, and the topology and geometry of the polygons are both corrected.

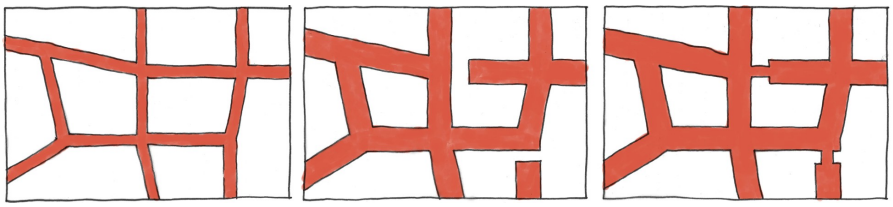

Figure 3.6: The polygon OSM street network and the Urban Atlas polygon datasets are merged and dissolved into one polygon.

Having one polygon dataset that represents the street network, the Medial Axis algorithm can be used in order to extract the polygon centreline. Two different solutions can be used in order to compute an approximation of the medial axis for a polygon. The first solution requires the identification of the Voronoi vertices inside the polygon and the extraction of the Voronoi edges that connect two interior Voronoi vertices. The second solution finds the middle point of each polygon edge that is not covered by a Delaunay edge and marks all the Delaunay edges that correspond to the edges of the polygon. From this the approximate medial axis can be extracted. The second solution is suggested in this methodology in order to extract the polygon centreline, because can ensure faster computation time for large datasets.

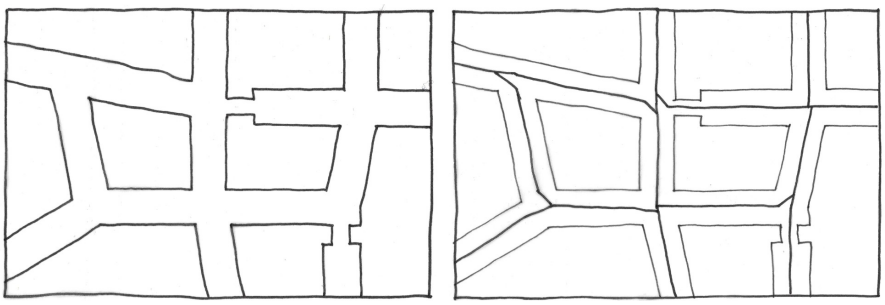

Figure 3.7: Centreline extraction using the Medial axis algorithm.

In case, the resulted network creates short dangled edges that needed to be removed. Afterwards, the street segments are simplified using the Douglas-Peucker algorithm, which retains the critical points on the dataset into a given threshold. Geometry and topology clean of the final dataset is required in order to eliminate duplicated and pseudo nodes.

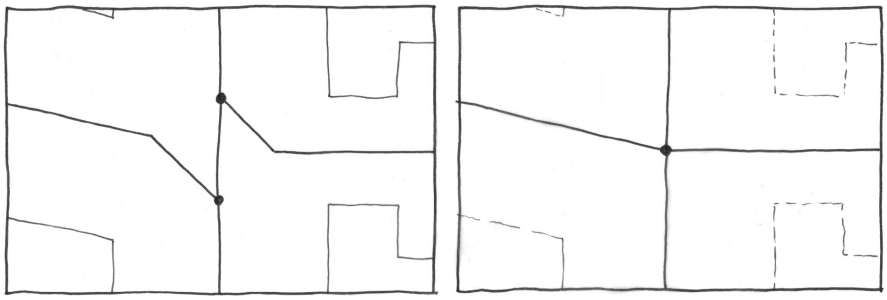

Figure 3.8: Node correction on the simplified street network.

As a last step the simplified street network is corrected with respects to the building footprints. In a few cases, the extracted polygon centreline may appears close to building footprints; a case that could affect the results of the visibility analysis. These segments are corrected manually and the average distance from the centroid of the buildings to the street network is calculated to ensure same distance of building-segment per street segment. This step can be implemented in PostGIS using the St_Offsetcurve function.

From the final simplified street network, the overpasses/underpasses need to be found. The overpasses/underpasses represent the intersections based on which the street network is divided into street segments.This step gives a final simplified street network, where each street segment represents one or more streets in the real street network and one street can be represented by multiple street segments. The Space Syntax plugin for QGIS and Python can be used for this purpose.

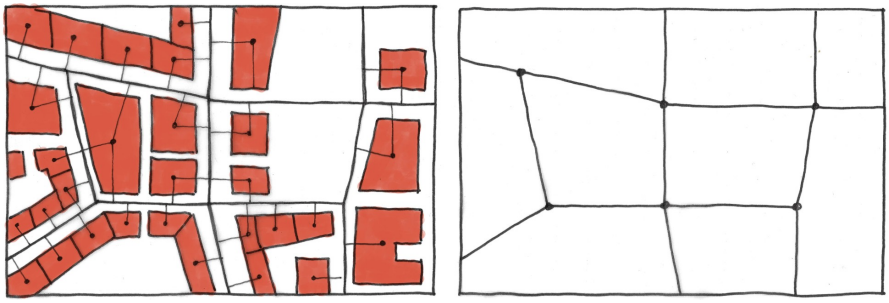

Figure 3.9: Correction of the simplified street network based on the building footprints.

The full workflow of the filtration and simplification of the OSM street network is represented in Figure 3.10.

To prepare the simplified street network as the input of the visibility analysis, the street network is transformed into 3D. This can be done, by assigning average height information to the street segments. The assigned height information is computed from the eye-level of a cyclist and the average height information obtained of the ground points of the LiDAR Point Cloud dataset.

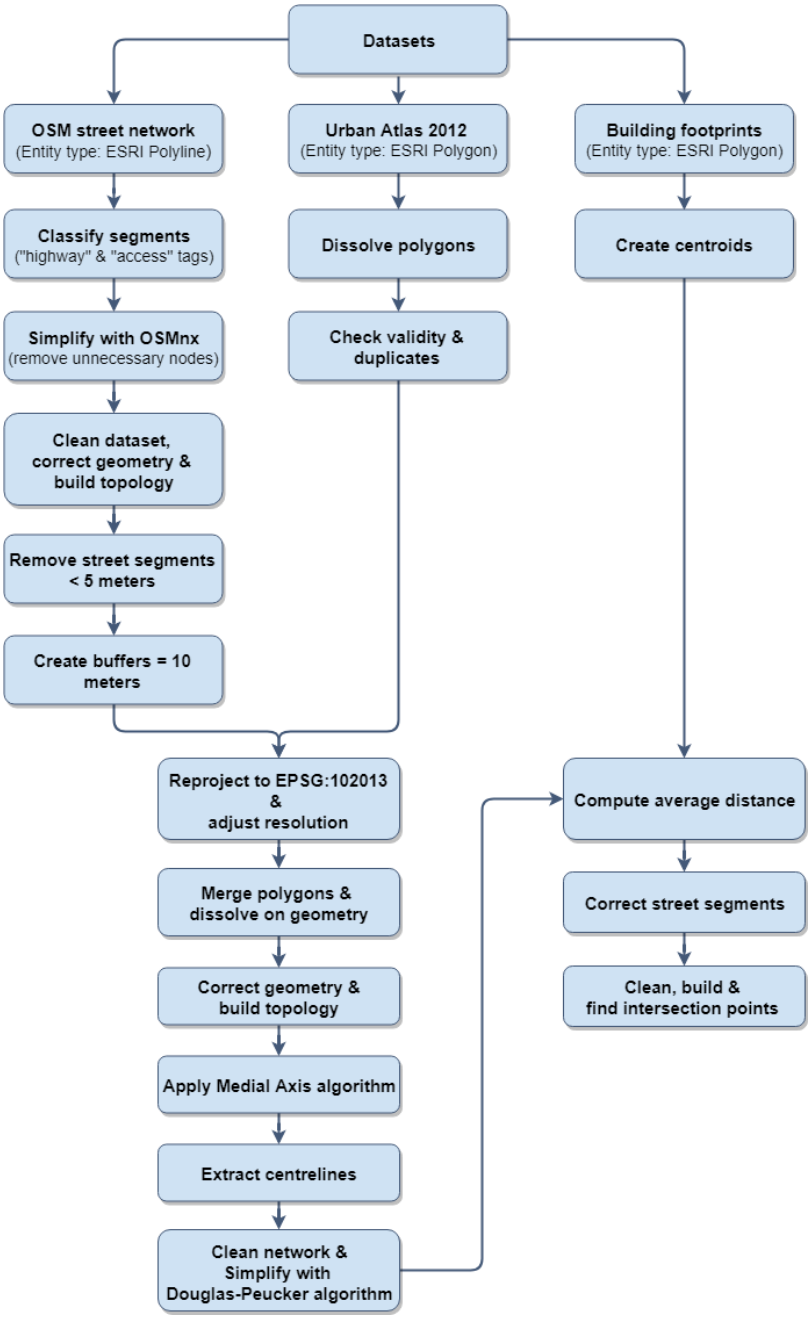

Figure 3.10: Steps for the filtration and simplification of the OSM street network.

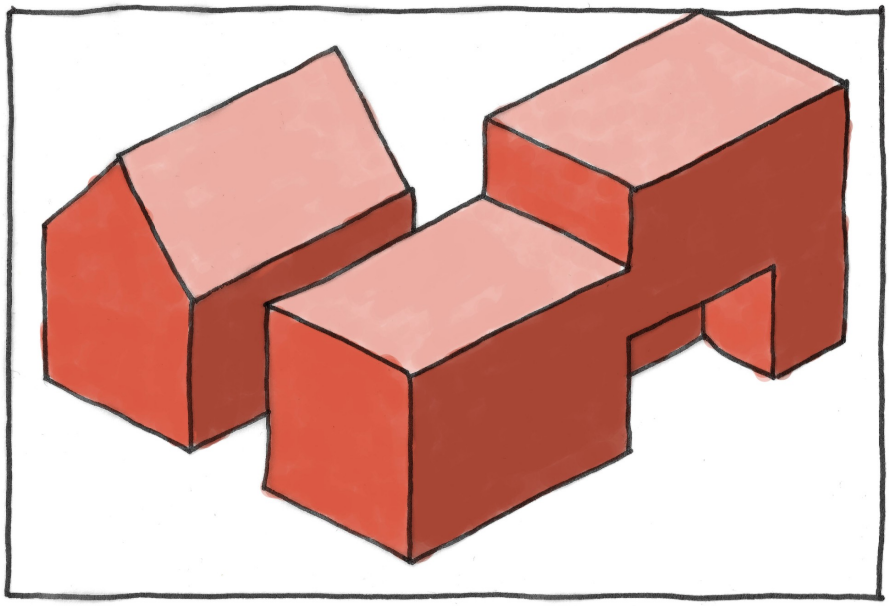

Figure 3.11: 3D buildings as a reference for the description of the process.

3.3.3 Generation of a 3D environment

To perform the visibility analysis, a 3D environment is required. In case the 3D environment is ready, this step can be skipped.

The current methodology is focused only on identifying the importance of the building forms in cyclists route choices. Therefore, only building footprints are used as an element of the built environment. These buildings are represented as LoD1 Breps (Figure 3.11). Further adaptations in the methodology are needed, if one chooses to include more elements of the built environment.

The beginning of the process starts with clipping and filtering the building footprints. Clipping is required in order to restrict the building footprints to the selected study area. Filtering the building footprints is required when temporal differences exist between the building footprints and the GPS routes. In this way, buildings that did not exist the time of the collection of the GPS data are excluded from the analysis. It is very useful when many details exist in the shape of the building footprints (i.e. many buildings close to each other) to either simplify the building footprints or set a distance threshold in between the building footprints. Either way improves the performance of the visibility analysis by reducing limitations of Rhino 3D regarding analysis on Breps. When ready, building footprints are imported to the database.

The process continues by clipping, cleaning, thinning and filtering the LiDAR Point Cloud dataset. In more detail, the dataset is clipped based on the administrative boundaries of the study area and is cleaned from possible existing noise. To reduce even more the size of the dataset and so make it easier to work with, the Point Cloud can be thinned at a specific threshold which depends on the amount of information needed for the analysis. Finally, a filtering of the dataset is needed in order to separate the needed 3D points. The needed 3D points are those classified as buildings. Before importing the building points of the Point Cloud to the dataset it is needed to be ensured that both datasets are on the same coordinate system.

To assign the height information to the building footprints, the PostGIS extension is used. The ST CONTAINS function of SQL computes the median elevation value for each building footprint and stores these values in a new table. The ST CONTAINS function tests whether the second geometry lies within the first geometry, and can be used to compute statistics like average, minimum, maximum and percentiles [66]. As the median is the 50th percentile, a value of 0.50 is used in the percentile_cont function. The median is chosen over the average because the median is less sensitive to outliers in the data (extremely high or low values) than the average. Outliers could be represented as points on chimneys for example. Alternatively, one can use the 10^{th} and 90^{th} percentile of the heights for each building footprint. This decision is up to the user.

The median heights within buildings are later exported and joined to the building footprints as a newly created height field. This procedure can be performed in QGIS.

Different ways can be followed to perform the extrusion of the building footprints and transform them to 3D. The way followed in this methodology imports the data to Rhino 3D with Grasshopper and makes the extrusion based on the previously stored height field. When extrusion is performed, the Breps are created. Preference towards the transformation of the buildings to Breps instead meshes is because of the limitations of Rhino 3D working with meshes. Finally, the Breps are capped to avoid openings on the buildings and the 3D buildings are checked for possible invalid geometries.

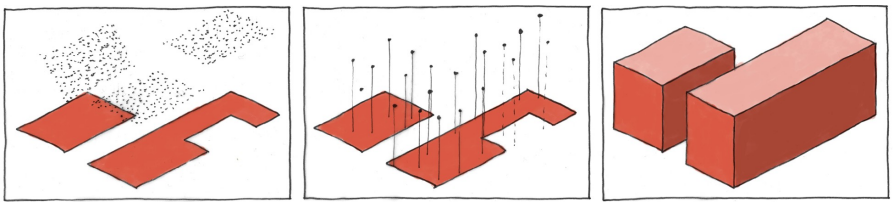

Figure 3.12: Extrusion of building footprints based on a LiDAR Point Cloud dataset.

The workflow of this process is represented in Figure 3.13.

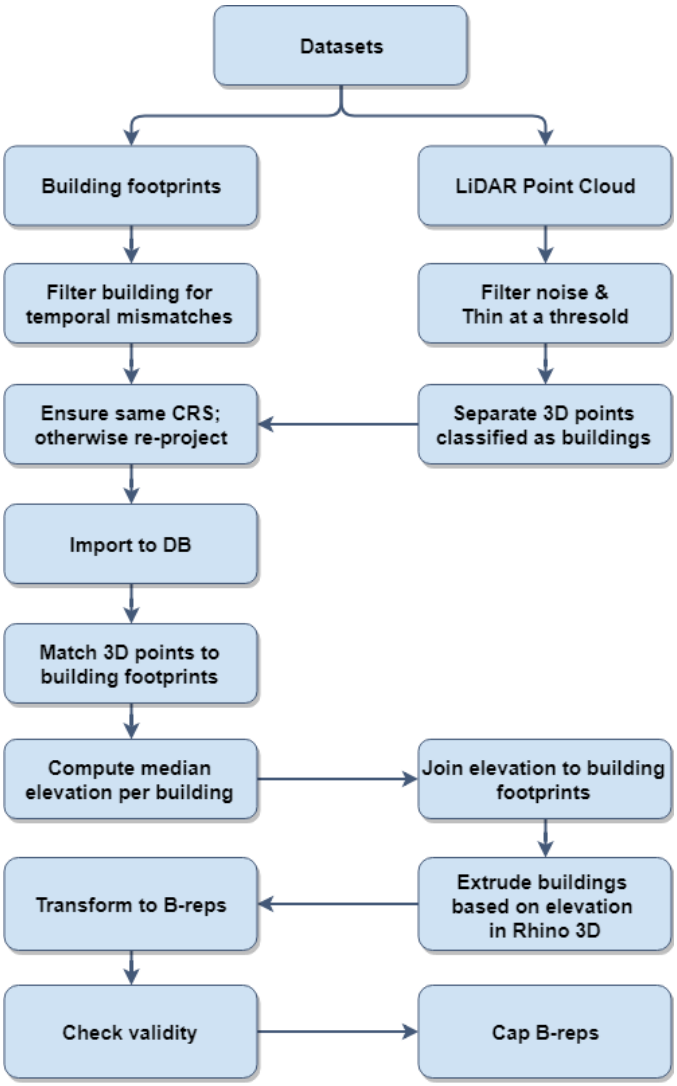

Figure 3.13: Steps for the generation of the 3D environment.

3.3.4 Visibility analysis

This step describes the implementation of the visibility analysis using a backward ray-tracing algorithm. Opposite to the forward ray-tracing, when the backward tracing is chosen, the rays are traced from the eye-level of an observer directly to a 3D object/target. If a ray hits the object then the 3D object is visible to the observer. The target is not visible when an obstacle involves in the 3D space and obstructs partially or totally the direct visibility of the observer by creating a shadow to the target [Scratchapixel].

The visibility analysis (from the preparation of the data in the 3D environment to the extraction of the metrics) implemented, using Rhino 3D and Grasshopper. A description of the steps required for the implementation is following. The workflow shown in Figure 3.14 depicts the full process.

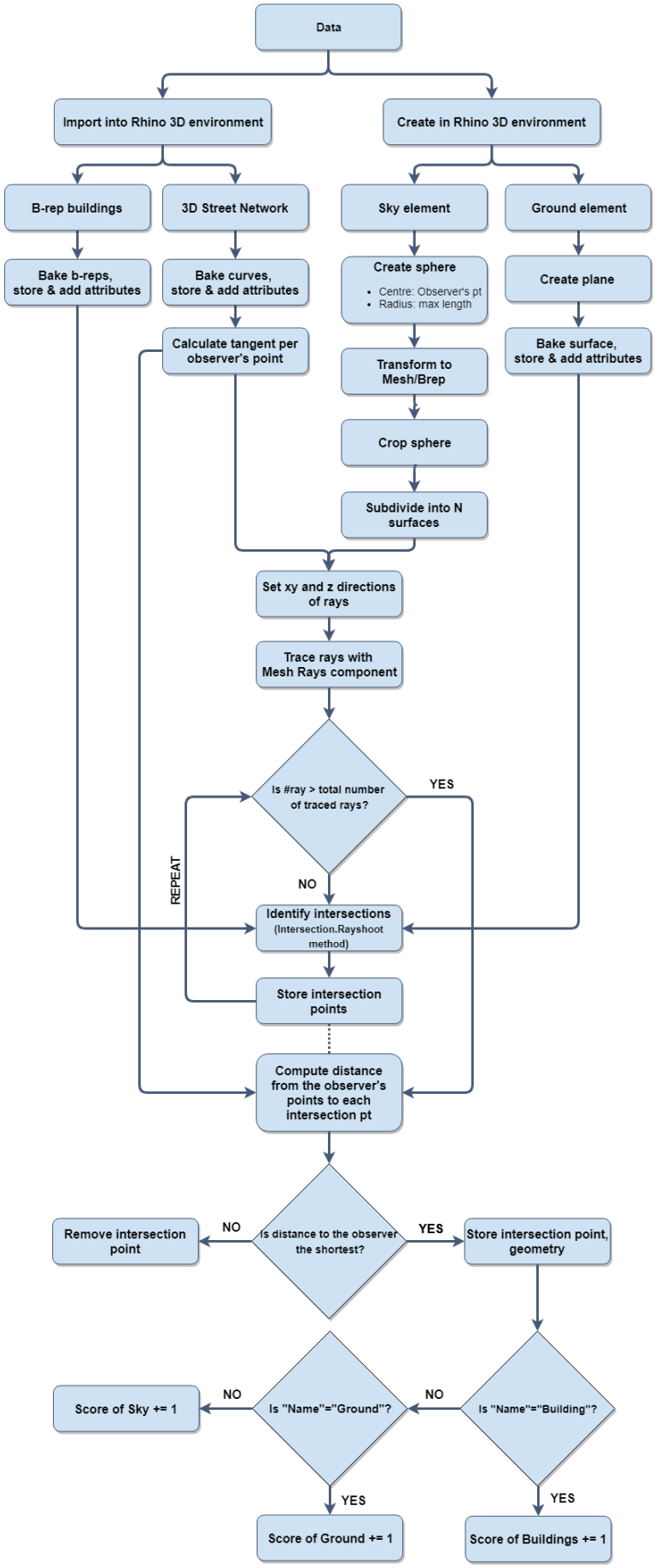

Figure 3.14: Description of steps of the visibility analysis process.

All required data need to be imported into the 3D Rhino environment using the Grasshopper plug-in. It is essential to ensure a common CRS for all datasets, meaning that re-projections are required, beforehand. Grasshopper gives the possibility of re-projecting the datasets directly via its environment, and so one can also follow this option.

The B-rep buildings are already into the 3D Rhino environment, but need to reference the B-rep buildings back to Grasshopper (as Brep), using the Elefront plug-in of Grasshopper. This ensures that the attributes of the buildings (such as Globally Unique IDentifier (GUID), year of construction etc.) will be maintained after importing them into Grasshopper [Plugin]. It also helps to assign an additional attribute based on the Rhino layer they belong to (i.e. layer: buildings) and the type of the geometry.

On the other hand, the 3D street network, the ground, and the sky are still out of the 3D Rhino environment and need to be imported.

The 3D street network is imported as an Autocad DWF file and is baked. The street network is reference to Grasshopper as curves using again the Elefront plug-in. For each 3D street segment, the tangent at each observer's point is calculated. The tangent indicates the direction of the visibility.

In this methodology, the ground element is represented as a plane, created by the user in Rhino 3D. This plane should cover the whole study area. Elefront is used to reference the geometry in Grasshopper as well. Height information is not added to the plane, although this step could augment the realism of the 3D environment. Nevertheless, because of the absence of details on the ground or the road infrastructure (such as pavements, bumps or bridges), this decision little affects the results.

At this moment, our 3D environment looks like the one in the Figure 4.19.

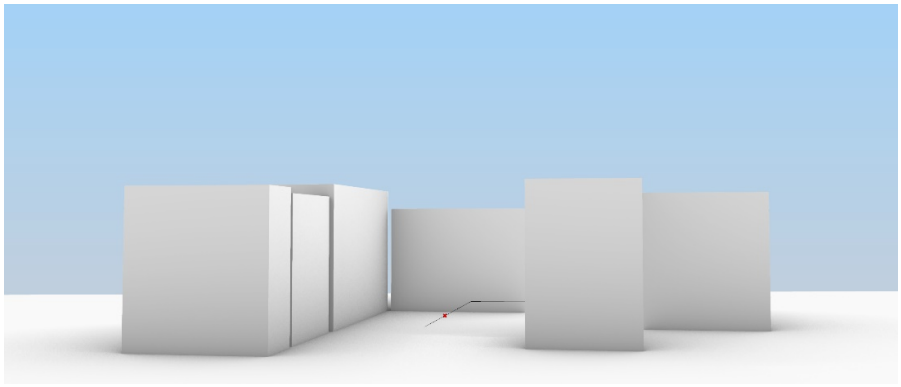

Figure 3.15: Representation of a 3D environment used for visibility analysis. The buildings and ground elements as well as the 3D street network are present.

The sky element defines the maximum length and the resolution of the visibility analysis. The way to determine the maximum length of visibility can be found in Preparation for implementation. The sky element is created on Grasshopper (with the sphere component), giving as the centre: the observer's location and as a radius: the maximum length of visibility. The sphere is represented as B-rep and needs to be cropped at a level below the ground element. Following, the B-rep is capped in order to ensure that the hole created by cropping it, is now closed. Finally, the sky element should be transformed into a mesh that approximates the B-rep geometryFigure 3.16).

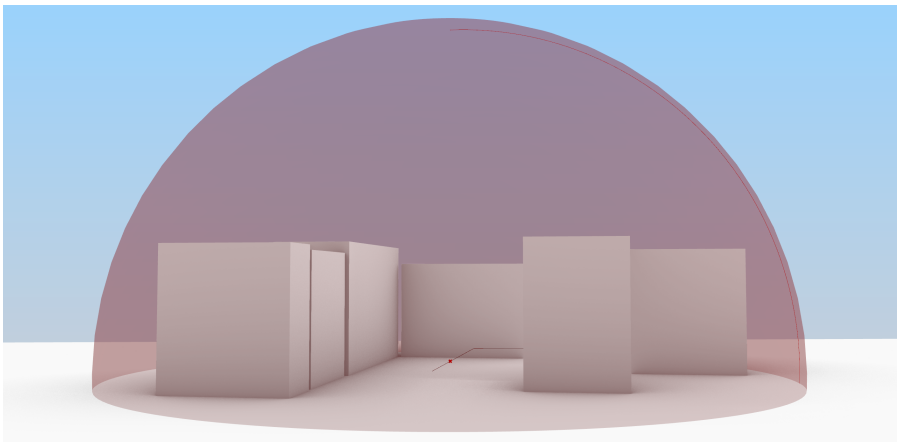

Figure 3.16: Representation of the complete 3D environment used for visibility analysis.

The sky element is subdivided into sub-surfaces creating a grid (Figure 3.17). The resolution of the grid depends on the desired level of detail of the visibility analysis, although the user should consider possible increment of the computation time. The suggested resolution in this methodology is 100, meaning that 100 rays will be traced by the observer's point. This value is the maximum possible used considering the computation time. A smaller value will give less detail to the visibility analysis and should be avoided when one works with complex 3D environments.

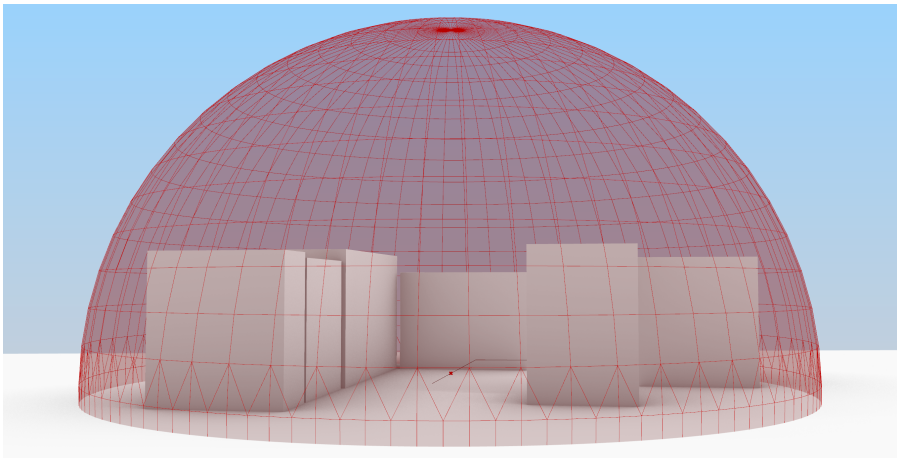

Figure 3.17: Division of the sky element into smaller sub-surfaces.

Following, rays are traced from the observer's point to each of these sub-surfaces. For this step, the location and the direction of the observer's point are required. One should set the direction of the vector to xy-direction and z-direction with an interval. This interval corresponds to the horizontal and vertical angles of the visibility. To determine both angles, this methodology takes into consideration the human field of vision (Figure 3.18). Therefore, the angles set to a. horizontal angle = 75° and b. vertical angle = 60°. These values succeed to capture a realistic representation of the visible views of the observer. Eventually, the mesh ray component of Grasshopper is used to trace the rays to the sky element. The amplitude of the rays is represented in Figure 3.19.

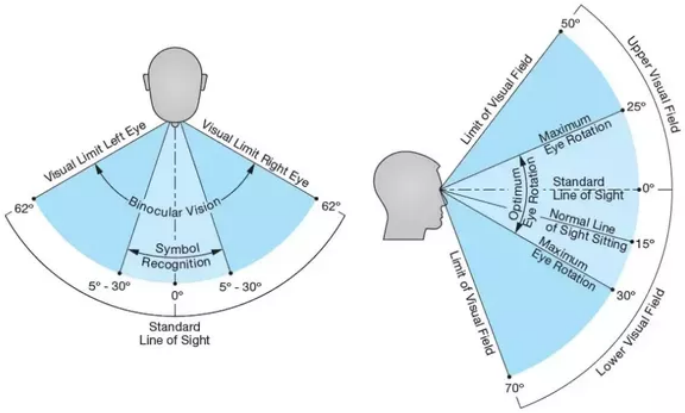

Figure 3.18: Human field of vision.

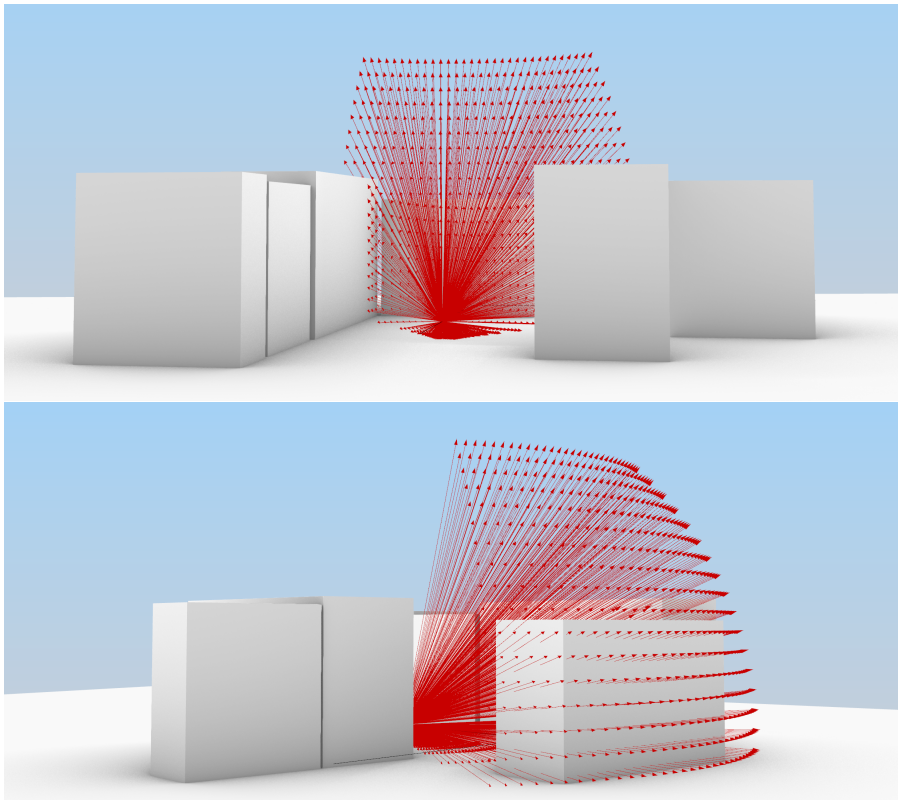

Figure 3.19: Rays traced to the sky element in a cone.

Having traced the rays to the sky element, the next step is to identify the intersections of these rays with the buildings and the ground elements. The Intersection.Rayshoot method of Grasshopper was used for this purpose. The method is not yet available in Python but it is available in C# or VB programming languages. The programming language C# used in this process. The Intersection.Rayshoot method takes as input the 3D rays, the geometry and an integer that represents the maximum reflections [Rhino3D]. The 3D rays were created in the previous step. The geometry refers to the geometry type of the obstacles (refers as Geometry.Base in Grasshopper), and the maximum number of reflections; an integer value that can be between [1,

1000]. In addition to this input, the observer's point is also required but will be used outside of the method. The output of the method is an array of 3D points that represent the hits to the input geometries (Point3d.Unset property). In our case, these geometries are the buildings and the ground. A known limitation regarding the Intersection.Rayshoot method, is the way reflections are created when trimmed geometries exist [Rhino3D]. The GUIDs and the geometry type are accessed inside the script. These values are needed to determine which element is visible to the observer. The script runs repeatedly for every input geometry. In every iteration, a new 3D Point that represents the hit of the ray is created and stored in the array. If the 3D Point already exists in the array, then is skipped. Additionally, if no 3D Point exists, the value is set to null. When a null value exists in the array, the sky element scores one hit. After the whole iteration is finished, an array with the total number of hits from all geometries is ready. At this moment, it is needed to filter these hits based on the distance from the observer's point. We need the closest hit to the observer because this is his visible view and so the Point3d.DistanceTo method is used. The hit with the smaller length is stored in a newly created list together with the GUID, the name and the type of the geometry and the distance from the observer's point (i.e. the lengths of the rays). The same process is repeatedly implemented for all the rays of the observer's point. The output is represented in Figure 3.20. The number of hits per object and the lengths of the rays are transformed into different data trees with a self-implemented script in ghPython.

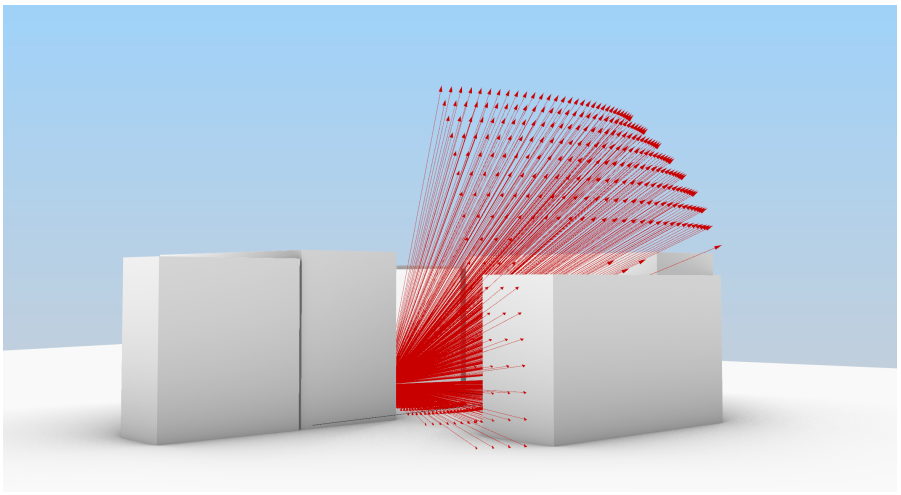

Figure 3.20: Isovists represented as rays in a 3D environment.

3.3.5 Preparation for implementation

Street segments in the simplified street network may vary extremely on their lengths. The fact that there may be street segments of 10 meters but also street segments of 400 meters length makes it difficult for a universal decision on the number of observer's points to be created. For this purpose three additional but complementary steps are needed to be followed before running the visibility analysis of the whole street network.

Categorization of street segments based on the length

All the unique IDs of the street segments together with their lengths can be used 1) to create a histogram of the lengths of the street segments and 2) to compute the normal distribution of the lengths of the street segments. In case the normal distribution is skewed to the left or right, then the computation of a Poisson distribution may be more suitable. These two graphs will be used to specify the way the street segments will form categories.

One of the ways to decide on the categorization of the street segments is to take different percentiles of the data. This methodology suggests the 20^{th}, 40^{th}, 60^{th}, 80^{th} and 100^{th} percentiles to categorize the street segments. However, when extreme length values still exist in these categories, one should consider to create more categories that separate these extreme length values.

The graphs of this step were created using the Matplotlib and Numpy libraries of Python.

Decision on maximum length of visibility

Using the defined categories of street segments, visibility analyses are performed in order to decide on the maximum length of visibility. The decision on the values of the maximum length of visibility tested in this step should be in line with the purpose of the study.

Considering that this value will remain steady during the whole implementation, it is important to describe as strongly as possible the 3D environment. This pass/fail test relies on the repetition of the visibility analysis process and can be applied only on the intersection points of a smaller sample of the dataset. In this way, a reduction of the computation time and power is ensured. However, two points need to be taken into consideration:

1. The smaller selected sample should include street segments of all defined categories.

2. The intersection points used to test the maximum length of a cyclist's visibility can be shared by several street segments. Therefore, possible duplicated intersection points may exist in the dataset. These duplicated points are retained because of the facts that a. their direction is changing based on the direction of the street segment and b. they represent the entry too- and the exit from- the street segment that a cyclist traverses.

The test finishes when one value can successfully represent our 3D environment from the observer's points.

Granularity test

The categories of street segments, as these formed in the previous step, and the maximum length of visibility will be used for a granularity test. This test is important in order to decide the number of observer's points per category. In this way, a more representative result of the built environment and a reduction of the computation time of the visibility analysis will be ensured.

The granularity test in the proposed methodology suggests the investigation of the visibility analysis of the street segments in four different cases. These distinct cases are:

1. Park: A street segment that crosses a park or at least a park is located alongside.
2. Water: A street segment that represents a bridge or a canal/water is present alongside.
3. High density buildings: A street segment that has a high density of buildings.
4. Low density buildings: A street segment that has a low density of buildings, or the buildings are away, or the buildings are very low.

These four cases are applied to each category of street segments. The metrics used in this step are the percentages of visible sky, visible building and visible ground, and the kurtosis. These four metrics are later compared with Google street view and Google maps in order to check whether they successfully represent the real environment.

This test gives a number of observer's points per category and can be implemented in Rhino 3D/Grasshopper. The graphs used to compare the results per category of street segments can be created in Excel.

3.3.6 Run the visibility analyses

When the categorization of the street segments and the granularity test are completed the procedure is ready to run. The implementation is performed repeatedly, meaning that each category of street segments is running separately. Each observer's point is giving as output a. a list of the lengths of all the rays and b. the number of rays that hit the sky, the buildings, and the ground. These data are stored temporarily for the computation of the metrics.

3.4 METRICS

The output of the previous step gives a list of the lengths of the rays and the number of hits to the sky, the buildings and the ground per observer's point. These data were used as the main input of this module. Moreover, the module explains a. the metrics and the way of calculating them per observer's point, b. the aggregation of each metric to a street segment level, c. the way of matching the GPS and alternative routes to the street segments and d. the aggregation of the metrics to a route level. By the end of this process, each route has one score which describes one metric and supports the comparison between the GPS routes and the alternatives.

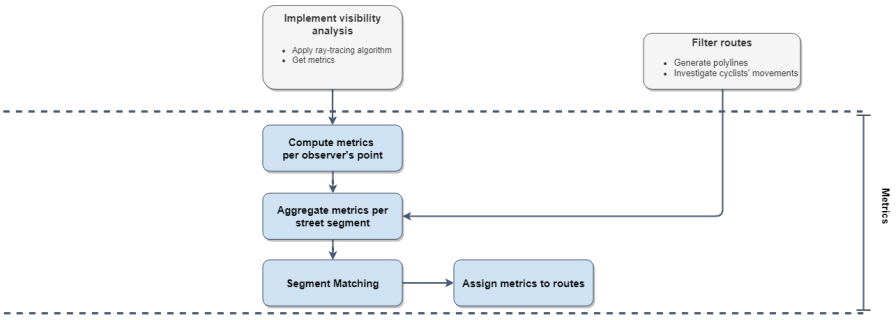

Figure 3.21: Generic overview of the module "Metrics".

3.4.1 Introduction to the metrics

In this research, the computed metrics can describe both the spatial openness and the shape of the 3D isovist per observer's point.

- **Spatial Openness**
  To measure Spatial Openness the transformation of the number of rays' hits to an element (i.e. sky, buildings, and ground) is required. This simple transformation is performed in Grasshopper by multiplying the total number of the hits to an element by 100 and later dividing this output with the total number of all hits.

  1. *Percentage of visible sky*
     The percentage of visible sky indicates the amount of sky that a cyclist sees while travelling. The metric has a maximum value of 51.6% which is found in highways, avenues or rural areas. Because the metric is normalized, its summation with the percentage of visible buildings and the percentage of visible ground results in the total 100% of visible views of the cyclist. The meaning of the metric is also depicted in the sketch C. of Figure 3.22.
  2. *Percentage of visible buildings*
     The percentage of visible sky indicates the number of buildings that a cyclist sees while travelling. The metric has a maximum value of 89.9%. Maximum value can be seen mainly in narrow streets of the city/town centre or in old parts of a city/town. Since the metric is normalized, its summation with the percentage of visible sky and the percentage of visible ground results in the 100% of visible views of the cyclist. The meaning of the metric is also depicted in the sketch A. of Figure 3.22.
  3. *Percentage of visible ground*
     The percentage of visible ground indicates the amount of ground that a cyclist sees while traveling. The metric has a maximum value of 48.3%. Maximum value can be found in highways, avenues or other spacious streets. Because the ground in this case includes also auxiliary traffic area, greenery, parks, and water/-canals, the maximum value may also be present in paths crossing parks or streets alongside canals. Since the metric is normalized, its summation with the percentage of visible sky and the percentage of visible buildings results in the 100% of visible views of the cyclist. The meaning of the metric is also depicted in the sketch B. of Figure 3.22.

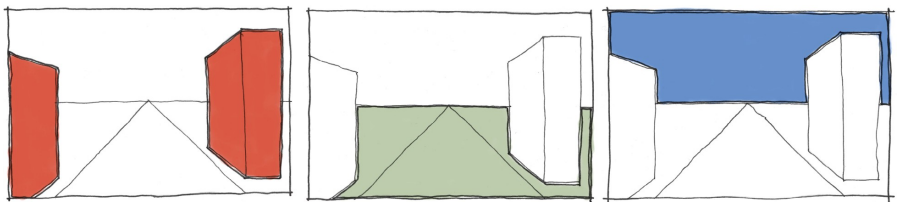

Figure 3.22: Representation of the metrics:percentage of sky, percentage of buildings and percentage of ground.

Apart from the use of the aforementioned metrics to describe Spatial Openness, three additional metrics are introduced in order to investigate the significance of these metrics when combined. If the buildings

would not influence a cyclist in his route choice, would the buildings in relation to the sky be more important to him? This type of questions are answered by measure the following metrics.

4. *Visible Buildings:Sky ratio*
   The visible Buildings:Sky ratio measures the visible buildings in relation to the visible sky. The values of both the buildings and the sky are derived from the result of the metrics #2 and #1, respectively. The opposite ratio would not be possible since the percentage of the visible buildings can equals 0.
5. *Visible Buildings:Ground ratio*
   The visible Buildings:Ground ratio measures the visible buildings in relation to the visible ground. The values of both the buildings and the ground are derived from the result of the metrics #2 and #3, respectively. The opposite ratio would not be possible since the percentage of the visible buildings can equals 0.
6. *Visible Sky:Ground ratio*
   In a similar way as the two previous metrics, the visible Sky:Ground ratio measures the visible sky in relation to the visible ground. The values of both the sky and the ground are derived from the result of the metrics #1 and #3, respectively.

- **Shape of the 3D isovist**

  To describe the shape of a 3D isovist the following metrics are used. The sketches created to describe these metrics are represented from the top view for a clearer interpretation.

  1. *Median of rays' lengths*
     The median length of all the rays represents the centrality of the data. This means that when a mean value is close to the maximum length of visibility, an almost complete 3D isovist shape is depicted.

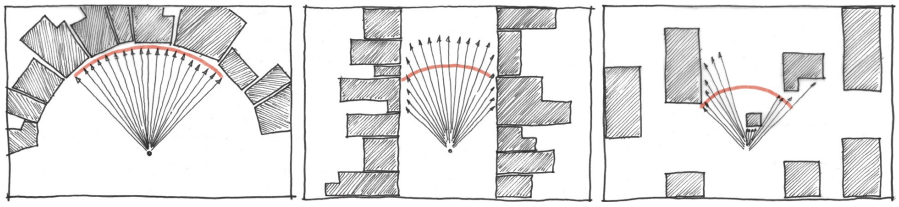

Figure 3.23: Representation of the median length of all the rays traced from an observer's point.

  2. *Kurtosis*
     Kurtosis indicates extreme variations of the rays' lengths by measuring the outliers in the data. Rather than measuring peaks, this metric describes the differences in the shape of the 3D isovist [Kenton]. Kurtosis is defined as [NIST]:

$$\mathcal{K} = n * \frac{\sum_{i=1}^{n}(x_i - x_a vg)^2}{(\sum_{i=1}^{n}(x_i - x_a vg)^2)^2} \tag{3.1}$$

     This metric is very often challenging to be interpreted and can be positive or negative [Kenton]. The sketch of Figure 3.24 shows the interpretation of different kurtosis values regarding an isovist.

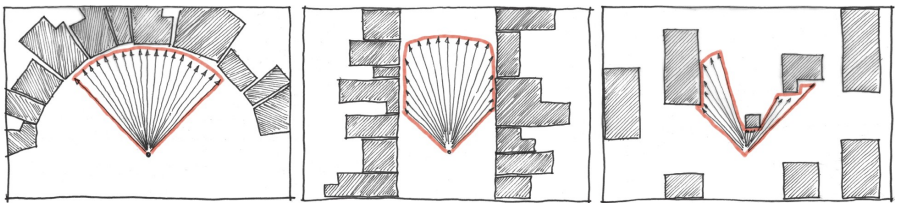

Figure 3.24: Representation of the kurtosis of all the rays traced from an observer's point.

3. *Standard deviation of rays' lengths*
   Standard deviation of the lengths of all the rays depict possible variations in the street profiles or only the heights of the buildings. The difference with the kurtosis is the fact that the standard deviation is not affected by the density of the data. This means that although both measure distributions, two values with different types of kurtosis may share the same standard deviation value. The sketch of Figure 3.25 represents the way that standard deviation is interpreted in this methodology.

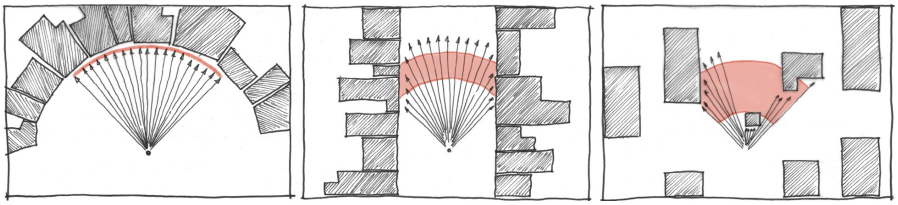

Figure 3.25: Representation of the standard deviation of all the rays traced from an observer's point.

3.4.2 Street profiles

The core metrics that describe spatial openness (i.e. % of visible sky, % of visible buildings, and % of visible ground) can be used to identify different street profiles. These street profiles form seven different categories. The process is conceptual, but the categorization of the street profiles can be an additional metric to describe the street segments. Figure 3.26 represents the different categories and their brief description.

The categories of the street profiles were created by analyzing the visibility of a small sample of the street segments and by taking into consideration possible locations of the observer. Other metrics (such as the kurtosis values) ignored during this categorization because of the extreme detail that would add to the categories and the number of possible interpretations of the street profiles that would produce.

The numbers of each street profile were used as the metric assigned to each observer's point. The criteria for the assignment are based on the percentages of sky, building and ground as these are represented in Table 3.2.

Table 3.2: Street profiles and their meanings regarding the sky, buildings and ground percentages.

Street profile	Values (%)
1	Buildings = 0.0
2	Buildings <= 20.0
3	20.0 <Buildings <=30 and Sky<Ground
4	20.0 <Buildings <=30 and Sky>=Ground
5	30.0 <Buildings <= 55.0
6	55.0 <Buildings <65.0
7	Buildings >65.0

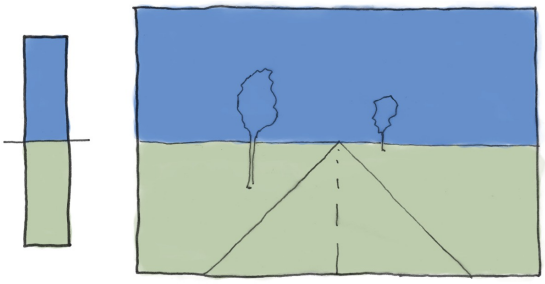

Street profile 1

Ideal open space where no buildings exist.

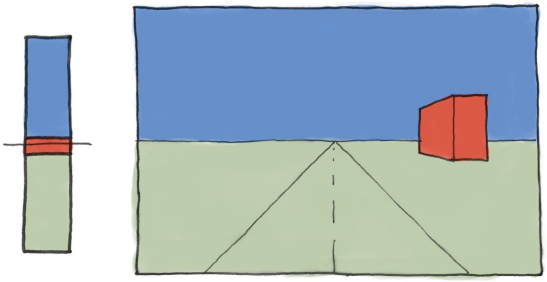

Street profile 2

Streets with a few buildings further away from the observer and their heights do not influence the view of the observer.

A. The buildings are located further away of the street.

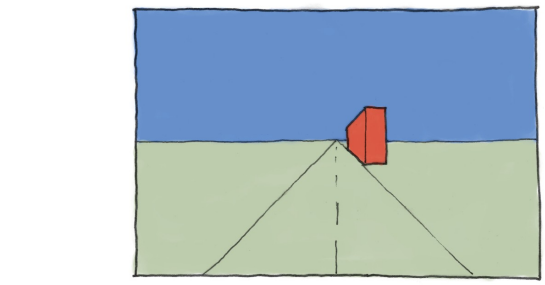

B. The buildings are located near the street.

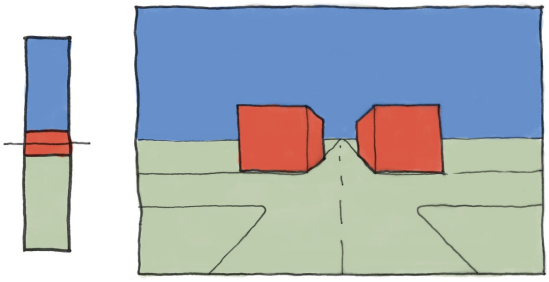

Street profile 3

Streets with low buildings on both sides or buildings on one side of the observer. Crossroads may also exist.

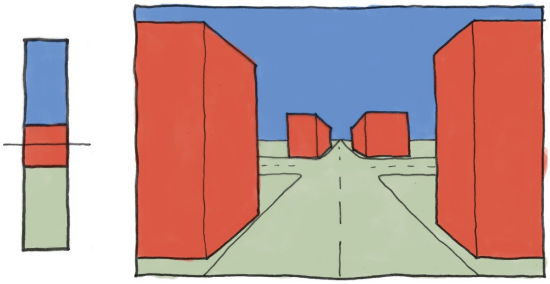

Street profile 4

A. Streets with low buildings on both sides of the observer. Crossroads may also exist.

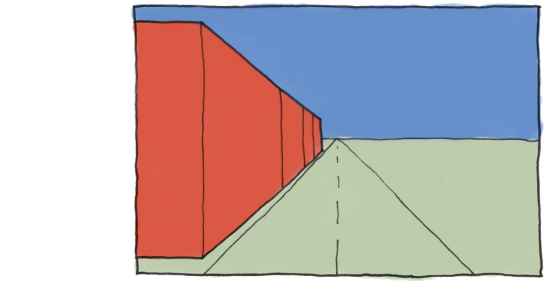

B. Streets with buildings on one side of the observer. Crossroads may also exist.

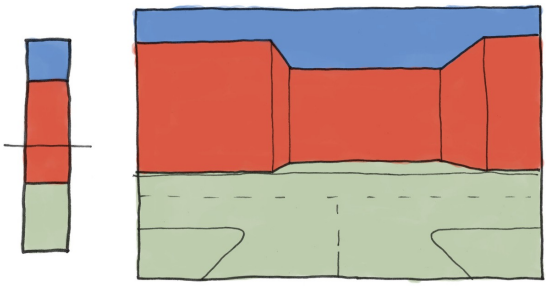

Street profile 5

A. Building(s) in the front view of the observer

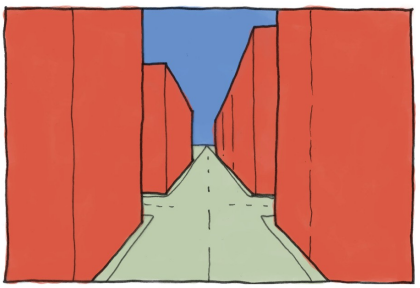

B. Narrow direct streets with buildings on both sides of the observer. Narrow crossroads may exist.

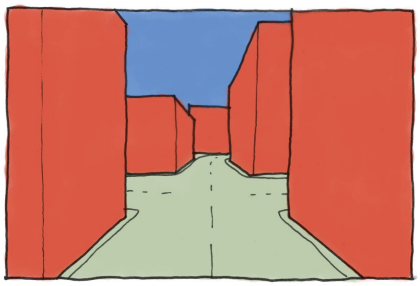

C. Normal streets with turns and buildings on both sides of the observer. Wider crossroads exist.

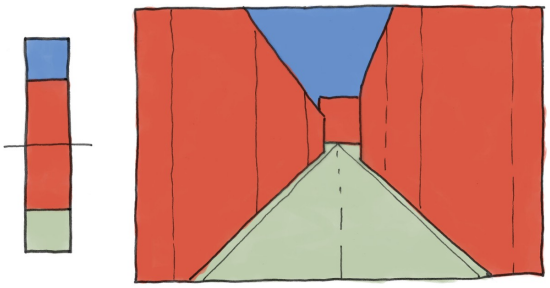

Street profile 6

Normal streets and buildings on both sides of the observer. No crossroads. Building on the front view of the observer exists.

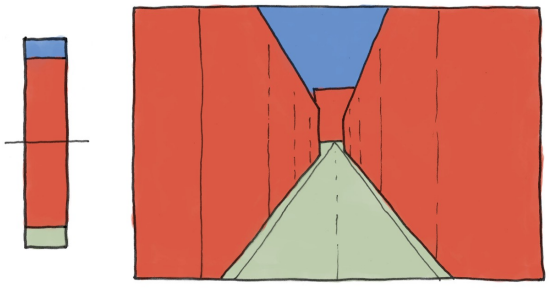

Street profile 7

Narrow streets and buildings on both sides of the observer. No crossroads. Building in the front view of the observer exists.

Figure 3.26: Identified street profiles in the built environment based on the percentages of sky, buildings and ground elements.

3.4.3 Assignment to the routes

The aforementioned metrics correspond to each observer's point. However one aggregated value per metric that characterizes the whole street segment is needed.

1. **Aggregation of metrics per street segment**
   In this step the metrics collected for each observer's point are aggregated in a street segment level (Figure 3.27). Different metrics are using different aggregation methods as shown in Table 3.3. The aggregation methods suggested in this methodology were decided based on the need to maintain all the valuable information.

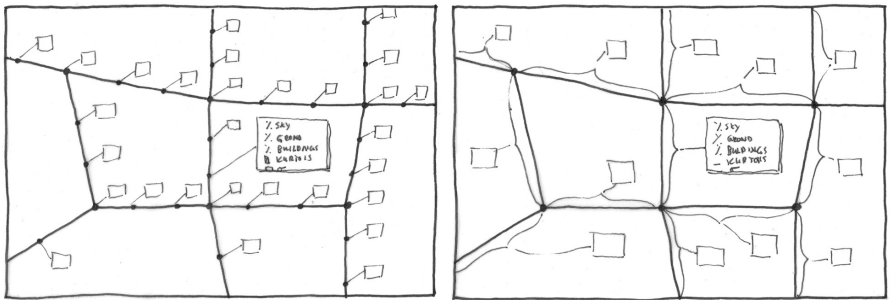

Figure 3.27: Aggregation of the metric per observer's point in a street segment level.

Table 3.3: Decision on aggregation methods per metric in a segment level.

Metric	Aggregation Method	Meaning
Sky (%)	Geometric Mean	Indicates the change of the amount of sky from one observer's point to the next
Buildings (%)	Geometric Mean	Indicates the change of the amount of buildings from one observer's point to the next
Ground (%)	Geometric Mean	Indicates the change of the amount of ground from one observer's point to the next
Buildings:Sky	Geometric Mean	Indicates the change of the ratio of buildings and sky from one observer's point to the next
Buildings:Ground	Geometric Mean	Indicates the change of the ratio of buildings and ground from one observer's point to the next
Sky:Ground	Geometric Mean	Indicates the change of the ratio of sky and ground from one observer's point to the next
Median	Geometric Mean	Indicates the change of the size of the isovist from one observer's point to the next
Kurtosis	Standard Deviation	Indicates the isovist's shape from one observer's point to the next
Standard deviation	Geometric Mean	Indicates the change of the homogeneity of the built environment from one observer's point to the next
Street Profile	Mode	Indicates the street profile that is most often seen in the street segment

Most of the metrics were aggregated by using the geometric mean. The geometric mean multiplies a series of data points and then uses the n number of data points to find the nth root of that product [4]. This means that the geometric mean is used when we want to calculate the mean of consecutive growth factors. Therefore, for the set of changing factors $x_1, x_2, ..., x_n$ the geometric mean is calculated as:

$$\prod_{i=1}^{n} x_i = \sqrt[n]{x_1 x_2 ... x_n} \tag{3.2}$$

The units of the geometric product are not the same as the input values. Instead, they are dimensionless and they apply only to positive values. The geometric mean adds depth and stability to the mean value.

Although the geometric mean can be applied to the kurtosis values, the fact that the kurtosis can acquire negative values adds a difficulty in performing the computation. For that purpose, kurtosis was aggregated based on the standard deviation of the values, a statistical measure used to quantify the amount of variation between individual points.

Finally, the street profiles assigned as a metric to each observer's point. This metric acquires values between 1 and 7 as shown in Figure 3.26 based on the table 3.2. This metric was aggregated based on the most often seen value (mode), giving a general description of the segment itself.

2. **Segment matching to routes**
The purpose of this step is to assign the aggregated metrics per street segment to the GPS or the alternative routes (Figure 3.28). This step requires the generation of a new table in the database where the ID of the route, the type of the route (GPS or alternative) and a sequence of the street segments are all included. The segment matching of the simplified street network and the routes can be performed in PostGIS using the ST_HausdorffDistance function. This function returns the Hausdorff distance between two polylines (or other geometries) by measuring the similarity of the polylines [67]. A strict threshold is required. Using ST_HausdorffDistance function the aggregated values are matched with the street segments of each route.

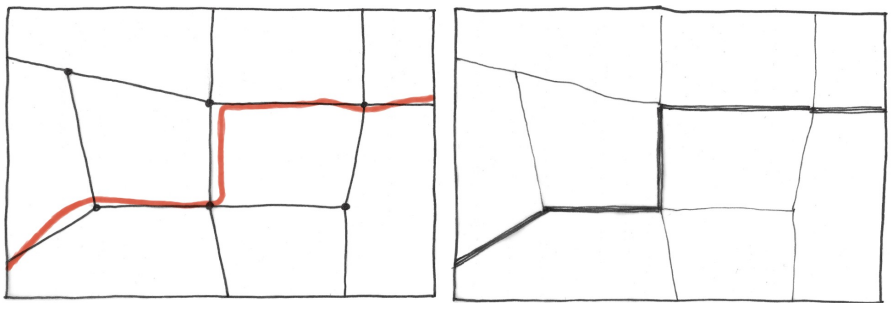

Figure 3.28: Segment matching of the routes to the OSM street network.

3. **Aggregation of metrics per route**
The aggregation of metrics per route is the last step of processing and simulation. This step produces one value for every metric for the GPS or an alternative route (Figure 3.29). The aggregation methods used for each metric are shown in Table 3.4. The selection of the aggregation methods is in line with the selection of the aggregation of metrics per segment.

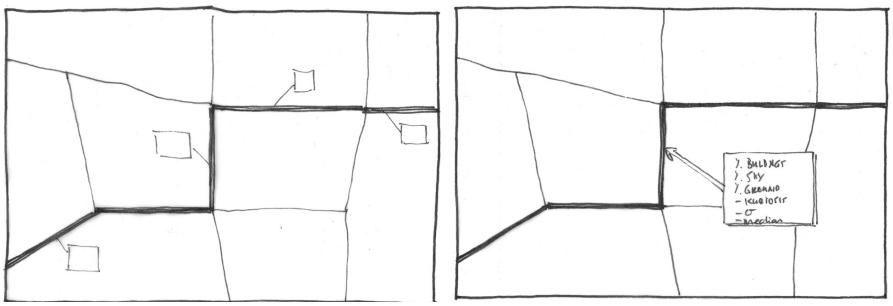

Figure 3.29: Aggregation of the metrics per street segment in a route level.

Table 3.4: Decision on aggregation methods per metric in a route level.

Metric	Aggregation Method	Meaning
Sky (%)	Median Standard Deviation	Indicates the amount and the possible variations of the visible sky of the route
Buildings (%)	Median Standard Deviation	Indicates the amount and the possible variations of the visible buildings of the route
Ground (%)	Median Standard Deviation	Indicates the amount and the possible variations of the visible ground of the route
Buildings:Sky	Median Standard Deviation	Indicates the amount and the possible variations in the ratio of buildings and sky of the route
Buildings:Ground	Median Standard Deviation	Indicates the amount and the possible variations in the ratio of buildings and ground of the route
Sky:Ground	Median Standard Deviation	Indicates the amount and the possible variations in the ratio of sky and ground of the route
Median	Median Standard Deviation	Indicates the amount and the possible variations of the open space of the route
Kurtosis	Median Standard Deviation	Indicates the isovist's shape and the possible shape variations of the route
Standard deviation	Median Standard Deviation	Indicates the amount and the existence of homogeneity in the built environment of the route
Street Profile	Mode	The street profile that is most often seen in the route.

3.5 COMPARISON OF THE GPS AND ALTERNATIVE ROUTES

The aggregated metrics per route, as computed in the previous step, used to compare the actual GPS routes with their alternatives. The multiple comparisons require both qualitative and statistical analyses in order to extract conclusions. Figure 3.30 shows the steps followed in this module.

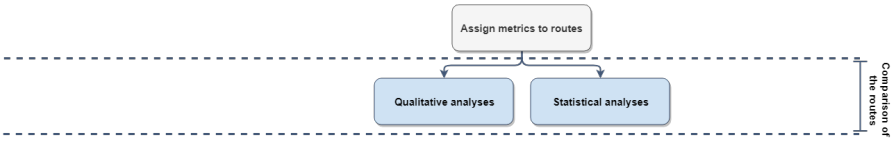

Figure 3.30: Generic overview of the module "Comparison of the GPS and alternative routes".

3.5.1 Qualitative analysis

Qualitative analysis applied to a street network level and the output is divided into two categories based on the street choices of the cyclists. In this way, we aim to investigate possible differences between the selected and the non-selected street segments of the street network.

The analysis is based on a. the percentages of visible sky, b. percentages of visible buildings, c. percentages of visible ground, and d. street profile. Therefore, we aim to examine only the preferences of cyclists regarding spatial openness and street profiles. The shape of the 3D isovist is excluded because of its complexity to be described and interpreted qualitatively. All graphs used for the qualitative analysis are created in Excel.

3.5.2 Statistical analyses

The Analysis of the variance (ANOVA) method considered suitable for the statistical analyses of the results since it compares different groups. ANOVA is useful for normal distributions when there is a need to check if the means of two or more (unrelated) groups are significantly different from each other [Field]. It is important that the analysis requires groups of equal or at least similar sizes. This means that even if a recommended by OSM route matches the fastest or the shortest routes, it should be stored and analyzed as well.

Regarding the data, the dependent variable should be categorical, and the independent variables can be factors (categorical variables) or covariates (continuous variables). In this case the dependent and independent variables are:

- Outcome (Independent variables):
  - GPS route
  - shortest alternative
  - fastest alternative
  - recommended alternative
- Predictors (Dependent variables):
  - Median and StDev of Sky
  - Median and StDev of Buildings
  - Median and StDev of Ground
  - Median and StDev of Kurtosis
  - Median and StDev of Median length rays
  - Median and StDev of Standard deviation of length of rays
  - Distance
  - Median and StDev of ratio buildings/sky
  - Median and StDev of ratio buildings/ground
  - Median and StDev of ratio sky/ground
  - Mode of street category

The statistical analysis can be performed in Statistical Package for the Social Sciences (SPSS) after making two essential decisions. The first refers to the definition of the contrasts using weights. The contrasts are defined in order to indicate to the system which dependent variable needs to be compared to [Field]. Different levels of contrasts applied based on the purpose of the analysis. In our case a contrast 1 is performed since we need to compare the GPS routes with the alternatives. However, in the case we wanted to compare also the fastest alternative with the shortest or the recommended, this would require an extra level of the contrasts (contrast 2).

To create the contrasts it is needed to apply weights to the dependent variables. The way the weights would be applied, is based on the dependent variables and on the additional requirement of getting a 0 coefficent total. In principle, the control group which in our case is the GPS routes is assigned by a negative weight, whereas the alternatives are getting a positive weight [Field]. Since there are 4 groups that we need to compare in total, we can code the GPS route with -3 and the alternatives with +1 for each route. The second decision refers to the post hoc tests that it needs to be used. Post hoc procedures are often called data mining because they used for cases that there are no specific predictions of the data and the differences between the groups [Field]. Because many post hoc tests consists the list, one should be aware of the types of the errors that could characterize the statistical analysis. In our methodology a more conservative choice, the Tukey's test used to reduce possible errors that affect the results when multiple ANOVA analyses performed. Because Tukey's test assumes homogeneity of variances, the Games-Howell post hoc test is also suggested. The outputs of this step are the descriptive statistics regarding the variables, a homogeneity of invariance test (Levene's test) that tests the assumption that the variances of the four groups are equal, the Brown-Forsythe and the Welch's F-ratios that used when the aforementioned assumption is fault and the means plots [Field].

3.6 CONCLUSION AND FUTURE RESEARCH

A discussion on the results and their interpretation regarding cyclists route choices for the selected study area is the next step (Figure 3.31). The interpretation of the results reflects on the route preferences of the cyclists and the actual application of the revealed information on the development of design guidelines for the street network. This thesis concludes with an assessment of the proposed methodology and potential limitations of it and gives recommendations for future research and adaptations.

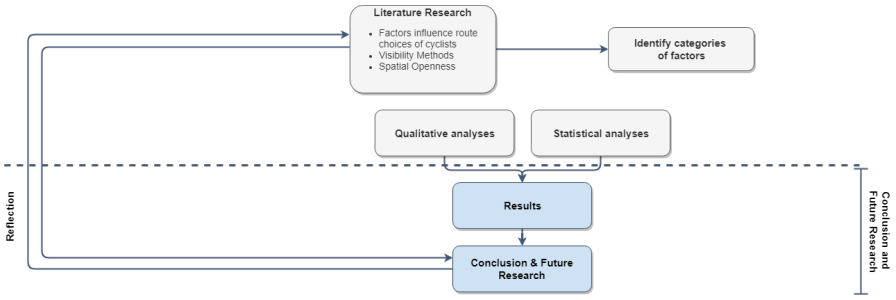

Figure 3.31: Generic overview of the module "Conclusion and Future research".

3.7 SYNTHESIS

This chapter gave a description on the methodology that is suggested in order to explore the extent that the visible views of the urban environment affect the route choosing of a cyclist while traveling. For this purpose, GPS trajectories are compared with alternative routes suggested by OSM via the OpenRouteService Directions API. The suggested alternatives can be either

the fastest routes, the longest routes or those recommended by OSM (in terms of travel distance, travel time or safety.

The suggested methodology is based on the visibility of the cyclist. The visibility analysis is using the ray casting algorithm in a 3D environment and gives as an output 3D isovists. The 3D isovists are used in order to measure the spatial openness as the ratio of the amount of visible sky, visible buildings and visible ground, as well as the shape of the 3D isovist itself. Opposite to similar researches that are performing the visibility analysis on the actual GPS routes, this thesis project applies the visibility analysis to a simplified version of the OSM street network in the centre of Amsterdam. The simplified OSM street network consists of street segments, the nodes of which represent real road intersections. The output of the visibility analysis per street segment is later mapped to the GPS trajectories and the alternative routes as an aggregated value. A detail overview of the steps followed can be seen in Figure 3.32.

In the next chapter, the suggested methodology tested with real data in order to explore potential advantages and limitations. For this purpose, the methodology is applied in the city of Amsterdam, the Netherlands.

RQ: To what extent the directly visible views of the urban environment influence the route choices of the cyclists and how these views can be measured?

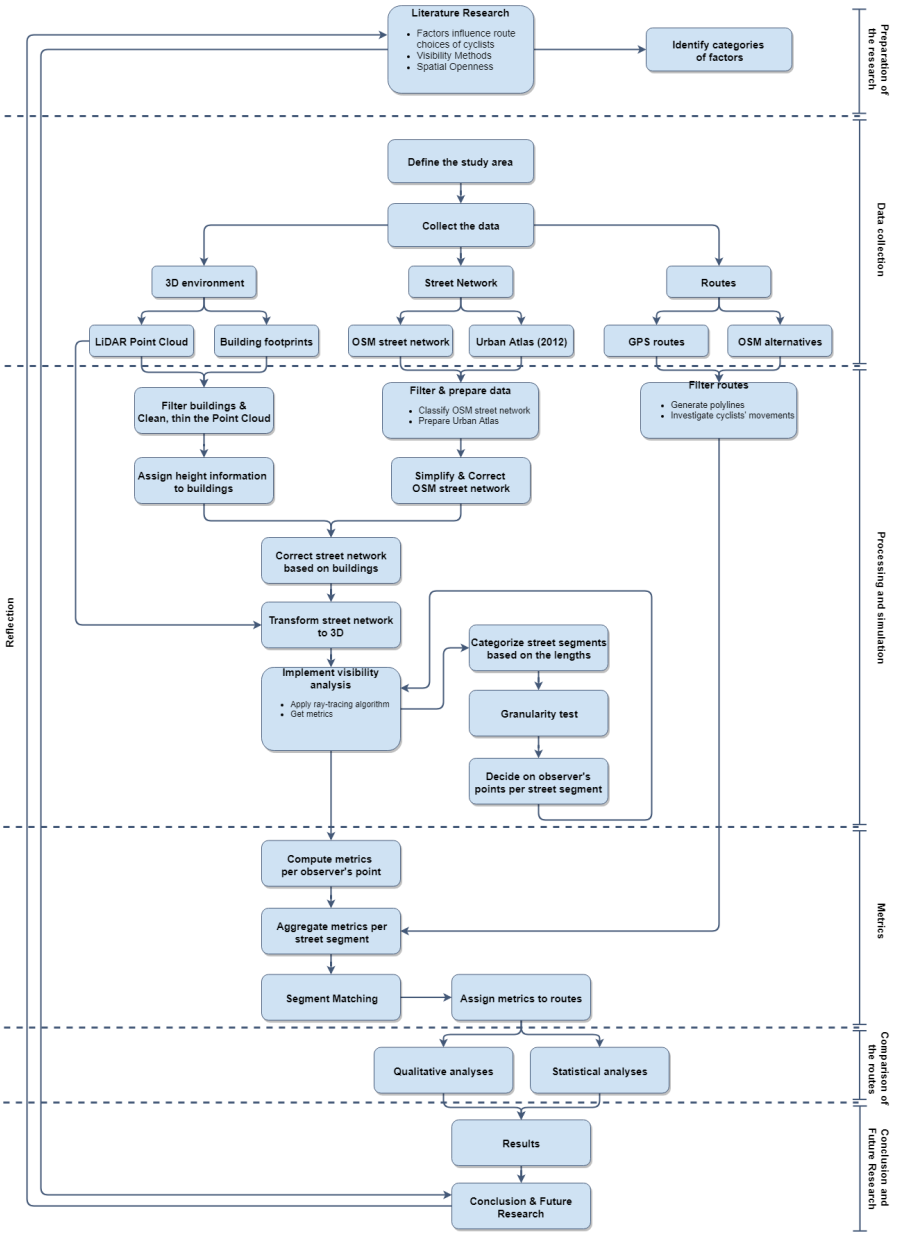

Figure 3.32: Generic overview of the modules of the suggested methodology.

4 CASE STUDY: AMSTERDAM, NL

In this thesis the suggested methodology was tested in the city of Amsterdam in the Netherlands. The city is located in the province of North Holland, in the west of the country (Figure 4.1). As the capital city of the Netherlands, Amsterdam has a population of 851,373 within the city proper, 1,351,587 in the urban area, and 2,410,960 in the Amsterdam metropolitan area. The city consists of 22 areas with their own characteristics and urban morphology. These are the Centrum Oost, Centrum West, Oud Noord, Noord West, Oud Oost, De Pijp, Watergraafsmeer, Oud Zuid, Slotermeer, Slotervaart, Osdorp, Indische Buurt, Ijburg, Buitenveeldert, Westerpark, Westpoort, Oud Oost, Bos en Lommer, De Aker, Bijlmer Oost, Bijlmer Centrum and Driemond. Cycling is key to the city's character. As mentioned in previous chapter, 32% of the traffic movement is done by bicycle and 63% of the citizens use their bicycle on a daily basis (Veen, 2017). In 2013, there were about 1,200,000 bicycles in Amsterdam outnumbering the amount of citizens in the city (Wikipedia, 2017).

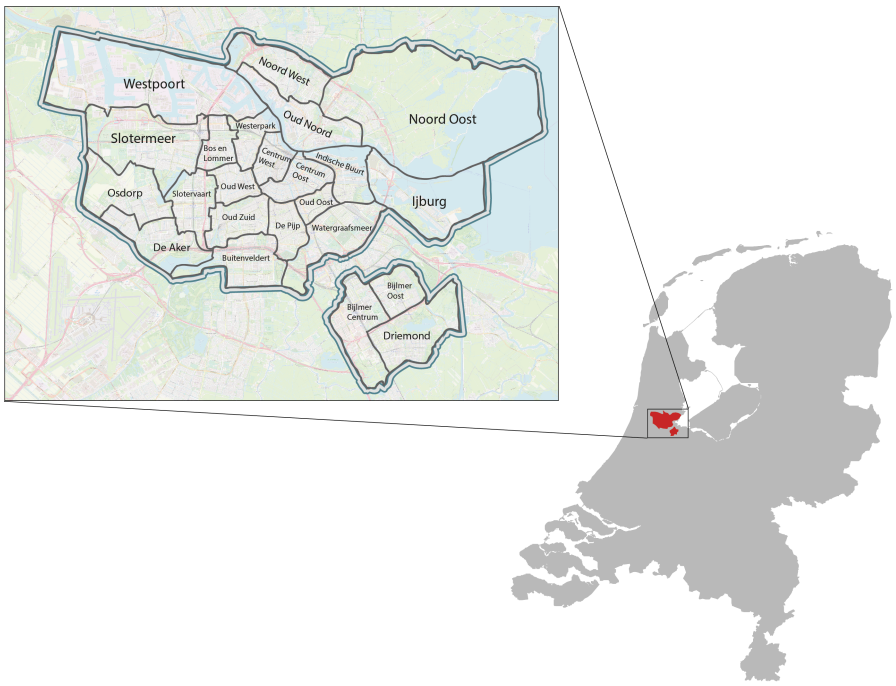

Figure 4.1: The city of Amsterdam, NL and the areas included.

4.1 GETTING TO KNOW THE CYCLISTS' ROUTES

Although this immense use of bicycles, there is limited knowledge on the bicycle movements and patterns in the Dutch cities. Fietstelweek organized

for that purpose. Fietstelweek occurs for one week in September during which cyclists can decide to track their routes using the Fiestel-app. In this way, they provide valuable information to the Dutch municipalities, organizations or/and universities. A part of the Fietstelweek dataset is becoming openly available through the homonymous website. The Fietstelweek dataset of 2015 used during this thesis to provide us with the GPS routes of the cyclists. The complete dataset was offered by the Department of Transport and Planning of the Faculty of Civil Engineering and Geosciences at TU Delft and with special permission by the Municipality of Amsterdam. Although later versions of the dataset exist, the one of 2015 has the advantages of being both pre-processed (cleaned and matched to the OSM street network) and available to the providers (permission of use).

The Fietstelweek dataset contains a total number of 10,500 cycling routes, where each route represented as point data. Because these point data rely on the OSM street network, no pre-processing was required. Each point in dataset described by attributes, such as the origin and destination neighborhoods of the route, the unique id of the route, and the OSM street segment that each point relies on (i.e. the wayID). Figure 4.2a shows all the attributes that describe a cyclist's point in the dataset. The origin and destination neighborhoods of the route are provided as the postal codes of the neighborhoods. Other information, such as the OD pairs, is not included in the dataset for privacy reasons. This means that each first and last point in the dataset does not reflect a real Origin-Destination pair. What it is known, however, is a point after the origin and a point before the destination of the cyclist's route. For simplification reasons, we consider these locations as our OD pairs.

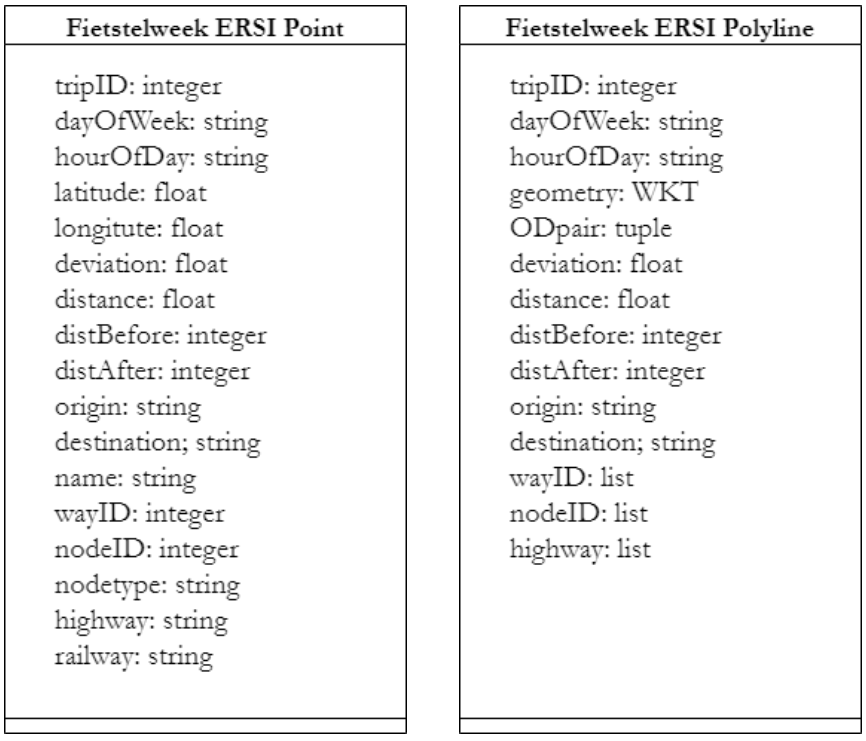

Figure 4.2: Stored attributes of the Fietstelweek data (a) Attributes of a cyclist's point. (b) Attributes of a cyclist's route.

The routes created by transforming the point data into polylines with a unique identity (i.e. tripID) in QGIS. Each polyline described by the attributes indicated in Figure 4.2b. These attributes inherited by the point data and adapted to the new geometry. A complete overview of the Fietstelweek routes represented in Figure 4.3.

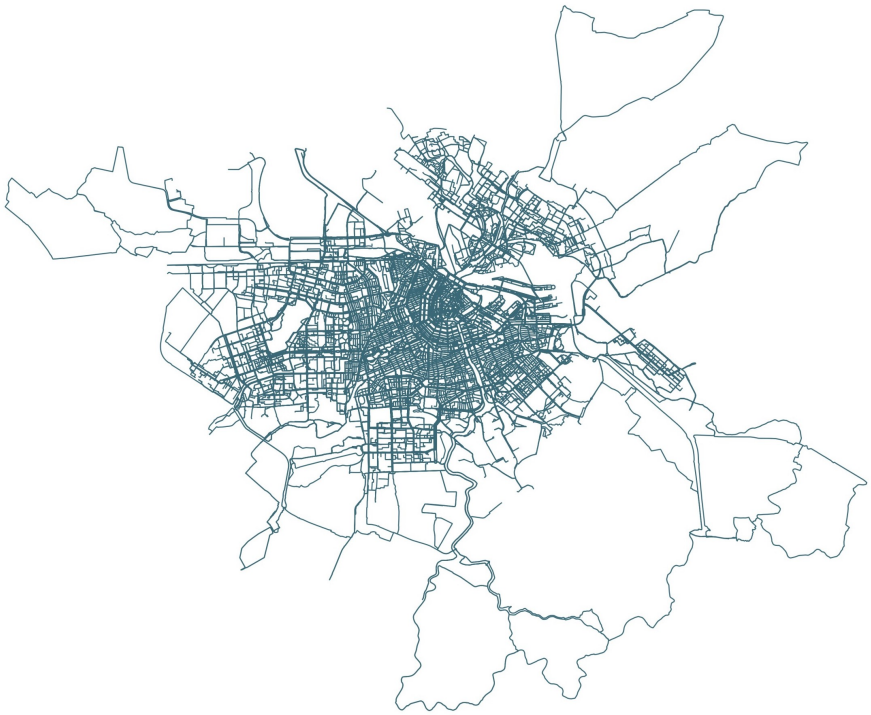

Figure 4.3: Cyclists' routes in the city of Amsterdam based on the Fietstelweek dataset of 2015.

4.1.1 Choosing the GPS routes

To get a better understanding of the way our cycling routes are distributed in the city of Amsterdam, the directions and the OD pairs of the routes examined. By geocoding the coordinates of the OD locations included in the Fietstelweek dataset, two different flow maps designed. The first type of flow maps examines the directions of the different trips and the origin and destination locations of the cyclists (Figure 4.4). This flow map reveals to which areas the cyclists tend to travel more when they are leaving a particular area. As Table 4.1 indicates, Centrum West and Oost and Indische Buurt are the most popular origin locations in our dataset. All of them have as most popular destination area Centrum Oost. On the other hand, the areas Centrum Oost, Oud Zuid and Oud Noord found to be the most common destinations of the cyclists.

Figure 4.4: Flow mapping of the cyclists' movements in the city of Amsterdam.

Table 4.1: Top 3 popular origin areas and destination areas in the city of Amsterdam based on the flow mapping of the Fietstelweek dataset 2015.

Origin Areas	Destination areas
Centrum West	Centrum Oost
Centrum Oost	Oud Zuid
Indische Buurt	Oud Noord

The second type of flow maps shows the most traversed areas in the city of Amsterdam (Figure 4.5). The difference from the previous flow maps is that this time only the routes with the same origin and destination areas investigated. The resulting map reveals that Centrum Oost is the most traversed

area of the city of Amsterdam. The Centrum West, De Pijp, and Watergraafsmeer areas are all following with a number of 52-124 trips, whereas areas such as Slotervaart and Oud Noord had no related information.

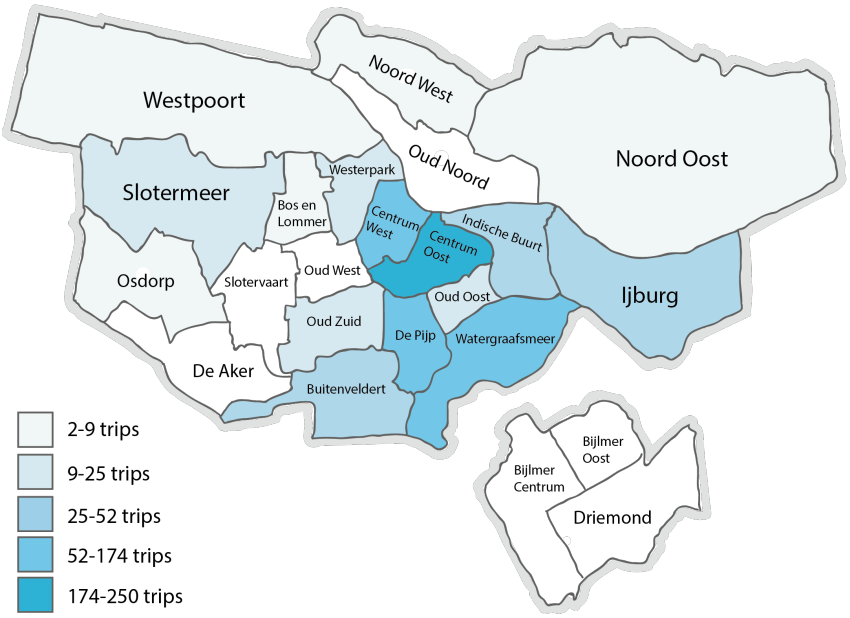

Figure 4.5: Cyclists' routes in the city of Amsterdam based on the Fietstelweek dataset of 2015.

The popularity of Centrum Oost for the cycling routes it was expected mainly because of the area's characteristics. Centrum Oost hosts major institutions, the National Maritime Museum, the Amsterdam Public Library, and the central train station. Newer parts of the city such as Oosterdokseiland can also be seen in the northern part of the area, which has lots of greenery and water. Moving southern to Centrum Oost one can find a less quiet part of the area that hosts cafes, bars but also theatres and other cultural facilities. Part of the south Centrum Oost, is the Grachtengordel neighborhood, the canal ring, which is more crowded and is characterized by the orthogonal and rational layout of its streets, canals, and blocks. Together with Centrum West, Centrum Oost combines the historic heart of the city of Amsterdam (Figure 4.6). Centrum West appears as the next popular area in the flow map. This area consists of five zones, each one with a unique character. For example, Haarlemmerbuurt accommodates restaurants, shops, and houses, Westelijke Eilanden is the base of warehouses and docks, the western part of Grachtengordel has museums and shops/restaurants/cafeterias, while Joordan gives a place for businesses and cafes. The morphology of the two areas exhibits differences in several neighborhoods. For example, the Joordan neighborhood of the western part of the center consists of blocks with narrow streets and historic buildings, whereas the Plantage neighborhood of the eastern part of the center described by more open space and greenery. The urban morphology of the center of Amsterdam depicted in Figure 4.7.

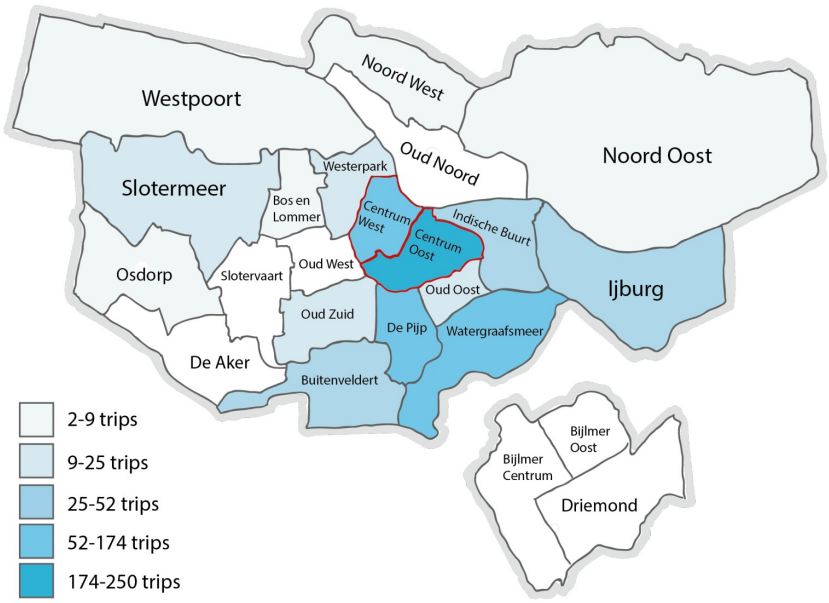

Figure 4.6: Amsterdam Centrum as the selected study area of the thesis.

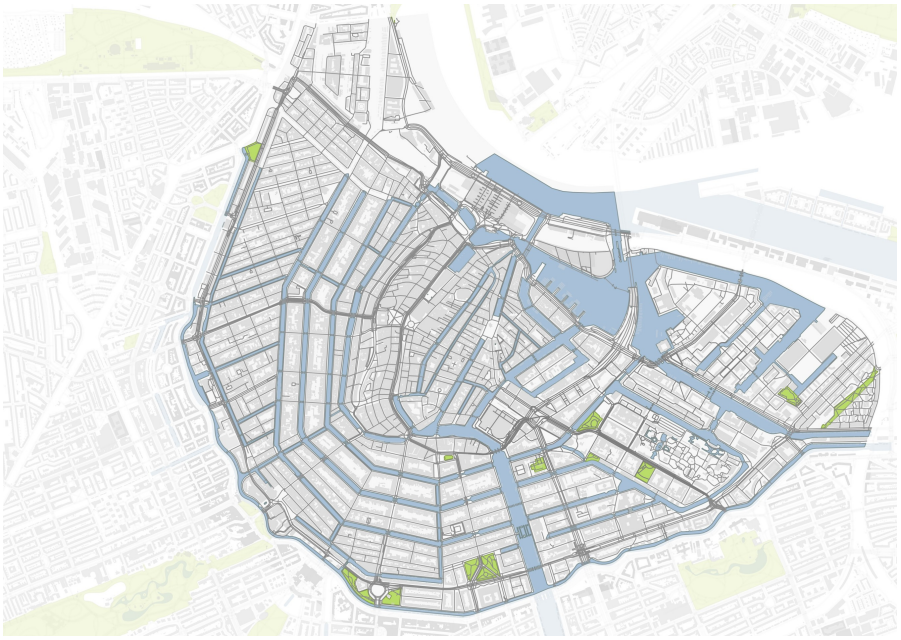

Figure 4.7: Representation of the center of Amsterdam and its urban morphology.

4.1.2 Calling for alternative routes

The OD pair of the GPS routes in Centrum Oost used to call the OSM alternatives via the Openrouteservice Directions API. As mentioned in chapter 3 (3.2.2), Directions API uses the POST method to return in JSON format up to 3 alternatives, under the user's request. These alternatives are the fastest, shortest or recommended by OSM routes. The request of the fastest route and the OSM response are both depicted as screenshots in Figure 4.8. The

response (encoded geometry), decoded to an ESRI polyline and stored in the database together with other information that described the route (i.e. settings). The resulting OSM alternatives represented in Figure 4.9. At first glance, we can see that OSM suggests routes which are using main streets and streets with bicycle lanes.

```
import requests

body = {"coordinates":[[4.905717,52.359085],[4.922028,52.37152]],"attributes":["avgspeed","detourf
actor"],"extra_info":["waycategory"],"preference":"fastest","geometry":"true"}

headers = {
    'Accept': 'application/json, application/geo+json, application/gpx+xml, img/png; charset=utf-8',
    'Authorization': '[redacted]'
}
call = requests.post('https://api.openrouteservice.org/v2/directions/cycling-regular', json=body,
 headers=headers)

print(call.status_code, call.reason)
print(call.text)
```

```
- "routes": [
- {
+ "summary": { /* 2 items */},
- "segments": [
+ { /* 5 items */}
],
- "bbox": [
4.90125,
52.358462,
4.922091,
52.371508
],
"geometry": "qkq~Hqc}\\dAdHBRBN?@WJHz@Db@z@bH@P@VC@a@JK@E@GB}DrAOFE_@QeBY}CAKWqB
- "way_points": [
0,
132
],
- "extras": {
+ "waycategory": { /* 2 items */}
}
}
],
+ "bbox": [ /* 4 items */],
- "metadata": {
"attribution": "openrouteservice.org | OpenStreetMap contributors",
"service": "routing",
"timestamp": 1555250057571,
+ "query": { /* 7 items */},
+ "engine": { /* 2 items */}
```

Figure 4.8: Example of a query and the response using the Openrouteservice API.

Figure 4.9: The OSM alternatives in Centrum Oost.

The rest of this chapter was mainly described with a specific GPS route taken as an example (Figure 4.10). Figure 4.11 pictures this example GPS route together with its fastest and shortest OSM alternatives. The recommended alternative matches the fastest route and for this reason is not represented on the map, although saved and analyzed as well.

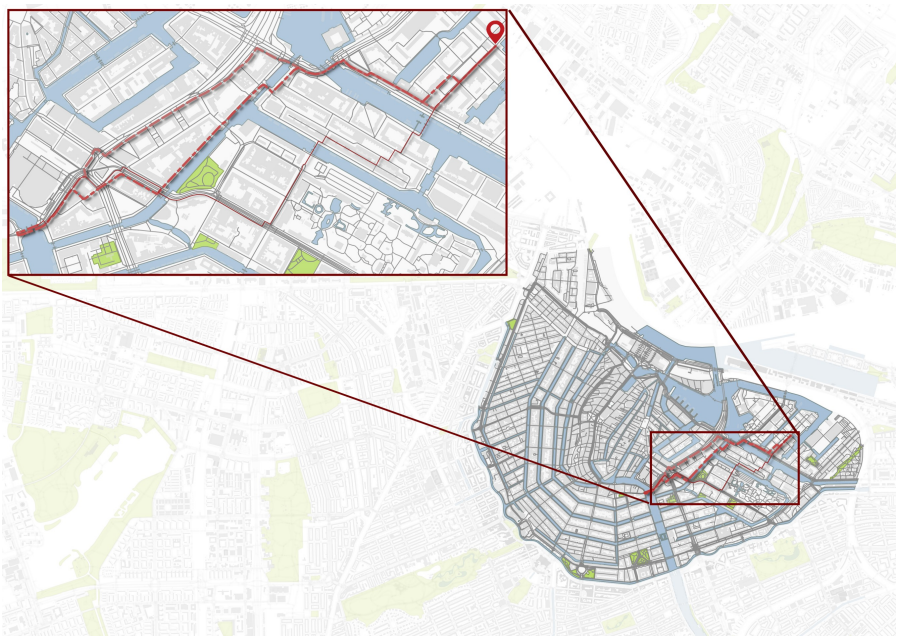

Figure 4.10: Location of the example GPS route and its alternatives in Centrum Oost.

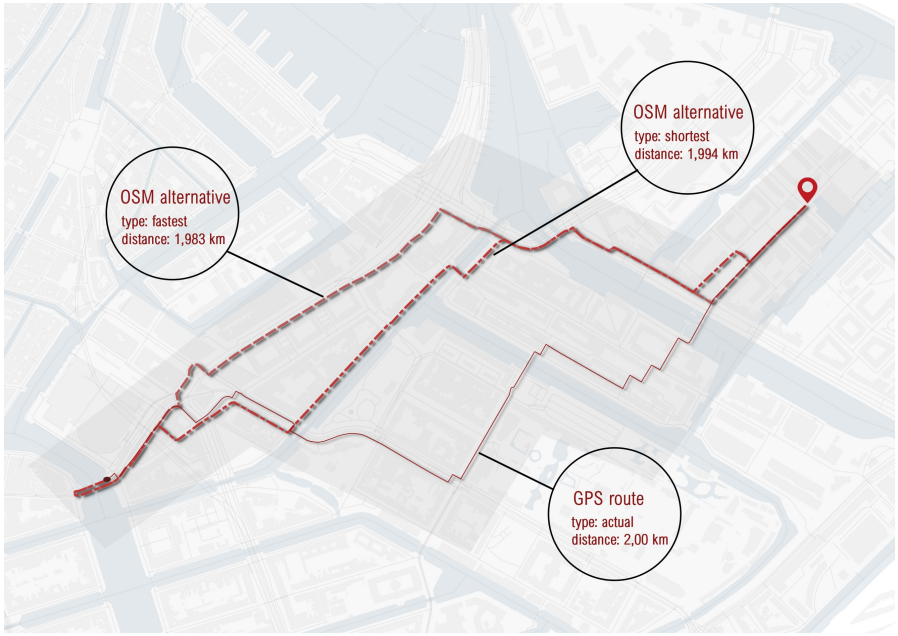

Figure 4.11: Information on the example GPS route and its OSM alternatives.

4.2 CREATING THE 3D ENVIRONMENT

This phase of the process includes the preparation of the OSM street network and the generation of the 3D buildings of Amsterdam Centrum. The preparation of the OSM street network consists of the filtration of the OSM street network, and its simplification by applying the rules and the methodology introduced in 3. The generation of the 3D buildings consists of the filtration of the building footprints and their extrusion using the building points of the LiDAR Point Cloud dataset. The output of this phase is the generation of the 3D center of Amsterdam on which the visibility analyses performed.

4.2.1 Preparing the street network of Amsterdam

The preparation of Amsterdam's street network starts by filtering and classifying the OSM street network of the whole center of Amsterdam. As mentioned before, the fact that the OSM alternatives use street segments of both parts of Amsterdam Centrum leaded to the decision of including in the analyses street segments of the whole center of Amsterdam. 4.12 shows the downloaded OSM street network clipped in the study area. The clipped street network consists of 6,086 segments and 26,426 nodes and the complete table with the information is shown in (Table 4.2).

Figure 4.12: The OSM street network clipped in the center of Amsterdam.

Table 4.2: Information on the OSM network. The units are in meters.

Network	Number of segments	Length										Number of nodes
		Min	Max	Mean	Median	StDev	Minority	Majority	1st Quartile	3rd Quartile	IQR	Coefficient of variation	
OSM	6086	0.10966	2487.01803	69.578810	32.083215	119.4276695	0.10966	3.38003	11.78447	79.20152	67.41704	1.71643	26426

Both the table and the figure indicates that the provided information is much more than needed and that a significant number of small segments were present in the whole street network. To reduce this information the classification of the OSM street network performed by filtering the 'highway' and 'access' tags. Table 4.3 reports the number of segments per highway tag and its significance to cyclists. Street segments tagged as ″construction″, ″platform″ and ″track″ removed from the dataset as non-relevant to our goal. Those tagged as ″unclassified″ remained in the dataset as the methodology also suggests. The second filtration on the remaining street segments performed based on the ″access″ tag as Table 4.4 indicates. In this context, street segments tagged as ″private″ or ″no bicycle use″ excluded from the dataset as well.

Table 4.3: Classification of the OSM street segments based on the ″highway″ id.

″Highway″ tag	Number of segments	Bicycle	″Highway″ tag	Number of segments	Bicycle
primary	84	(no)	pedestrian	487	(no)
primary_link	2	(no)	steps	159	
secondary	212	(yes)	track	1	no
secondary_link	4	(yes)	trunk	10	
residential	326	(yes)	trunk_link	4	
living street	5	yes	unclassified	1084	
service	415	(yes)	platform	1	no
tertiary	143		crossing	2	yes
path	16	yes	construction	3	no
cycleway	537	yes	null	1488	(yes)
footway	1101	(no)			

Table 4.4: Classification of the OSM street segments based on the ″access″ id.

″Access″ tag	Total number of segments	″Highway″: service	″Highway″: Unclassified	Bicycles
yes	25	2	2	1
no	294	217	11	8
customers	47	5		
permissive	26	8	1	8
private	187			
psv	2	2		
public	12			
restricted	14			
none	5473			88

The number of unnecessary nodes and by extent the small segments that are present in the street network simplified using the OSMnx package of Python. The resulting street network of this step contained orphan segments, duplicates and discontinues lines that needed geometry and topology correction. In addition, street segments smaller than 5m with naked nodes eliminated. As mentioned before, this is because most of the segments indicated small streets leading to houses (inrit). Afterward, the geometry of the street network cleaned and its topology built. Buffers of fixed distance equal to 10 meters created from the street segments of the street network. Each polygon buffer represented a street segment of the OSM street network as (Figure 4.13) indicates. The buffers dissolved into one polygon (figure b.) in order to get merged with the Urban Atlas polygon dataset.

Both the OSM and the Urban Atlas polygons were re-projected to the EPSG:102013 (European Conic projection) CRS in order to get the same projection of the datasets and to transform the units from degrees to meters.

The polygons of the ″Roads and associated land use″ data of the Urban Atlas dissolved in order to transform the initial three polygons into one polygon with all the information (Figure 4.13). A check of the validity of the polygons and existing duplicates in the dataset was a requirement in this step. The two polygon datasets (i.e. the Urban Atlas and the OSM network) merged and dissolved based on their geometry. Finally, the geometry of the polygons corrected and the topology built.

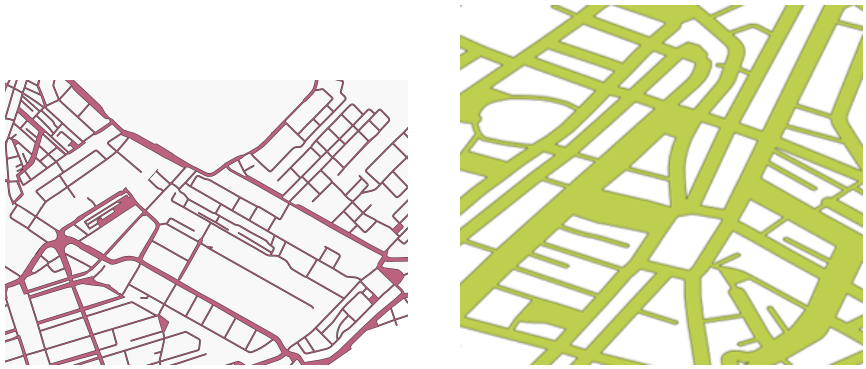

(a) Urban Atlas **(b)** OSM

Figure 4.13: Datasets with dissolved polygons.

To extract the centreline of the dissolved polygon, the Medial Axis algorithm used. The result of this step can be seen in Figure 4.14. The resulting network produced short dangled edges that required removal. The centreline was simplified using the Douglas-Peucker algorithm with a threshold of 5 meters. A clean of the geometry and topology of the final dataset was essential in order to eliminate duplicated geometries and pseudo nodes. From

the final simplified network, the intersections were found using the Space Syntax plugin of QGIS. The final output can be seen in Figure 4.16 and a comparison of the statistics between the initial OSM street network and the simplified street network is represented in Table 4.5.

Figure 4.14: Extraction of the centreline from the polygon.

Figure 4.15: Before the simplification process of the OSM street network.

Figure 4.16: After the simplification process of the OSM street network.

Table 4.5: Statistics about the simplified network and the OSM network

Statistics		Network	
		OSM	Simplified Network
Number of segments		6086	2701
Number of nodes		26426	5402
Length	Min	0.10966	9.0
	Max	2487.01803	624.0
	Mean	69.578810	77.80340
	Median	32.083215	62.0
	StDev	119.4276695	58.32972
	Minority	0.10966	9.0
	Majority	3.38003	28.0
	1st Quartile	11.78447	38.0
	3rd Quartile	79.20152	100.0
	IQR	67.41704	62.0

As a last step the simplified street network was checked with respect to the building footprints. In a few cases, the extracted polygon centreline appeared closed to building footprints; a case that could affect the results of the visibility analyses. These street segments corrected manually and the distance from the centroid of the buildings to the street network was calculated to ensure same distance of building-segment per segment. This step can be seen in Figure 4.17.

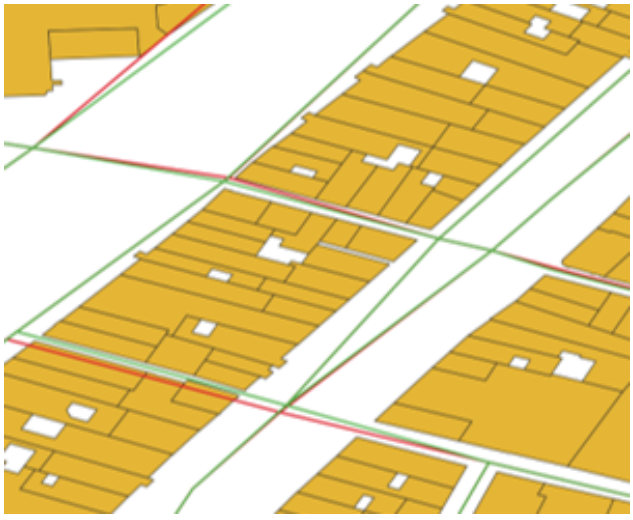

Figure 4.17: Correction of the street network based on the building footprints.

In order to make ready the simplified network for the visibility analysis, the street network was transformed to 3D. This was done by assigning the average height of the ground points of the AHN3 Point Cloud to the street segments.

4.2.2 Preparing the 3D buildings

For the creation of the 3D buildings, three national datasets used, namely the Basisregistratie Grootschalige Topografie (BGT), the Basisregistratie Adressen en Gebouwen (BAG) and the AHN3 LiDAR Point Cloud datasets. The first two datasets provided by the Publieke Dienstverlening op de Kaart

(PDOK) and used to obtain the building footprints. BGT constitutes the large-scale topographic map of the Netherlands that gives information on the buildings' location. The BAG dataset contains data for all buildings in the Netherlands that fall in the category of either premises, accommodation, number indication, public area, and residences. The data contain a number of attributes from which the gebruiksdoel (function) and bouwjaar (the year of construction) of the buildings were used during the filtration of the BGT buildings. On the other hand, the AHN3 LiDAR Point Cloud dataset used to assign the height information on the building footprints. AHN3 consists of an enormous number of 3D points where a classification is applied to the individual points. Each 3D point is assigned to one of the 5 classes: unclassified, ground, buildings, water and artifact. In this case, only the building points (classification code: 6) were relevant.

The BAG dataset and the BGT datasets used for the filtration of the building footprints in our study area. To avoid the presence of overlapping features in the BGT building layer, buildings with values in the eindregistratie field were filtered out. To get the bouwjaar and gebruiksdoel attributes that are part of the BAG layer into the BGT layer, the BAG building footprints were joined to the BGT building footprints based upon the identificatie field (Figure 5.5a). Once all the non-null eindregistratie features were filtered out, there were no mismatches in the join, and all buildings joined 1-1 perfectly. Finally, all BGT buildings with bouwjaar newer than 2015 were removed from the dataset ((Figure 5.5b). Although this filtration removed only a number of 11 buildings, it was necessary in order to avoid temporal mismatches with the Fietstelweek dataset.

After this step, a total number of 7171 building footprints remained in Amsterdam Centrum.

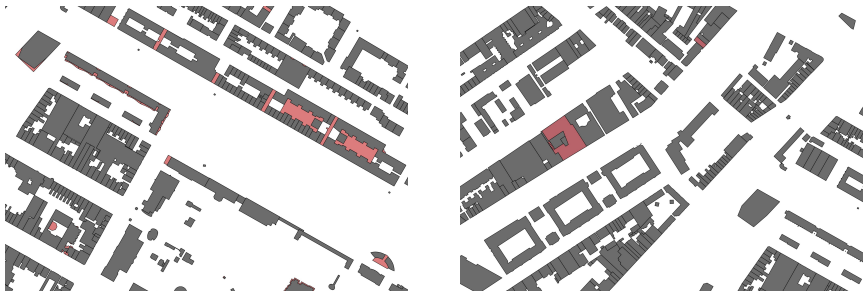

(a) Mismatches between BGT (grey) and BAG (orange).

(b) Building footprints created later than 2015 (orange).

Figure 4.18: Filtration of the building footprints.

The next step of this phase was the assignment of the height information on the building footprints. The output of this step is a collection of 3D buildings located in the area of Amsterdam Centrum. The process required to clean the noise of the AHN3 Point Cloud dataset, clip the dataset in the study area and thin it with an interval of 4 points in order to reduce the size.

The median elevation value of the "Building" (classification code 6) points within each building footprint computed and assigned as the elevation of the building footprints. A spatial database was created in PostGIS, and the building layer along with the class 6 LIDAR points imported into the database. SQL was used to compute the median elevation value for each building footprint and store these values in a new table. The median heights

within buildings were later exported and joined to the building footprints and stored as a newly created height field. Finally, the shapefile of the building footprints and their heights were imported into Grasshopper and extruded to B-reps based on the height field. The 3D buildings were checked for their validity and capped creating the 3D buildings of Figure 4.19.

Figure 4.19: Creation of the LoD1 buildings in the center of Amsterdam.

4.3 EXPLORING THE VISIBLE VIEWS

4.3.1 Categorizing the street network

All the street segments created a chart based on their length. The histogram of the lengths and their distribution are shown in Figure 4.20. Here we can see that the data are skewed to the left and the most values of the streets have a length of 28 meters.

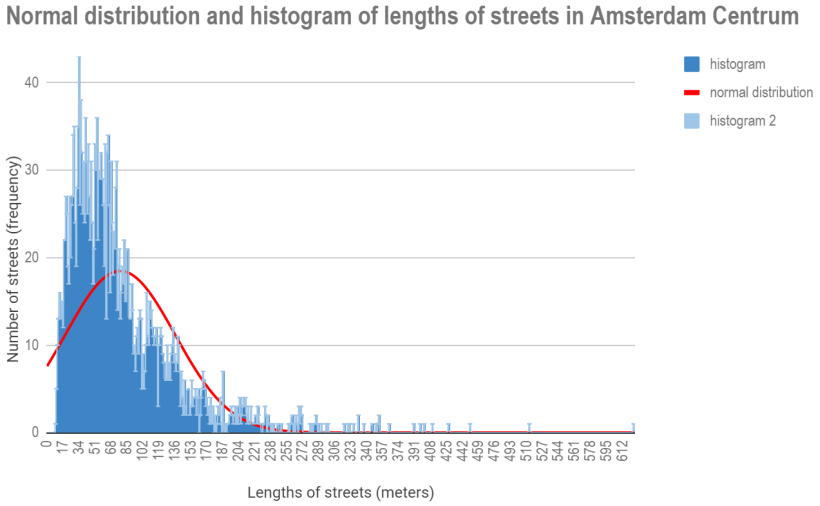

Figure 4.20: Histogram and normal distribution of the street segments based on their lengths.

In order to investigate what would be the most suitable number of observer's points per street segment, a categorization of the segments was

made. This categorization was based on the percentiles of the distribution. Every 20th percentile a new category of street segments was created. Because in the 20th and 80th percentiles, big differences of lengths existed between the street segments, two more percentiles (the 5th and the 95th) created as well. These percentiles included the extreme lengths of the dataset. In this context, the categories of the street segments formed as shown in Table 4.6 and the Figure 4.21.

Table 4.6: Categorization of the street segments based on the nth percentile.

Category	Percentile (Pi)	Lengths (m) intervals	Number of segments
A	P5	[5, 19)	145
B	P20	[19, 34)	411
C	P40	[34, 53)	550
D	P60	[53, 73)	518
E	P80	[73, 113)	549
F	P95	[113, 194)	405
G	P100	[194, 624]	136

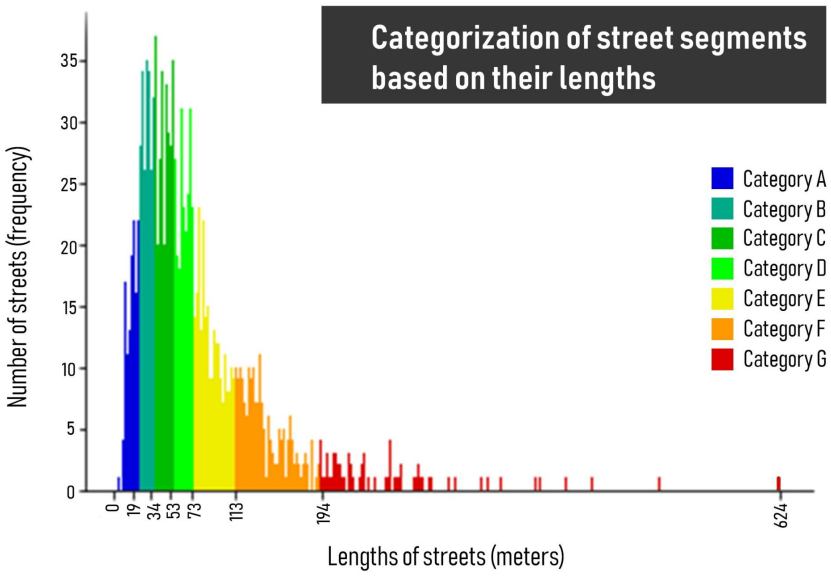

Figure 4.21: Histogram of street segments in the center of Amsterdam showing the categorization of them based on the percentile they belong to.

Both the histogram and the categorization of the segments show that the majority of the street segments belong to the categories C, D and E. In general, short segments can be seen in the heart of the centre of Amsterdam, whereas longer segments were found mainly in the Grachtengordel neighborhood, close to the train station and on the administrative boundaries of Amsterdam Centrum (Figure 4.22). Segments of the first category (Category A - [5m, 19m)) constituted mainly bridges and short paths of the same street, whereas segments of the last category (Category G - [194m, 624]) highways and primary/main streets.

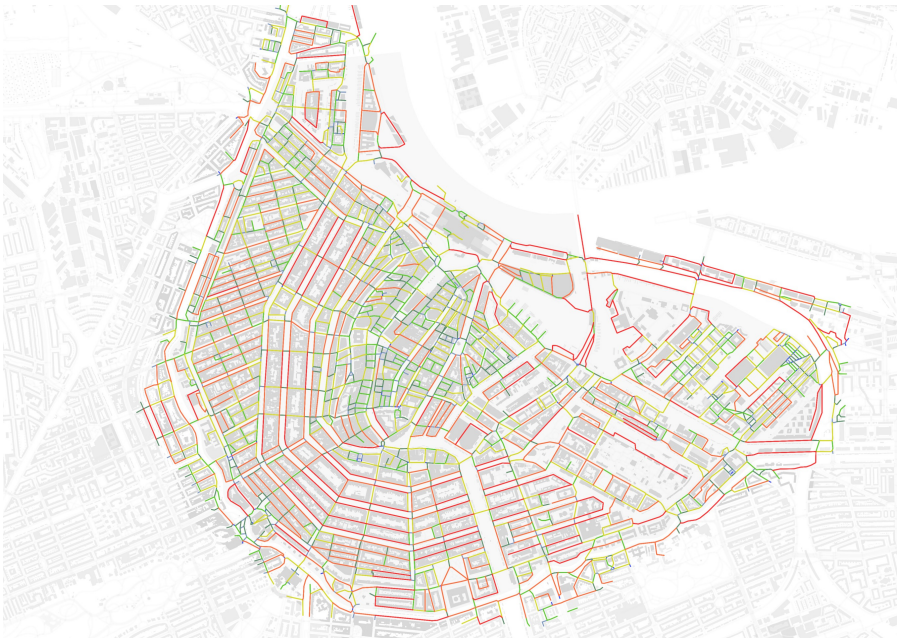

Figure 4.22: Representation of the categories of the street segments in Amsterdam Centrum based on their lengths.

4.3.2 Setting the maximum distance

This paragraph describes the decision on the maximum distance used to describe the view of an observer's point and a whole segment as well. A street segment in the street network starts from an intersection and ends in the next intersection. These intersection points used as the first and last points of each segment. This means that although duplicates of the intersection points may exist (at least two street segments share the same point), the points maintained in the data for two reasons. The first reason is that the direction of the different points on an intersection was changed based on the direction of the street segment and secondly because they represented the entry to- and the exit from- the street segment.

Three possible maximum distances used to test the visibility from an observer's point; a 150m, a 100m and a 50m distance. Considering the fact that all street segments (length independently) needed to have the same maximum distance to ensure the lack of bias, a maximum length value that was smaller than 50m was not taken into consideration. This is because street segments would require a big amount of observer's points that could increase the computation time. For this test 50 street segments were used as a smaller sample in order to reduce the computational time. This sample includes streets from all 7 categories with segment lengths between 7m and 450m.

- 1st case: 150 meters maximum distance Setting the maximum distance to 150m, a good result can be seen regarding the percentages of visible buildings in the intersections of high density streets. This result was expected since the ray intersects a number of buildings. May the rays extend to the horizontal axis, however it creates a realist result for the point. What affects the result and let us decide that this distance is not considered suitable for the network is how the length affects the percentage of the visible sky. In cases with segments that belong to

the Categories A, B and C, and especially short segments of the Category A such as bridges the visible sky is highly affected by buildings that belong to other streets or buildings just at the end of the bridge. Regarding the computation time, running 50 points with maximum distance 150m took 45 minutes approximately.

- 2nd case: 100 meters maximum distance Similar results as the previous case, could be seen also when setting the distance to 100 meters. Here, the Categories A,B were the most sensitive to a non representative percentage of sky, although were already more improved than the first case. However, because of the incomplete representation of the visible views, this case considered unsuitable for the analyses as well. Regarding the computation time, running 50 points with maximum distance 100 meters took 35 minutes approximately.

- 3rd case: 50 meters maximum distance A maximum distance of 50 meters considered the best of the three options for all categories and types of streets. Even for smaller street segments, with different street profiles, the distance succeeded to capture the difference between sky, buildings and ground and represented in a satisfying way the street. The quality of the results for smaller street segments that exist in the street network but not in the sample data, will be ensured by adding a midpoint in each of these street segments. Regarding the computation time, running 50 points with a maximum distance of 50 meters took 26 minutes approximately.

4.3.3 Granularity

Having decided on the maximum distance of the visibility analysis from an observer's point, a granularity test performed in order to decide on the number of observer points that each category of segments should have. Four different cases of streets were taken into account for this decision, namely 1) a street with water/canal nearby or a bridge, 2) a street that goes through a park and passes near a park, 3) a street with low buildings' density and 4) a street with high buildings' density.

The table Table 4.7 summarizes the results of the granularity together with the reasoning of the decisions and the information on the categories of the street segments. This analysis performed by trying different number of observer's points and checking how the results correspond to each case. Google street view used to check our results as well. For most of the categories, one can see that the street segments going through or nearby a park require in general less points in order to describe the street segments, possibly because of the limited changes in the environment. For example, even if a building is included in the park this can be captured in the result as well. Furthermore, the rest of the street cases had a role on the granularity. This decision took into consideration both the percentages of sky, buildings and ground, as well as the kurtosis (i.e. the sudden differences in the visible views). The kurtosis values could capture the points close to intersections, the points with a building in a park and other changes in the street profiles. The moment that the results stopped revealing new information (e.g. Category F with 6 points on park) or altered the street profile (e.g. Category G: 8 points in high density streets or Category C with 4 points in bridges), the decision could be made.

Table 4.7: Granularity for the street segments in the center of Amsterdam per category of segments.

Category	Percentile (Pi)	Lengths (m) intervals	Number of segments	Granularity	Reasoning
A	P5	[5, 19)	145	3 pts	It succeeds to capture the cases of water (bridges), high and low density streets. The case of park needs an extra point.
B	P20	[19, 34)	411	4 pts	It succeeds to capture the cases of water (bridges), high and low density streets. The case of park needs an extra point.
C	P40	[34, 53)	550	4 pts	It succeeds to capture the cases of water (bridges), high and low density streets. The case of park needs an extra point.
D	P60	[53, 73)	518	5 pts	It succeeds to capture the cases of water (bridges), high and low density streets. The case of park can be captured with 4 pts.
E	P80	[73, 113)	549	5 pts	It succeeds to capture the cases of park, water (bridges) and low density streets. The case of high density streets can be captured with 4 pts.
F	P95	[113, 194)	405	6 pts	It succeeds to capture the cases of parks, high and low density streets. The case of water (bridges) can be captured with 5 pts.
G	P100	[194, 624]	136	8 pts	It succeeds to capture the cases of water (bridges), high and low density streets. The case of park can be captured with 7 pts.

As an example, a street segment of Category G with high density of buildings is described. The street is called Nieuwe Kerkstraat and it has a length of almost 220 meters. Figure 4.23 shows both the location of the street on the map and a picture of the Google street view.

Figure 4.23: Nieuwe Kerkstraat was assigned to Category G.

On this street, different numbers of observer's points tested and each test formed a different case. All cases can be seen in Figure 4.24. All graphs until the one with 6 points, so a loss of valueable information regarding the percentages of visible sky, visible buildings and visible ground, as well as, regarding the kurtosis values. Although the case that we assign to the street segment with 6 points could give an indication of the street profile, it again failed to capture the differences that the kurtosis value could reveal. Between the last two graphs with 7 and 8 points respectively, the graph with 8 points indicated in a clearer way the moment that the cyclist entered the intersection (point 7 on graph) but also showed a better stability of the kurtosis until that moment. In this context, it represented better the street profile and the potential existing differences on the heights of the buildings. For these reasons, the case of 8 observer points on Nieuwe Kerkstraat considered the best choice. A similar thinking process on the graphs followed for all the cases and categories. The granularity test for each category of street segments can be found in **??**.

Figure 4.24: Granularity on Nieuwe Kerkstraat.

4.3.4 Running the visibility analyses

For the implementation of the visibility analysis the ray tracing algorithm used for each observer's point as explained in Chapter 3. Based on the maximum distance and the granularity test performed in the previous step, the radius of the sphere set to 50 meters. The sphere cut, capped, transformed to an approximation of a mesh and subdivided based on the suggested resolution. Furthermore, the sphere cut based on a horizontal angle of 124 degrees and a vertical angle of 90 degrees with regards to the human vision and its representation in the created 3D environment. By cutting the skydome, the cone was created. Rays traced from every observer's point to the skydome and the intersections of rays and both the 3D buildings and the ground found using C. Eventually, the points of the cut skydome and the intersection points formed the rays of Figure 4.25.

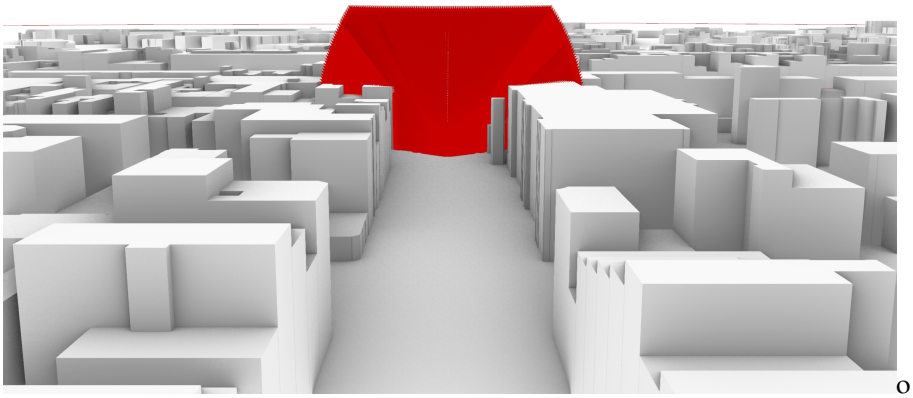

Figure 4.25: 3D isovist created by the rays to the sky, the buildings and the ground.

4.4 OUTPUT

As mentioned also in the methodology, the list of the lengths of the rays and the number of hits to an element of the 3D environment used to compute our metrics. These metrics were either describing the spatial openness (a. the percentages of sky, b. buildings and c. ground, d. building:sky ratio, e. building:ground ratio and f. sky:ground ratio) or the shape of the 3D isovist per observer's point (a. median, b. kurtosis, c. standard deviation). The way these metrics computed is provided in Section 3.4.

4.4.1 Getting the first metrics

In this step, the spatial openness and the shape of the 3D isovist per observer's point calculated and later aggregated to a street segment level. The main aim of this process was to get one value for every metric in order to describe a street segment. The metrics of the mean and standard deviation of the length of the rays and those describing the spatial openness aggregated using the geometric mean. The kurtosis values aggregated by using the standard deviation method and the street profiles by finding the mode value. The complete table of the used aggregation methods and the reasoning behind these decisions can be found in Section 3.4.3). The aggregation of the values per observer's point performed in Python and stored in the database for further analyses.

This step produces interesting outputs in a street network level that provide a description of the streets in the center of Amsterdam and a brief validation of the procedure. Following, the percentages of the visible sky, the visible buildings and the visible ground, and the street profiles for the street network of Amsterdam Centrum are introduced. The rest of the metrics are available on Appendix B.

Figure 4.26 shows the percentages of the visible sky per street segment. As expected, the least amount of the visible sky is essentially found in the heart of the city center and in the western part of Amsterdam Centrum that is characterized by denser lots. On the other hand, the main streets (such as those towards the central train station) and also streets nearby canals scored the biggest amount of the visible sky.

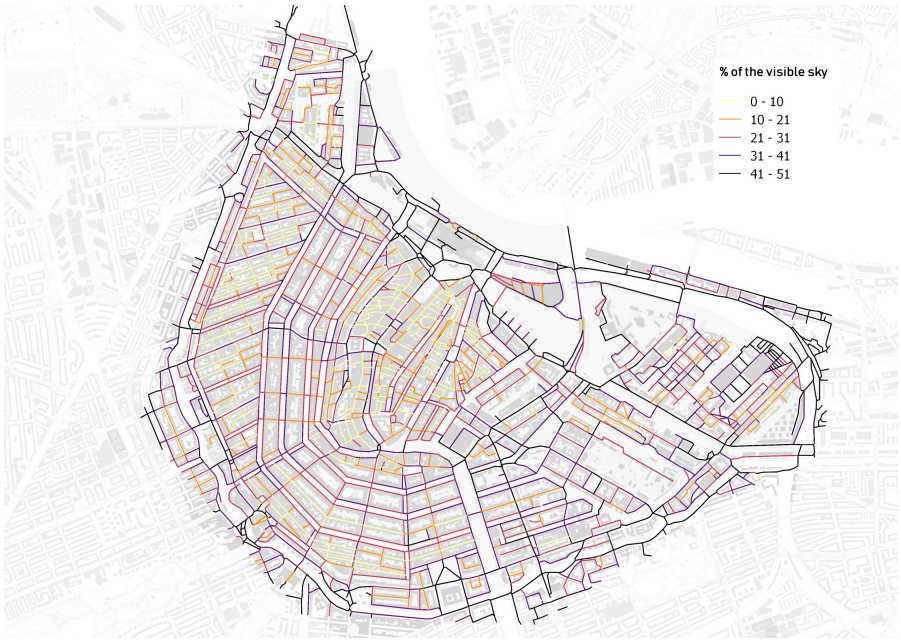

Figure 4.26: Percentage of the visible sky per street segment in the center of Amsterdam.

Furthermore, high percentages of the visible buildings can be found in the biggest part of the Amsterdam's center. However, main streets on the administrative boundaries of the center and streets near or inside parks found to score the lowest amount of visible buildings. Figure 4.27 represents how the street of Amsterdam Centrum scored regarding the values of the visible buildings.

Figure 4.27: Percentage of the visible buildings per street segment in the center of Amsterdam.

Similarly to the amount of the visible buildings, the percentages of the visible ground are high in almost all the center of Amsterdam. The higher values however, found in street segments that represent bridges or streets near the canals. Figure 4.28 depicts the percentages of the visible ground in Amsterdam Centrum.

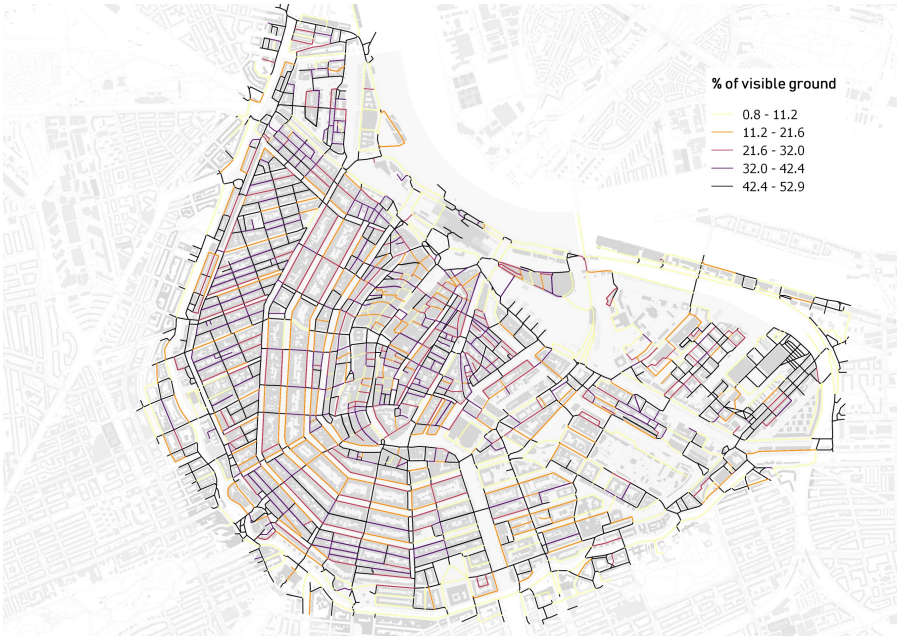

Figure 4.28: Percentage of the visible ground per street segment in the center of Amsterdam.

The last map is visualizing the results of the street profiles in Amsterdam Centrum. Interestingly, we see significant deviations between the way that the values describe the street profiles and the way we defined the street profiles in Section 3.4.2. As seen in Figure 4.29 many street segments in the center of Amsterdam correspond to an ideal street profile, something that is not true in reality. The fact, however, that narrow street segments and street segments located in the heart of Amsterdam Centrum scored as either street profile 6 or 7, shows a potential of the use of the metric as a descriptor of the spatial openness. This potential of use, however, requires the redefinition of the used aggregation method and/or the way that the street profiles are translated to values in the future. Because the aggregated street profiles failed to capture the whole street network are excluded for now from the rest of the analyses.

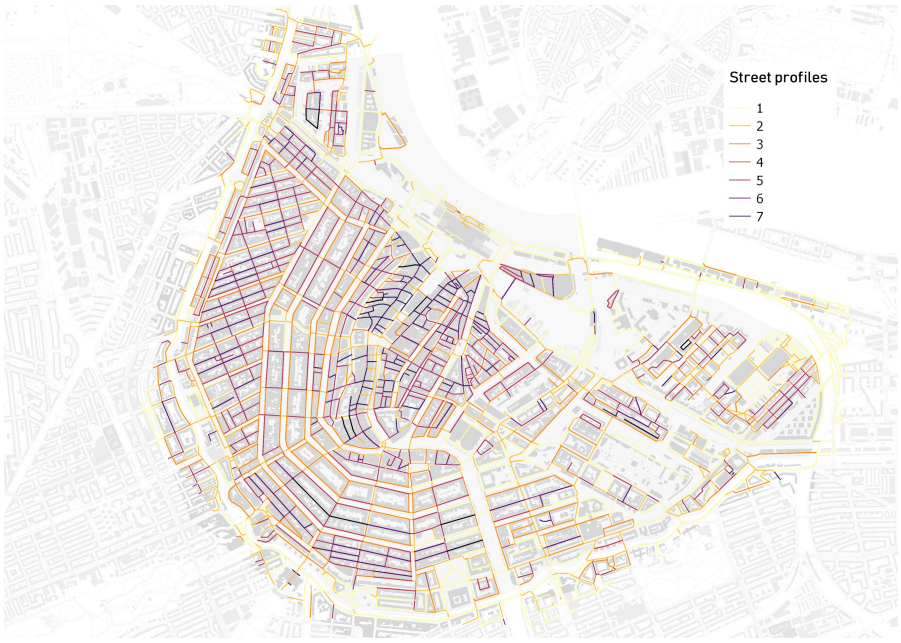

Figure 4.29: Street profiles of the street segments in the center of Amsterdam.

4.4.2 Visible views in a route level

All the metrics computed in the previous step needed to be assigned to the GPS and alternative routes. This assignment was required in order to have only two values of each metric per route and so, to be able to compare the different types of routes in the next phase.

To do this, the segment matching performed beforehand between the routes and the street segments. Furthermore, the HausdorffDistance computed with a threshold of 0.1 in order to match the routes with the closest street segments of the street network. The output of this step is a table that contains a. each route (ID and geometry), b. the street segment IDs that the route matched on and c. all the metrics computed for the particular street segment ID.

For each route, all metrics (except the street profiles) aggregated by calculating the median and the standard deviation of the values. The output of the aggregation is a table with the metrics for each route. A screenshot of this table is represented in the Figure 4.30 below. The interpretation of this output is further discussed in the next chapter.

tripid integer	median_sky double precision	Std.Dev_sky double precision	median_blds double precision	Std.Dev_blds double precision	median_grd double precision	Std.Dev_grd double precision	median_kurtosis double precision	Std.Dev_kurtosis double precision	median_median double precision	Std.Dev_median double precision	median_stDev double precision	Std.Dev_stDev double precision
583355313	37.64053093	9.881262743	13.09038075	12.79632207	47.18296895	5.282846727	0.119533986	0.908967076	21.18355174	11.85934794	21.00282264	1.753844923
583547983	32.05523011	13.98992161	19.31017207	16.23135044	45.34726209	7.671030937	0.196155746	1.426435813	16.04261876	10.01230302	20.15365019	4.748306016
584244033	29.84223853	11.82134499	22.54540586	15.80861606	44.70199862	2.485896957	0.244490623	0.457363693	12.15415634	11.26972269	20.39363364	2.348997148
589116080	32.64939025	12.08311047	19.19265313	18.33938592	46.08772936	10.19524142	0.237758016	1.698547411	20.56537877	9.967593521	20.60144892	3.238388006
591512884	33.58011556	11.38745835	17.2268856	16.54079242	44.6577443	6.651303594	0.22673725	1.382636793	17.27140157	9.760459815	20.27029994	2.125045794
591580491	30.32346469	9.707456108	23.56762264	10.00460894	44.35916673	2.65330954	0.310727912	0.74810825	12.8372377	6.17868658	20.32278367	2.577535443
591715484	26.56294392	14.08391437	26.54951826	16.27295718	45.76667277	1.984365877	0.404776325	0.549683823	15.85736771	12.75072295	19.57399762	3.098697902
592027612	34.76089046	11.13848614	18.11236513	13.98469113	46.04947328	5.413157797	0.140565556	0.457418839	19.76870996	11.8924107	20.76082419	1.942725989
592384567	32.64939025	8.585108165	20.65952309	11.80300989	45.42860168	5.706384237	0.271370564	0.433086591	14.46335789	7.015141418	20.37836804	1.787975144
593403756	32.90347903	9.38123872	21.08872122	13.0426178	46.04947328	5.912795894	0.185977638	0.432267618	14.13435302	7.950560979	20.56388902	1.923901482
595859229	31.4810827	10.21051027	22.75613533	11.78074173	44.55569599	3.33909482	0.220040903	2.42210808	12.77540654	8.969963649	20.3577974	2.872475478
596424426	31.12088163	8.031986122	21.48969393	11.22085627	44.81938517	2.227508311	0.203100887	0.319122422	12.45802433	5.175462354	20.44812221	1.968024911
596598382	32.59899525	11.82057568	21.08872122	17.76041186	46.08772936	9.855867347	0.199749869	1.644915996	20.08679697	9.169091879	20.38819946	3.101919138

Figure 4.30: Aggregated metrics per route in Amsterdam Centrum.

4.5 SYNTHESIS

This chapter described the application of the methodology in the city of Amsterdam, the Netherlands. The center of Amsterdam (Centrum Oost and Centrum West) selected as the main area to be examined after investigating the cyclists' GPS routes provided by the Fietstelweek dataset of 2015. The GPS routes analyzed only for Centrum Oost, although the street network of all Amsterdam Centrum used in the visibility analyses. The OSM street network of the center of Amsterdam simplified until the point that the street network consisted of segments and nodes at the real intersections. The simplification methodology for the street network leaded to a reduction of 3,385 street segments and more than 15,000 nodes from the initial OSM street network. The 3D environment created by using three national datasets, the BGT and BAG that provided the building footprints and the AHN3 Point Cloud dataset which gave the height information of the buildings. After the end of the data preparation, the visibility analyses performed repeatedly based on the lengths of the street segments. The output of the analyses which aggregated in a street segment and a route level will be discussed in the next chapter.

5 RESULTS

This chapter aims to communicate the resulting visible views of our example routes (GPS and alternatives) in a qualitative and statistical way. Qualitatively, the three core metrics that define spatial openness (i.e. % of the visible sky, % of visible buildings and % of the visible ground) displayed for the whole street network of Amsterdam Centrum. On the other hand, the ANOVA statistical method explored potential differences between the GPS routes and the alternatives acknowledging all metrics but discussing only those found significant between the routes. The output of this chapter is the base on which the discussion of Chapter 6 has formed.

5.1 QUALITATIVE ANALYSIS

For the qualitative analysis, the aggregated metrics: a. % of the visible sky, b. % of the visible buildings and c. % of the visible ground have investigated. The effect of these metrics on the cyclists' route choices is analyzed on the street network of Amsterdam Centrum. In a street network level, the qualitative analysis aims to discover possible differences between the street segments traversed by cyclists based on the GPS routes and those that were not selected. The charts bollow depict the results in the whole street network of Amsterdam Centrum.

Figure 5.1 depicts the differences on the percentages of the visible sky between the selected and the non-selected street segments. At first glance, we can see that the selected street segments have a higher amount of visible sky, although not significant differences exist. Figure 5.1 shows the selected street segments and the non-selected streets in the street network. Although, it is clear that the cyclists chose to follow the streets with higher percentages of sky, the data cover the biggest part of the center of Amsterdam and so it is difficult to extract conclusions. Street segments that were not selected, are mainly located at Centrum West and a few close to the train station. This was rather expected since no GPS routes were selected from the eastern part of the center of Amsterdam.

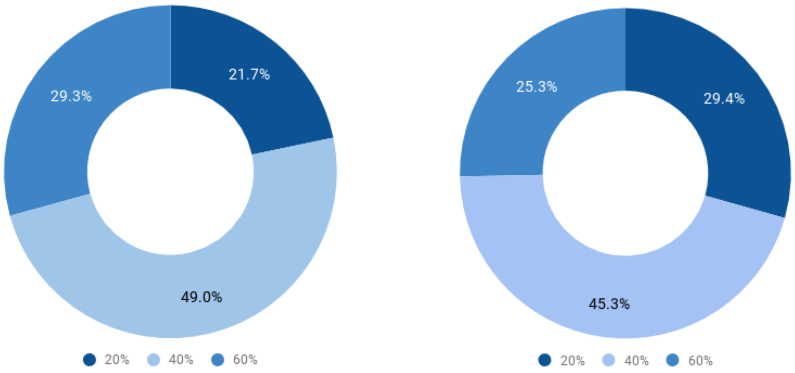

(a) Selected **(b)** Not selected

Figure 5.1: Percentage of visible sky in the street network of Amsterdam Centrum. The used data correspond to the aggregated output per street segment.

Figure 5.2: Representation of the percentage of visible sky in the street network of Amsterdam Center. The traversed street segments by the cyclists are represented with thick lines.

The second chart regarding the percentages of the visible buildings reveals a variation on the amount of buildings at the chosen street segments and differences between specific intervals as well (Figure 4.26). It seems that cyclists tended to follow streets with a low density of buildings (0%-20%) and avoid streets with higher density of buildings (above 40%). However, when the cyclists had to pass through the heart of the center of Amsterdam they did not avoid narrow or highly dense streets that may let them reach directly their destination (Figure 6.7).

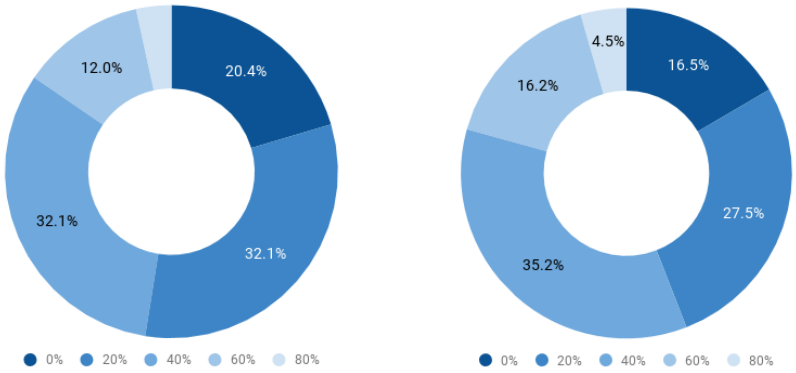

(a) Selected **(b)** Not selected

Figure 5.3: Percentage of visible buildings in the street network of Amsterdam Centrum. The used data correspond to the aggregated output per street segment.

Figure 5.4: Representation of the percentage of visible buildings in the street network of Amsterdam Center. The traversed street segments by the cyclists are represented with thick lines.

The last chart indicates the percentages of the visible ground in the street network of the center of Amsterdam Figure 4.26. Here the output is similarly high in both cases. However, cyclists would slightly prefer to go through streets with visible ground between 40% and 60% than from streets with lower value of ground. Having a look at the map of Figure 5.6 we can see that cyclists traversed mainly streets that belong to the Grachtengordel neighborhood (which is characterized by the ring canals) and even when they were traveling through the heart of the center, they selected streets with higher values of the visible ground. Finally, when we compare the three maps, we can see an importance of the visible ground on the selection of the street segments. In addition, we can assume that a higher level of

detail to represent the visible ground can potentially give an indication of the morphology of the center of Amsterdam.

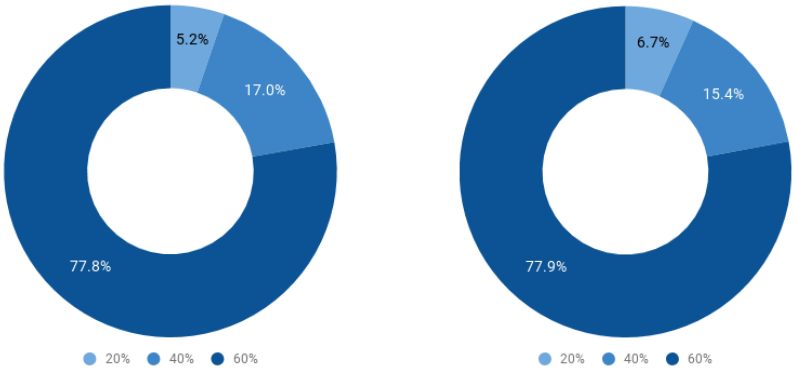

(a) Selected **(b)** Not selected

Figure 5.5: Percentage of visible ground in the street network of Amsterdam Centrum. The used data correspond to the aggregated output per street segment.

Figure 5.6: Representation of the percentage of visible ground in the street network of Amsterdam Center. The traversed street segments by the cyclists are represented with thick lines.

5.2 STATISTICAL ANALYSIS

One-way ANOVA analysis used in SPSS to perform the multiple comparison tests between N=227 GPS routes and their alternatives (the fastest, the shortest and the recommended OSM routes). All these routes assigned as the grouping variables of the analyses and coded as follows:

- 1 = GPS route
- 2 = Fastest route
- 3 = Shortest route
- 4 = Recommended route

From all the metrics defined in the previous chapter, the following dependent variables are described here as being the most significant results:

- StDev of Sky,
- StDev of Buildings,
- StDev of Ground,
- StDev of Standard deviation of length of rays,
- StDev of ratio buildings/sky,
- StDev of ratio buildings/ground, and
- Distance

To perform the statistical analysis it is important to adjust two settings beforehand. The first setting refers to the weights of the grouping variables. As discussed also in 4.5, the coefficient of the routes coded to -3 for the GPS, to +1 for the fastest routes, to +1 for the shortest routes and to +1 for the recommended routes. The Post Hoc test set the Tukey's and the Games-Howell test. The overview of all settings can be seen in Table 4.5.

SPSS output of Figure 5.7 represents the Levene's test of homogeneity of the variances or in other words, it explores whether the variances of the four groups have significant differences between them. We can see from the table that the a. standard deviation of the sky, b. the standard deviation of the buildings, c. the standard deviation of the ground and d. the distance appear to be identical. On the other hand, Levene's test appears to be significant for a. the standard deviation of the median, b. the standard deviation of the standard deviation, c. the standard deviation of the ratio blds:sky and d. the ratio blds:ground, all with p_i=0.05. This values indicate that the variances of our groups are significantly different. As [Field] indicates that this result requires rectification since it violates one of ANOVA's assumptions. The Welch's or/and the Brown-Forsythe's test could be used instead.

Test of Homogeneity of Variances

		Levene Statistic	df1	df2	Sig.
Std.Dev_sky	Based on Mean	.831	3	904	.477
	Based on Median	.662	3	904	.575
	Based on Median and with adjusted df	.662	3	887.539	.575
	Based on trimmed mean	.772	3	904	.510
Std.Dev_blds	Based on Mean	.707	3	904	.548
	Based on Median	.542	3	904	.654
	Based on Median and with adjusted df	.542	3	893.273	.654
	Based on trimmed mean	.664	3	904	.574
Std.Dev_median	Based on Mean	5.116	3	904	.002
	Based on Median	3.536	3	904	.014
	Based on Median and with adjusted df	3.536	3	831.094	.014
	Based on trimmed mean	4.303	3	904	.005
Std.Dev_stDev	Based on Mean	5.506	3	904	.001
	Based on Median	4.537	3	904	.004
	Based on Median and with adjusted df	4.537	3	889.622	.004
	Based on trimmed mean	5.293	3	904	.001
Std.Dev_bldssky	Based on Mean	24.352	3	904	.000
	Based on Median	10.608	3	904	.000
	Based on Median and with adjusted df	10.608	3	636.889	.000
	Based on trimmed mean	17.283	3	904	.000
Std.Dev_bldsgrd	Based on Mean	12.841	3	904	.000
	Based on Median	4.486	3	904	.004
	Based on Median and with adjusted df	4.486	3	821.177	.004
	Based on trimmed mean	10.392	3	904	.000
distance	Based on Mean	4.539	3	904	.004
	Based on Median	1.611	3	904	.185
	Based on Median and with adjusted df	1.611	3	537.024	.186
	Based on trimmed mean	2.255	3	904	.081

Figure 5.7: Differences between the GPS and alternative routes regarding the variations in buildings:sky.

Table 5.1 shows the ANOVA summary which is divided into the *Between Groups* effect and the *Within Groups* effect. This table reveals of whether statistically significant differences exist in the four groups. The *Combined* field of the *Between Groups* shows the complete effect and so it gives the significance and the F-ratio of the variable. The *Within Group* show the "unsystematic variations within the data" [Field]. The results of this table are discussed in the next paragraphs per each segment.

Table 5.1: ANOVA summary table.

Variable		Mean Square	F	Sig	Sum of Squares	df
StDev sky	Between Groups	26.017	4.207	.006	78.052	3
	Within Groups	6.185			5591.105	904
StDev buildings	Between Groups	62.343	3.363	.018	187.030	3
	Within Groups	18.536			16756.626	904
StDev ground	Between Groups	8.182	.618	.604	24.546	3
	Within Groups	13.243			11971.828	904
StDev stdev	Between Groups	7.072	9.664	.000	21.217	3
	Within Groups	.732			661.567	904
StDev buildings:sky	Between Groups	22.961	12.008	.000	682.784	3
	Within Groups	1.912			1728.523	904
StDev buildings:ground	Between Groups	13.015	4.821	.002	39.044	3
	Within Groups	2.699			2440.228	904
StDev median	Between Groups	27.953	3.982	.008	83.858	3
	Within Groups	7.020			6430.039	904
Distance	Between Groups	36778067.8	38.400	.000	68409200.4	3
	Within Groups	957764.334			865818958	904

Furthermore, regarding the standard deviation of the sky, we see a significant difference between the groups in the mean standard deviation of the visible sky as determined by one-way ANOVA **(F= 4,207 , p=0.006))**. However, at this point is still uncertain the exact way that the groups affected by the significance of the mean standard deviation of the visible sky. This is revealed on the post hoc Tukey's test of Table 5.2. The comparison shows that there is a significant difference between the GPS route and the fastest alternative (**p=0.019**), the shortest alternative **(p=0.036)** and the recommended alternative of **(p=0.013)**. *This means that the cyclists tend to follow routes with larger variations in the visible sky.*

Table 5.2: Multiple comparison test regarding the standard deviation of the visible sky.

	(I) Type of route	(J) Type of route	Sig.	95% confidence Lower Bound	95% confidence Upper Bound	Mean difference (I-J)	Standard Error
StDev sky	1	2	.019	.079725437	1.28136485	.68054514	.233435371
		3	.036	.029154687	1.23079410	.62997439	.233435371
		4	.013	.110051168	1.31169058	.71087087	.233435371

Significant difference between the groups can be seen also on the mean standard deviation of the visible buildings with **(p = 0.018)**. The Tukey's Post Hoc test of Table 5.3 shows that difference exist between the GPS route and both the fastest **(p = 0.046)** and the recommended alternatives **(p = 0.045)** but not with the shortest routes. *This means that the cyclists tend to follow routes with more variations in the visible buildings when routes are not the shortest.*

Table 5.3: Multiple comparison test regarding the standard deviation of the visible buildings.

	(I) Type of route	(J) Type of route	Sig.	95% confidence Lower Bound	95% confidence Upper Bound	Mean difference (I-J)	Standard Error
StDev blds	1	2	.046	.013705958	2.09397087	1.0538384	.404120743
		3	.051	-.00422951	2.07603540	1.03590295	.404120743
		4	.046	.014075283	2.09434020	1.0542077	.404120743

The mean standard deviation of the visible ground between the routes is not significant difference between the routes with **p = 0.604**. The multicomparison test is represented in Table 5.4.

Table 5.4: Multiple comparison test regarding the standard deviation of the visible ground.

	(I) Type of route	(J) Type of route	Sig.	95% confidence Lower Bound	95% confidence Upper Bound	Mean difference (I-J)	Standard Error
StDev grd	1	2	.686	-.50137764	1.25697345	.377797904	.341584450
		3	.604	-.45683703	1.30151405	.422338511	.341584450
		4	.830	-.58836065	1.16999043	.290814888	.341584450

For the rest of the variables we assume unequal variances between the four groups and so we are discussing them based on Games-Howell Post Hoc test.

Furthermore, the mean standard deviation of the standard deviation is considered significant difference of the routes as determined by the one-way ANOVA with **p = 0.000**. The Games-Howell test show big differences between the GPS route and all 3 alternatives (Table 5.5). *This means that the cyclists tend to follow a route with less homogeneity in the built environment.*

Table 5.5: Multiple comparison test regarding the standard deviation of the standard deviation.

	(I) Type of route	(J) Type of route	Sig.	95% confidence Lower Bound	95% confidence Upper Bound	Mean difference (I-J)	Standard Error
StDev StDev	1	2	.000	.167811501	.581155962	.37448373	.080297980
		3	.000	.155674372	.569018833	.36234660	.080297980
		4	.002	.101212859	.514557320	.30788509	.080297980

The mean standard deviation in the ratio buildings:sky is also a significant difference between the routes with **p = 0.000**. In this context, GPS routes tend to have a higher mean ratio of buildings:sky than all three other alternatives (Table 5.6). *This means that the cyclists tend to follow routes with higher variations in the ratio buildings:sky.*

Table 5.6: Multiple comparison test regarding the standard deviation of the ratio buildings:sky.

	(I) Type of route	(J) Type of route	Sig.	95% confidence Lower Bound	95% confidence Upper Bound	Mean difference (I-J)	Standard Error
StDev Blds:sky	1	2	.000	.308518970	1.04412329	.67632113	.142459082
		3	.000	.308231255	1.03551950	.67187538	.140825590
		4	.016	.062779336	.887490191	.47513476	.159875883

On the other hand, the mean standard deviation of the ratio buildings:ground is significantly different with **p = 0.007**. The ratio buildings:ground is higher in the GPS routes than the fastest and the shortest routes but not significantly different that the recommended routes (Table 5.7). *In general, this means that the cyclists tend to follow routes with higher variations in the ratio of the buildings and the ground but not when the route is a recommended.*

Table 5.7: Multiple comparison test regarding the standard deviation of the ratio buildings:ground.

	(I) Type of route	(J) Type of route	Sig.	95% confidence Lower Bound	95% confidence Upper Bound	Mean difference (I-J)	Standard Error
StDev Blds:grd	1	2	.007	.098577001	.892430873	.49550394	.154217290
		3	.005	.120571814	.914425686	.51749875	.154217290
		4	.079	-.02807067	.765783200	.368856264	.154217290

Finally, the mean distance appear to be one of the most significant differences between the routes with **p = 0.000** based on the one-way ANOVA analysis. According to the Games-Howell Post Hoc test (Table 5.8) *the cyclists tend to follow routes longer in their distance than faster, shorter or recommended alternatives.*

Table 5.8: Multiple comparison test regarding the distance of the GPS and alternative routes.

	(I) Type of route	(J) Type of route	Sig.	95% confidence		Mean difference (I-J)	Standard Error
				Lower Bound	Upper Bound		
Distance	1	2	.000	.074003251	.917004624	.49550394	.163411323
		3	.000	.113054485	.921934015	.51749875	.156754641
		4	.000	.08194246	.819654994	.368856264	.174812547

5.3 SYNTHESIS

This chapter provided a description of the output of the visibility analyses in a qualitative and a statistical way. The qualitative analysis performed in a street network level with the aim to find differences between the selected street segments and the non-selected street segments in the center of Amsterdam. These differences were referring to the core metrics that describe the spatial openness (i.e. the percentages of the visible sky, the visible buildings, and the visible ground). The analysis showed a preference towards street segments with more visible sky and ground, as well as street segments with lower buildings' density. On the other hand, the statistical analysis performed using the ANOVA method and the Tukey's and Games-Howell Post Hoc tests in order to identify potential differences between the GPS and OSM alternative routes. A sample of N=227 GPS routes showed that the cyclists of our dataset tend to follow less homogeneous routes with higher variations of the visible sky, visible buildings, ratio of buildings: sky, ratio of buildings:ground, as well as routes longer than their alternatives. The next chapter provides a further discussion on these results and presents possible applications of them in the urban design process.

6 DISCUSSION

This chapter aims to provide a discussion on the results of the qualitative and the statistical analyses as these reported in Chapter 5. The GPS route that introduced as an example in Chapter 4 is used here to provide a reflection on the results Figure 6.1. Together with the reflection, the chapter gives suggestions on potential applications of the results as urban design guidelines.

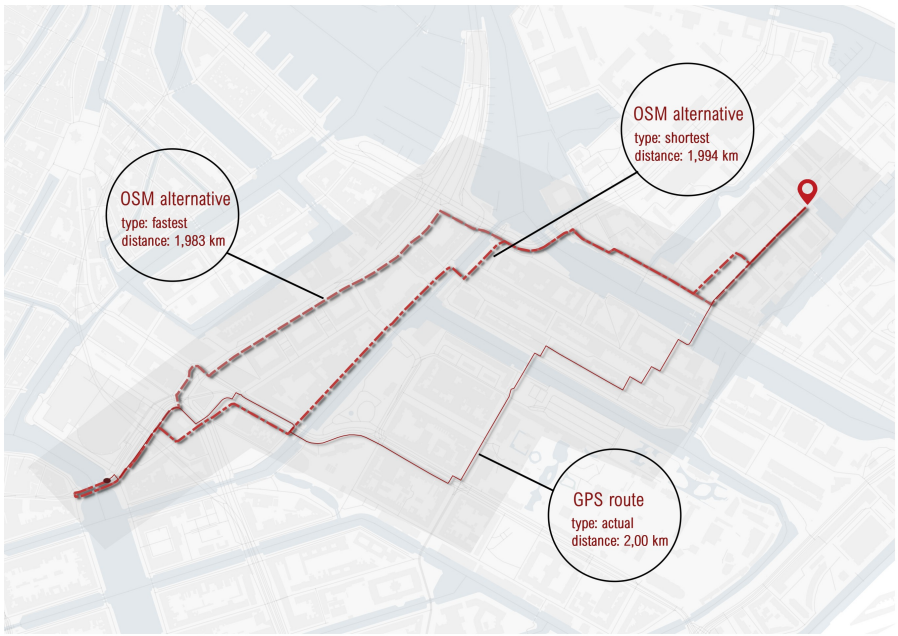

Figure 6.1: Information on the example GPS route and its OSM alternatives.

Both the statistical and qualitative analyses showed existing differences between the routes in the street network and route level. These differences are related to either metrics that define the spatial openness or metrics that describe the shape of the 3D isovists. An additional variable, the distance of the routes, added in the analyses in order to compare the GPS and the OSM alternatives. Distance appeared to be one of the most significant differences Figure 6.2. Eventually, the cyclist is the one that chooses longer routes, something that is depicted also in our example. This fact has addressed extensively by related studies and attributed to the fact that cyclists have often a different perception of their travel distance than the actual one. Either because it is a cycling routine or not, this result illustrates that the planning of cyclists' accessibility in the street network should be designed without considering only the shortest or the fastest routes.

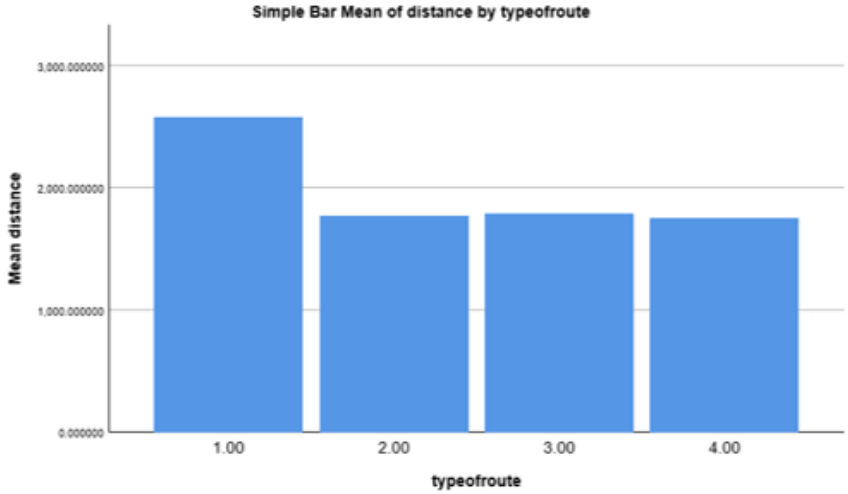

Figure 6.2: Differences between the GPS and alternative routes regarding the mean distance.

In the street network level, the cyclists seem to choose streets segments with higher amount of visible sky and less amount of visible buildings. Of course, they would not avoid to cross narrow streets and streets in densely built lots in the heart of Amsterdam Centrum in order to reach their destinations. In addition, variations of the amount of sky Figure 6.3 and the amount of the buildings Figure 6.4 found to affect the route choices of the cyclists in the city of Amsterdam. At this moment, we can assume that the second choice of the cyclist (except of the actual GPS route:1) would be the shortest OSM route (#3). Although these variations are statistically significant, they slightly differ between the GPS routes and their corresponding alternatives Figure 6.3. Another possible reason is that the cyclist made his choice influenced by factors such as the directness of his route or the possible avoidance of the traffic, meaning that deeper exploration of their significance is required.

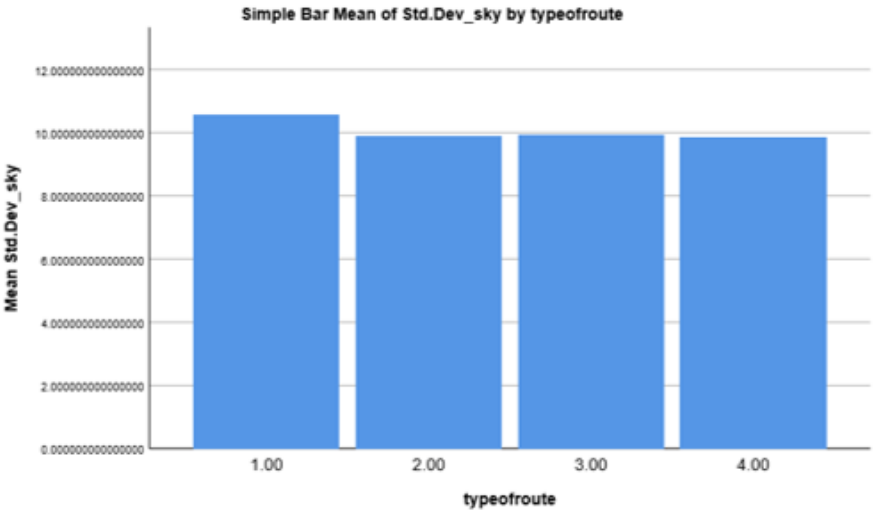

Figure 6.3: Differences between the GPS and alternative routes regarding the mean variations of the visible sky.

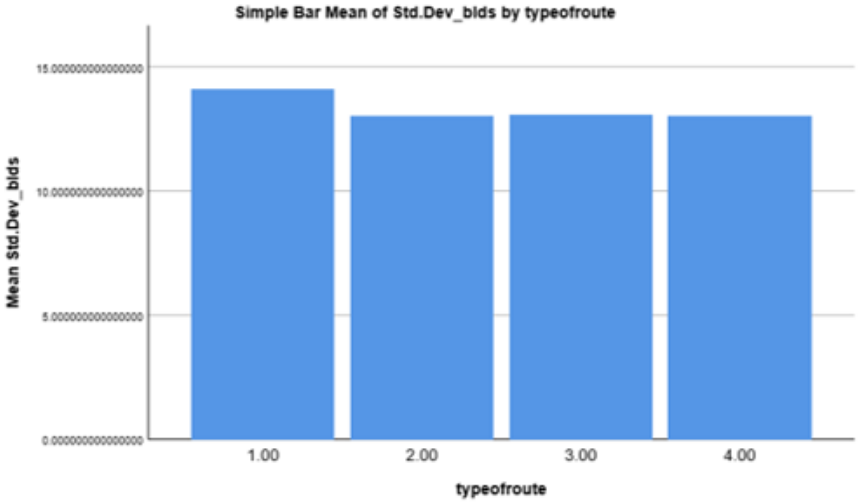

Figure 6.4: Differences between the GPS and alternative routes regarding the mean variations in the amount of visible buildings.

Furthermore, variations of the two ratios buildings:sky and buildings:ground found significant for the cyclists' route choices when the OSM alternative is not recommended. This means that the variations in the density of the buildings a street are important to a cyclist in order to decide on a shorter or faster OSM route. These observed differences are much higher than the before mentioned variables and so we could conclude that the variables that describe the spatial openness are more important to a cyclist when seen in relation to each other.

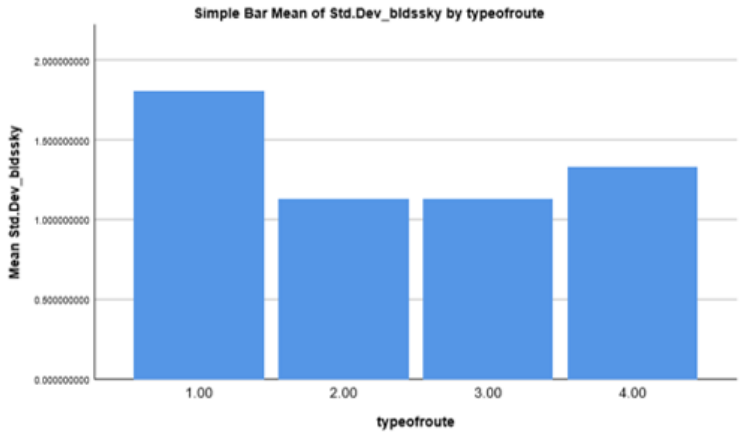

Figure 6.5: Differences between the GPS and alternative routes regarding the mean variations in buildings:sky.

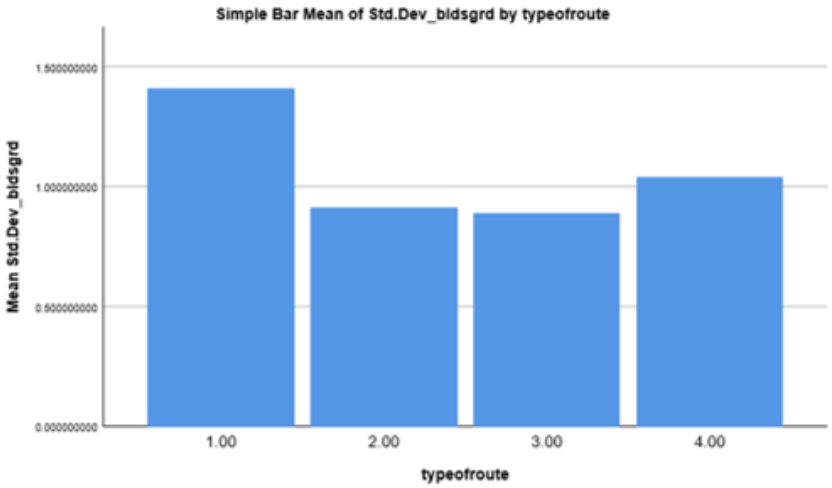

Figure 6.6: Differences between the GPS and alternative routes regarding the mean standard deviation of the % of the visible ground.

An interesting output of both analyses is the insignificant effect of the amount of the ground or the variations of the ground on the cyclists' routes or segments choices. This appears contradictory to prior studies that found the importance of the road infrastructure on cyclists' route choices. A possible explanation of this result relates to the way that the ground is represented in the methodology, meaning that a higher level of detail is required in order to extract conclusions. Furthermore, rather than the amount of visible ground, what possibly matters to the cyclist is elements of the ground such as the quality of the road, the existence of greenery and the canals.

An important difference between the GPS and the OSM alternatives is related to the homogeneity of the routes. Furthermore, cyclists seem to prefer routes with different street morphology per street segment. In our example, the cyclist follows a more natural movement in the space, with lots of turns and variations regarding the built environment. He crosses parks, bridges, narrow streets in building blocks until he reaches his destination. This lack of homogeneity of the GPS routes are also described as statistically significant variable for the route choices of the cyclists. The fastest and shortest routes although are more direct and organized with bicycle lanes on the main streets, are avoided by the cyclist.

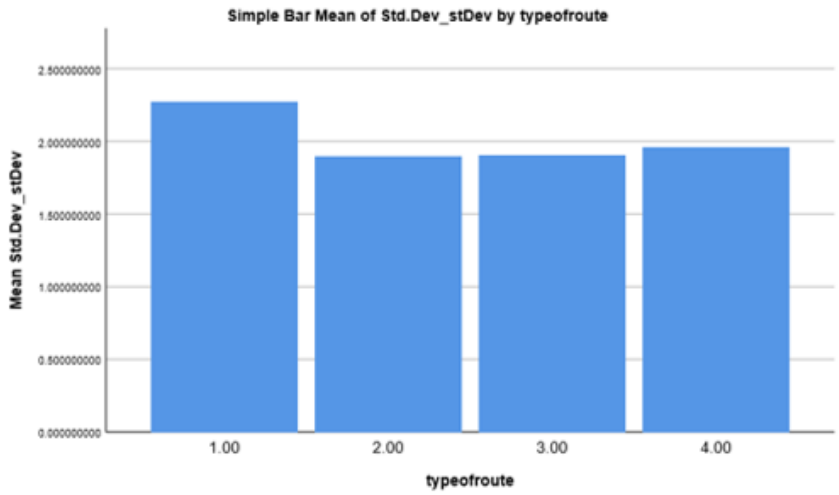

Figure 6.7: Differences between the GPS and alternative routes regarding the mean standard deviation of the % of the visible ground.

7 CONCLUSION AND FUTURE RESEARCH

7.1 CONCLUSION

This MSc Thesis project aims to describe the influence of the visible views of the urban environment on the route choices of the cyclists. For this purpose, actual GPS routes compared with their OSM alternatives using a geospatial approach that was based on the creation of 3D isovists. Parts of the approach includes the preparation for the research, the data collection, the processing and the simulation. In this context, three different categories of metrics introduced to describe the spatial openness, the street profiles and the shape of the 3D isovists. A post processing of these metrics was necessary in order to analyze the results both qualitatively and statistically.

The proposed methodology applied on the city of Amsterdam, the Netherlands, in order get a better insight of its advantages and limitations. The study area selected due to the availability of the GPS dataset, the Fietstelweek 2015, and because of the popularity of the cycling activity in the city. Flow mapping used to investigate the cycling movements which restricted the study area even more, to the level of Amsterdam Centrum. The alternative routes acquired via the Openrouteservice API owed by OSM and its contributors.

Instead of applying the visibility analysis on the GPS and OSM routes, the whole street network of Amsterdam used for this purpose. In this way, a deeper understanding of the morphology of the city center regarding the visible views and the choices of the cyclists gained. Although the numerous advantages of the OSM street network, the type and the number of the included information and also the topology and geometric issues required the filtration and simplification of the street network under pre-defined rules. The level of simplification is the point of having street segments and nodes that represent real intersections. The processing performed in Postgis, QGIS and Python. The simplified street network reduced the number of street segments for more than 50% and the nodes to more than 20,000. The street network is represented by the centreline of two merged polygon datasets, the OSM and the UA. The centerline corrected based on the location of the building footprints.

Although the extraction of the centreline succeed to give a representation of the real network, it limited the visibility analyses and specifically the position of the cyclist on the street. This means that bicycle lanes were not taken into consideration and, for this reason, we have no overview of the way this adaptation affected the results.

The street segments of the simplified network were categorized according to their lengths. The categorization of the street segments performed by defining one category every 20^{th} percentile, as well as two additional percentiles (the 5^{th} and the 95^{th}) to include the extreme length values. Based on these seven categories and the maximum length of the visibility, a granularity test performed. The granularity test aimed to place a specific number of observer's points per category of street segments; a number that could

succeed in giving a representative overview of the visible views from the observer's points. The number of points selected per category gave a satisfying output. However, after the granularity check we found different categories of street segments that could be described with the same number of points. These categories should be redefined and/or combined.

Next, the 3D environment was required as input of the visibility analysis. The BGT and BAG datasets used to get and filter the building footprints, while the AHN3 dataset used to assign the height information on the buildings. The building footprints transformed to B-reps of LoD1. This selected LoD1 represented in a satisfying way the building forms but lead to misinformation regarding tunnels or arcs that exist in the center of Amsterdam.

The visibility analyses performed into the Rhino 3D/Grasshopper environment. Four different elements used as input to the environment, the skydome, the plane that represented the ground, the B-reps buildings and the 3D street network. The ray tracing performed using C with the aim of tracing rays to the skydome and the intersections to the other elements. The process is quite fast but in narrow streets with high density of buildings, possible null values created. This required the filtration of the output and the repetition of the visibility analysis for the unsuccessfully implemented observer's points and so further adaptations are required.

The output of the visibility analyses defined two different categories of metrics, the spatial openness and the shape of the 3D isovist. The core metrics of the spatial openness used to identify 7 different street profiles which assigned as metrics as well. All the metrics aggregated per observer's point, however the street profiles produced different results than excepted. Furthermore, the mode as the selected aggregation method for the street profiles is considered unsuitable and the metric needs to be redefined.

The metrics aggregated for second time, but here on a route level. GPS and OSM alternatives matched on the street network and the metrics join on the routes. Although all these aggregations required, they resulted to loss of information, meaning that one should consider other possible techniques/methods for the aggregation.

The qualitative analysis of the results performed only on the core metrics that describe the spatial openness and with the aim to compare the selected with the non-selected street segments. Although no significant information revealed regarding the amount of visible ground, cyclists seem to choose routes with higher amount of visible sky and an average/low amount of visible buildings.

The ANOVA statistical analyses showed a significance of the distance, the variations and the lack of homogeneity on the cyclists' route choices. It also showed the importance of the spatial openness, when the metrics combined. ANOVA is a useful method to find differences between routes, however is comparing the routes using every dependent variable separately. This means that possible use of another statistical method, such as MANOVA should be discussed.

In a nutshell, the methodology showed satisfying results on characterizing the 3D built environment based on the visibility analyses and the 3D isovists. However, certain adaptations and corrections are still needed.

7.2 DISCUSSION ON THE RESEARCH QUESTIONS

- Which determinants of the urban environment that have been identified in prior studies can be implemented in the current research?

  An extensive list of determinants has been identified in the literature regarding the urban environment. These determinants can belong to different subcategories such as the road infrastructure, the network infrastructure, the scenery/aesthetics etc. Since building forms are part of the urban environment and shape the movements and patterns of people, we decided to use it as the main determinant of the current project. The analyses showed that buildings are important to a cyclist's route choices especially when seen together with the visible sky or the visible buildings.

- How the cyclists' route choices will be examined?

  The cyclists' route choices were examined by comparing actual GPS routes provided by the Fietstelweek dataset of 2015 and the OSM alternatives. This comparison was based on the visibility analyses performed on a number of observer's points. The formation of the observer's points performed with respect to the simplified version of the OSM street network. The two different datasets were mapped on the street network and the output of the visibility analyses was assigned to the routes. The ANOVA statistical method with the Games-Howell's and Tukey's Post Hoc tests performed in order to compare the GPS with the alternative routes.

- What is the added value of the point cloud as a method for investigating the visibility of cyclists in an urban environment, compared to the use of other 3D and 2D data?

  The added value of the point cloud in the project is the the height information that assigned to the building footprints. The point cloud used for the creation of the 3D environment, adding realism to the visible views.

- What is the role of space syntax in the current research?

  The space syntax methodology was used in different ways in the project. The most important was the measurement of the 3D environment by using 3D visibility analyses and the notion of the 3D isovist. Space syntax tools were used also for identification of the overpasses/underpasses during the simplification of the street network.

- Which cyclists' routes should be used for the current research and how they can be filtered?

  The cyclists' routes from the Fietsetweek dataset of 2015 were used for the city of Amsterdam. These routes filtered based on the origin and destination location and their direction. The most traversed area, Centrum Oost area was selected as the main study area of the project. In this way, routes with OD pair pairs inside Centrum Oost selected.

- What is the proper number of scenes to be created for the visibility analysis?

In the beginning, the street segments were categorized based on their length and the N percentile that they belong to. From this categorization, seven different categories of street segments created. The granularity test implemented in order to make a selection on observer's points based on the category and, by extent, the lengths of the street segments. For each category, four different cases selected to be examined; a street close to the water/canals or a bridge, a street that was going through or near a park, a street with high buildings' density and a street with low buildings' density. Afterward, these cases tested with different number of observer's points in order to decide on the number of the used observer's points that they could successfully represent the real street.

- What are the differences between the routes of the cyclists and the alternate routes?

  From the statistical analyses we see that the actual routes differed from the OSM alternatives on their variations on the building:ground ratio, buildings:sky ratio, the variations of the visible sky and the visible buildings and their distances. The GPS routes did not differ with their alternatives on the variation of amount of the visible ground, whereas differences on the street profiles could not be tested because of their limitation to represent the actual 3D environment.

- What route characteristics are considered significant for the cyclists during the trip?

  The route characteristics that are significant for the cyclists are the distance, the variations on the building-ground ratio, buildings-sky ratio, the variations of the visible sky and the visible buildings and the distance. Variations in the route and a route that consists of less homogeneous street segments are important to a cyclist in order to make a route choice.

7.3 FUTURE RESEARCH

The future research of this thesis should be focused mainly on three aspects; the street network and the statistical analyses.

Regarding the network simplification, a sensitivity analysis is required. This means that, although the extraction of the centrelines (in order to represent the street segments) resulted to a simplified street network that was easier to apply the visibility analyses, there is still an uncertainty of the extent that the centreline can capture a realistic view of the 3D environment. Different angles between the different bicycle lanes would result to different outputs, especially in cases such as streets with water or big highways.

The statistical analysis applied to the trips that cyclist travelled in Centrum Oost. More trips should be included in the center of Amsterdam and in different areas/cities in order to 1) have a bigger sample and so a better overview of the significance of the values and 2) have a comparison of the outputs of the visibility analyses based on different areas/neighborhoods. In this way it would give a better insight on advantages and the limitations of the proposed methodology on representing the different street profiles and building forms.

In addition, the start and end points of the street segments could be used to test a. the different views of the intersection points and b. the way that the views of the decision points can affect the route choice of the cyclist.

Future research can be done also with respect to the street categorization. The aggregation method used should be reconsidered or/and more categories of street profiles should be defined in order to get more detailed information on the street segments themselves.

The Space Syntax methodology should be compared with the proposed methodology in order to identify in a practical level advantages and weaknesses regarding mainly the visibility graph analyses.

BIBLIOGRAPHY

Boundary representation. Page Version ID: 823348954.

Churchill and the Commons Chamber.

Openrouteservice.

(2019). Geometric mean. Page Version ID: 888555713.

Alexander, M. Analyzing the behavior of cyclists at intersections.

Apparicio, P., Carrier, M., Gelb, J., Séguin, A.-M., and Kingham, S. Cyclists' exposure to air pollution and road traffic noise in central city neighbourhoods of Montreal. *Journal of Transport Geography*, 57:63–69.

Aultman-Hall, L. M. Commuter bicycle route choice: analysis of major determinants and safety implications.

Bator, M., Chmielewski, L. J., and Orlowski, A. Heuristic Assessment of Parameters of the Local Ground Approximation from Terrestrial LIDAR Data. In *Pacific-Rim Symposium on Image and Video Technology*, pages 88–97. Springer.

Beheshtitabar, E., Aguilar Ríos, S., König-Hollerwöger, D., Svat, Z., and Rydergren, C. ROUTE CHOICE MODELLING FOR BICYCLE TRIPS. 4(2).

Benedikt, M. L. To take hold of space: isovists and isovist fields. *Environment and Planning B: Planning and design*, 6(1):47–65.

Bergström, A. and Magnusson, R. Potential of transferring car trips to bicycle during winter. 37(8):649–666.

Bernhoft, I. M. and Carstensen, G. Preferences and behaviour of pedestrians and cyclists by age and gender. 11(2):83–95.

Biernat, E., Buchholtz, S., and Bartkiewicz, P. Motivations and barriers to bicycle commuting: Lessons from Poland. *Transportation Research Part F: Traffic Psychology and Behaviour*, 55:492–502.

Bovy, P. H. and Bradley, M. A. *Route choice analyzed with stated-preference approaches*. Number 1037.

Bovy, P. H. and Stern, E. *Route Choice: Wayfinding in Transport Networks: Wayfinding in Transport Networks*, volume 9. Springer Science & Business Media.

Broach, J., Dill, J., and Gliebe, J. Where do cyclists ride? a route choice model developed with revealed preference GPS data. 46(10):1730–1740.

Casello, J. M. and Usyukov, V. Modeling cyclists' route choice based on GPS data. 2430(1):155–161.

CBS Netherlands. CBS. *Statistics Netherlands*.

Coffeng, G. Goudappel Coffeng.

Corcoran, J., Li, T., Rohde, D., Charles-Edwards, E., and Mateo-Babiano, D. Spatio-temporal patterns of a public bicycle sharing program: the effect of weather and calendar events. 41:292–305.

Dill, J. and Gliebe, J. Understanding and measuring bicycling behavior: A focus on travel time and route choice.

DUTCH, B. Cycling in the rain.

Díaz-Vilariño, L., González-de Santos, L., Verbree, E., Michailidou, G., and Zlatanova, S. FROM POINT CLOUDS TO 3d ISOVISTS IN INDOOR ENVIRONMENTS. *International Archives of the Photogrammetry, Remote Sensing & Spatial Information Sciences*, 42(4).

Ehrgott, M., Wang, J. Y., Raith, A., and Van Houtte, C. A bi-objective cyclist route choice model. 46(4):652–663.

Emond, C. R. and Handy, S. L. Factors associated with bicycling to high school: insights from davis, CA. 20(1):71–79.

Engbers, L. H. and Hendriksen, I. J. Characteristics of a population of commuter cyclists in the netherlands: perceived barriers and facilitators in the personal, social and physical environment. 7(1):89.

Field, A. P. *Discovering Statistics Using SPSS: (and Sex, Drugs and Rock'n'roll)*. SAGE. Google-Books-ID: IY61Ddqnm6IC.

Fietsberaad Crow. Fietsberaad.

Fisher-Gewirtzman, D. and Wagner, I. A. Spatial openness as a practical metric for evaluating built-up environments. *Environment and Planning B: Planning and Design*, 30(1):37–49.

for Transport Policy Analysis, N. I. Cycling Facts | KiM.

Garrard, J., Rose, G., and Lo, S. K. Promoting transportation cycling for women: the role of bicycle infrastructure. 46(1):55–59.

Gemeente Amsterdam. Gemeente amsterdam.

Ghekiere, A., Van Cauwenberg, J., de Geus, B., Clarys, P., Cardon, G., Salmon, J., De Bourdeaudhuij, I., and Deforche, B. Critical environmental factors for transportation cycling in children: A qualitative study using bike-alongs. *Science & Sports*, 29:S18.

Gil, J. (2016). Using OSM Data for Street Network Analysis - From data to model to graph(s).

Girres, J.-F. and Touya, G. Quality Assessment of the French OpenStreetMap Dataset. *Transactions in GIS*, 14(4):435–459.

Grasso, N., Verbree, E., Zlatanova, S., and Piras, M. Strategies to evaluate the visibility along an indoor path in a point cloud representation. *ISPRS Annals of the Photogrammetry, Remote Sensing and Spatial Information Sciences*, 4:311.

Gröger, G. and Plümer, L. CityGML–Interoperable semantic 3d city models. *ISPRS Journal of Photogrammetry and Remote Sensing*, 71:12–33.

Handy, S., Wee, B. v., and Kroesen, M. Promoting Cycling for Transport: Research Needs and Challenges. *Transport Reviews*, 34(1):4–24.

Handy, S. L., Boarnet, M. G., Ewing, R., and Killingsworth, R. E. How the built environment affects physical activity: Views from urban planning. *American Journal of Preventive Medicine*, 23(2, Supplement 1):64–73.

Heinen, E., Maat, K., and van Wee, B. The effect of work-related factors on the bicycle commute mode choice in the netherlands. 40(1):23–43.

Hillier, B., Hanson, J., and Graham, H. Ideas are in things: an application of the space syntax method to discovering house genotypes. *Environment and Planning B: planning and design*, 14(4):363–385.

Hood, J., Sall, E., and Charlton, B. A GPS-based bicycle route choice model for san francisco, california. 3(1):63–75.

Hull, A. and O'Holleran, C. Bicycle infrastructure: can good design encourage cycling? *Urban, Planning and Transport Research*, 2(1):369–406.

Hunt, J. D. and Abraham, J. E. Influences on bicycle use. 34(4):453–470.

Hyodo, T., Suzuki, N., and Takahashi, K. Modeling of bicycle route and destination choice behavior for bicycle road network plan. (1705):70–76.

Institute, U. C. Choreography of cyclist behavior.

Izadpanahi, P., Leao, S., Lieske, S., and Pettit, C. Factors motivating bicycling in sydney: Analysing crowd-sourced data.

Jarjour, S., Jerrett, M., Westerdahl, D., de Nazelle, A., Hanning, C., Daly, L., Lipsitt, J., and Balmes, J. Cyclist route choice, traffic-related air pollution, and lung function: a scripted exposure study. *Environmental Health*, 12(1):14.

Kang, L. and Fricker, J. D. A bicycle route choice model that incorporates distance and perceived risk.

Kenton, W. Kurtosis.

Krenn, P. J., Oja, P., and Titze, S. Route choices of transport bicyclists: a comparison of actually used and shortest routes. *The International Journal of Behavioral Nutrition and Physical Activity*, 11:31.

Larsen, J. and El-Geneidy, A. A travel behavior analysis of urban cycling facilities in montréal, canada. 16(2):172–177.

Lawson, A. R., Pakrashi, V., Ghosh, B., and Szeto, W. Y. Perception of safety of cyclists in Dublin City. *Accident Analysis & Prevention*, 50:499–511.

Li, Z., Wang, W., Liu, P., and Ragland, D. R. Physical environments influencing bicyclists' perception of comfort on separated and on-street bicycle facilities. *Transportation Research Part D: Transport and Environment*, 17(3):256–261.

McCahil, C. and Garrick, N. The applicability of space syntax to bicycle facility planning. *Transportation Research Record: Journal of the Transportation Research Board*, (2074):46–51.

Menghini, G., Carrasco, N., Schüssler, N., and Axhausen, K. W. Route choice of cyclists in zurich. 44(9):754–765.

Mertens, L., Compernolle, S., Deforche, B., Mackenbach, J. D., Lakerveld, J., Brug, J., Roda, C., Feuillet, T., Oppert, J.-M., Glonti, K., Rutter, H., Bardos, H., De Bourdeaudhuij, I., and Van Dyck, D. Built environmental correlates of cycling for transport across europe. 44.

Miranda-Moreno, L. and Nosal, T. Weather or not to cycle: Temporal trends and impact of weather on cycling in an urban environment. (2247):42–52.

Morello, E. and Ratti, C. A digital image of the city: 3d isovists in Lynch's urban analysis. *Environment and Planning B: Planning and Design*, 36(5):837–853.

Nankervis, M. The effect of weather and climate on bicycle commuting. 33(6):417–431.

Netherlands, S. Netherlands' Safety Monitor.

NIST, S. Measures of Skewness and Kurtosis.

Parkin, J., Ryley, T., and Jones, T. Barriers to cycling: an exploration of quantitative analyses. *Cycling and society*, pages 67–82.

Peters, R., Ledoux, H., and Biljecki, F. Visibility Analysis in a Point Cloud Based on the Medial Axis Transform. In *UDMV*, pages 7–12.

Plugin, E. Elefront Plugin.

PostGIS. ST_contains.

PostGIS. $ST_Hausdorff Distance$.

Pucher, J. and Buehler, R. Making cycling irresistible: Lessons from the netherlands, denmark and germany. 28(4):495–528.

Raford, N., Chiaradia, A., and Gil, J. Space syntax: The role of urban form in cyclist route choice in central London.

Reynolds, C. C., Harris, M. A., Teschke, K., Cripton, P. A., and Winters, M. The impact of transportation infrastructure on bicycling injuries and crashes: a review of the literature. *Environmental health*, 8(1):47.

Rhino3D. Intersection.RayShoot Method.

Rietveld, P. and Daniel, V. Determinants of bicycle use: do municipal policies matter? *Transportation Research Part A: Policy and Practice*, 38(7):531–550.

Rybarczyk, G. and Gallagher, L. Measuring the potential for bicycling and walking at a metropolitan commuter university. *Journal of Transport Geography*, 39:1–10.

Sallis, J. F., Conway, T. L., Dillon, L. I., Frank, L. D., Adams, M. A., Cain, K. L., and Saelens, B. E. Environmental and demographic correlates of bicycling. 57(5):456–460.

Schmid, K. and von Stülpnagel, R. Quantifying Local Spatial Properties through LiDAR-based Isovists for an Evaluation of Opinion-based VGI in a VR Setup. In *Adjunct Proceedings of the 14th International Conference on Location Based Services*, pages 173–178. ETH Zurich.

Schramka, F., Arisona, S., Joos, M., and Erath, A. Development of Virtual Reality Cycling Simulator. *Arbeitsberichte Verkehrs-und Raumplanung*, 1244.

Schwenker, F., Scherer, S., and Morency, L.-P., editors. *Multimodal Pattern Recognition of Social Signals in Human-Computer-Interaction: Third IAPR TC3 Workshop, MPRSS 2014, Stockholm, Sweden, August 24, 2014, Revised Selected Papers*. Lecture Notes in Artificial Intelligence. Springer International Publishing.

Scratchapixel. Introduction to Ray Tracing: a Simple Method for Creating 3d Images.

Segadilha, A. B. P. and Sanches, S. d. P. Identification of factors that influence cyclistś route choice. 160:372–380.

Sener, I. N., Eluru, N., and Bhat, C. R. An analysis of bicycle route choice preferences in texas, US. 36(5):511–539.

Si, B., Zhang, H., Zhong, M., and Yang, X. Multi-criterion system optimization model for urban multimodal traffic network. *Science China Technological Sciences*, 54(4):947–954.

Sileryte, R. Analysis of Urban Space Networks for Recreational Purposes based on Mobile Sports Tracking Application Data.

Snizek, B., Sick Nielsen, T. A., and Skov-Petersen, H. Mapping bicyclists' experiences in Copenhagen. *Journal of Transport Geography*, 30:227–233.

Song, R., Ni, Y., and Li, K. Understanding cyclists' risky route choice behavior on urban road sections. 25:4157–4170.

Soren, J. Bicycle tracks and lanes: A before–after study.

Spencer, P., Watts, R., Vivanco, L., and Flynn, B. The effect of environmental factors on bicycle commuters in vermont: influences of a northern climate. 31:11–17.

Stinson, M. and Bhat, C. Commuter bicyclist route choice: Analysis using a stated preference survey. (1828):107–115.

Stinson, M. A. and Bhat, C. R. A comparison of the route preferences of experienced and inexperienced bicycle commuters. In *84th Annual Meeting of the Transportation Research Board, Washington, DC*.

Tang, U. W. and Wang, Z. S. Influences of urban forms on traffic-induced noise and air pollution: Results from a modelling system. *Environmental Modelling & Software*, 22(12):1750–1764.

Thomas, T., Jaarsma, R., and Tutert, B. Exploring temporal fluctuations of daily cycling demand on dutch cycle paths: the influence of weather on cycling. 40(1):1–22.

Tilahun, N. Y., Levinson, D. M., and Krizek, K. J. Trails, lanes, or traffic: Valuing bicycle facilities with an adaptive stated preference survey. 41(4):287–301.

Ton, D., Duives, D. C., Cats, O., Hoogendoorn-Lanser, S., and Hoogendoorn, S. P. Cycling or walking? determinants of mode choice in the netherlands.

Van Bilsen, A. How can serious games benefit from 3d visibility analysis? *Proc. of International Simulation and Gaming Association*.

Van Duppen, J. and Spierings, B. Retracing trajectories: the embodied experience of cycling, urban sensescapes and the commute between 'neighbourhood'and 'city'in utrecht, NL. 30:234–243.

Winters, M. and Cooper, A. What Makes a Neighbourhood Bikeable Reporting on the Results of Focus Gro - Google Search.

Winters, M., Davidson, G., Kao, D., and Teschke, K. Motivators and deterrents of bicycling: comparing influences on decisions to ride. 38(1):153–168.

Winters, M. and Teschke, K. Route preferences among adults in the near market for bicycling: findings of the cycling in cities study. *American journal of health promotion*, 25(1):40–47.

Yeboah, G. *Understanding urban cycling behaviours in space and time*. doctoral, Northumbria University.

A | GRANULARITY

Category A - [9m, 34m)

Park

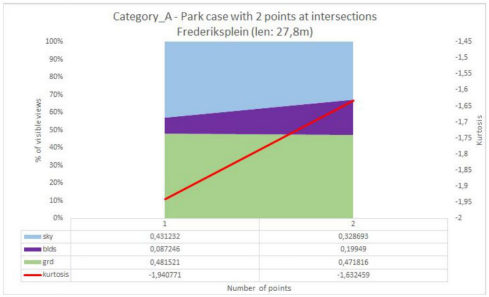

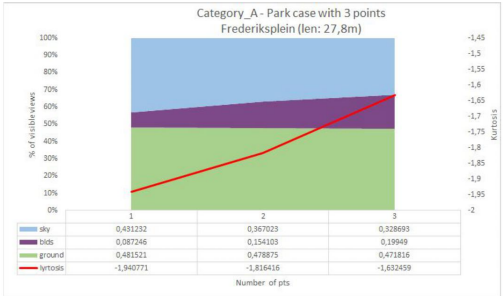

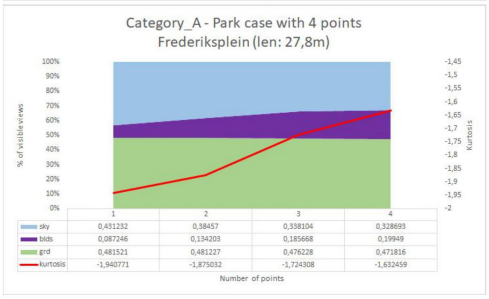

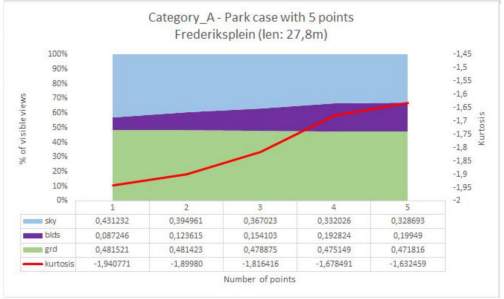

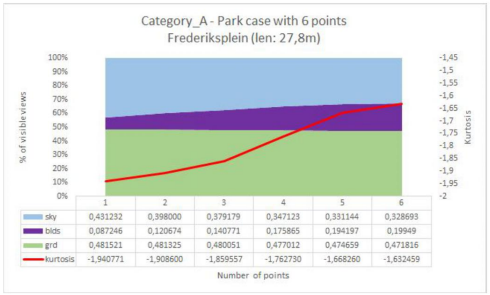

Water


Egelantiersgracht
Eerste Leliedwarsstraat

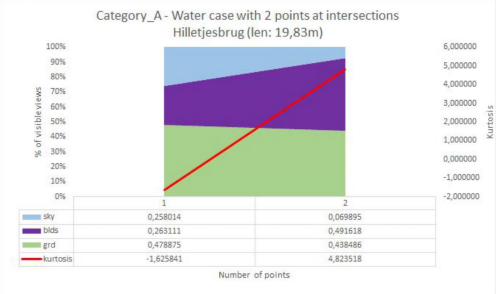
Category_A - Water case with 2 points at intersections
Hilletjesbrug (len: 19,83m)
% of visible views
Kurtosis
Number of points
sky 0,258014 0,069895
blds 0,263111 0,491618
grd 0,478875 0,438486
kurtosis -1,625841 4,823518

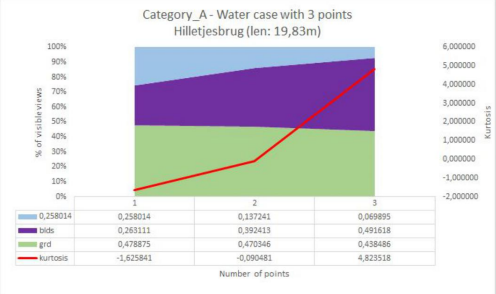
Category_A - Water case with 3 points
Hilletjesbrug (len: 19,83m)
% of visible views
Kurtosis
Number of points
sky 0,258014 0,258014 0,137241 0,069895
blds 0,263111 0,263111 0,392413 0,491618
grd 0,478875 0,478875 0,470346 0,438486
kurtosis -1,625841 -1,625841 -0,090481 4,823518

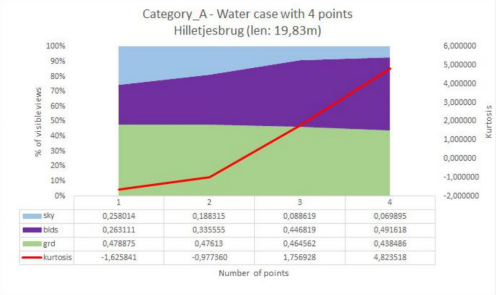
Category_A - Water case with 4 points
Hilletjesbrug (len: 19,83m)
% of visible views
Kurtosis
Number of points
sky 0,258014 0,188315 0,088619 0,069895
blds 0,263111 0,335555 0,446819 0,491618
grd 0,478875 0,47613 0,464562 0,438486
kurtosis -1,625841 -0,977360 1,756928 4,823518

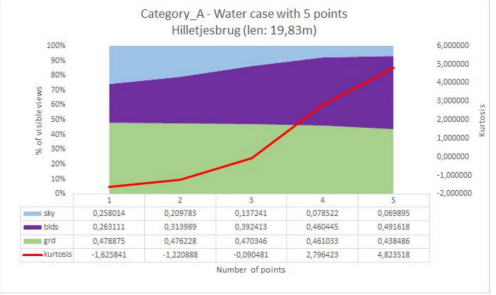
Category_A - Water case with 5 points
Hilletjesbrug (len: 19,83m)
% of visible views
Kurtosis
Number of points
sky 0,258014 0,209783 0,137241 0,078522 0,069895
blds 0,263111 0,313989 0,392413 0,460445 0,491618
grd 0,478875 0,476228 0,470346 0,461033 0,438486
kurtosis -1,625841 -1,220888 -0,090481 2,796423 4,823518

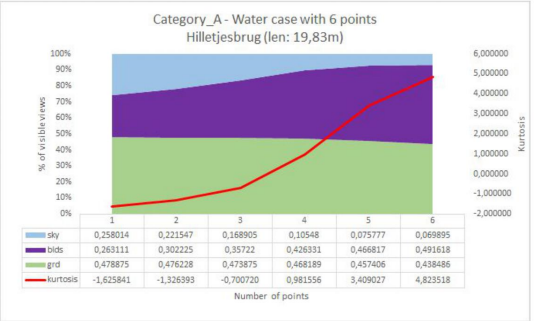
Category_A - Water case with 6 points
Hilletjesbrug (len: 19,83m)
% of visible views
Kurtosis
Number of points
sky 0,258014 0,221547 0,168905 0,10548 0,075777 0,069895
blds 0,263111 0,302225 0,35722 0,426331 0,466817 0,491618
grd 0,478875 0,476228 0,473875 0,468189 0,457406 0,438486
kurtosis -1,625841 -1,326393 -0,700720 0,981556 3,409027 4,823518

High Density

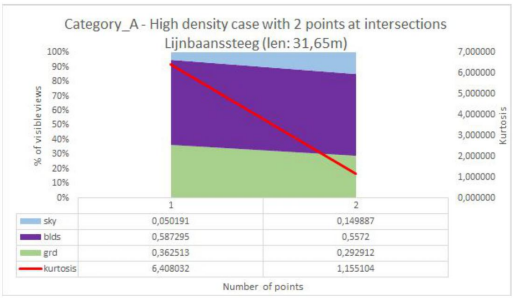

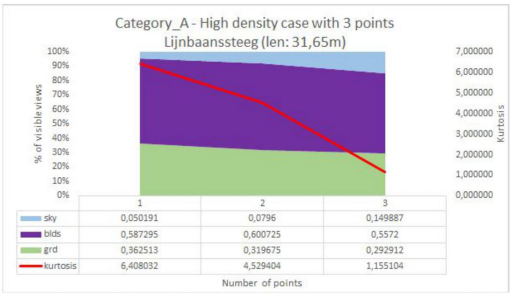

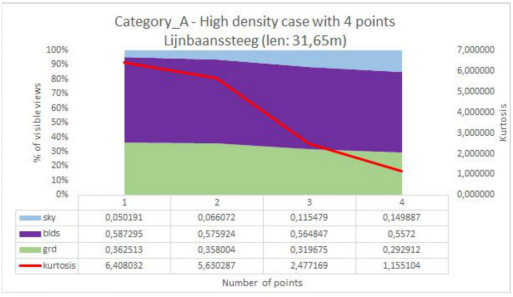

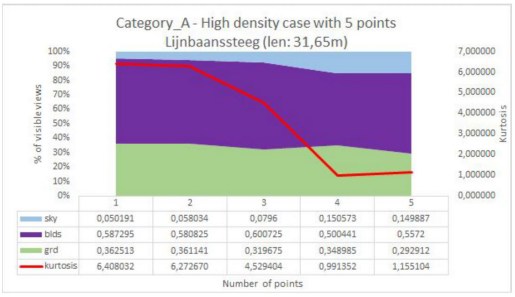

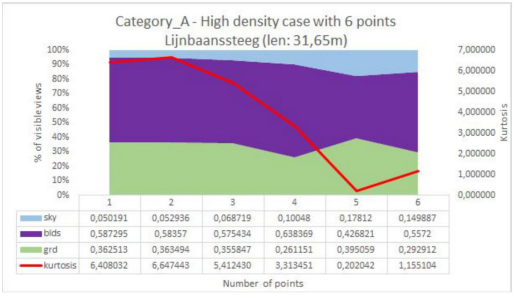

Category B - [34m, 53m)

Park

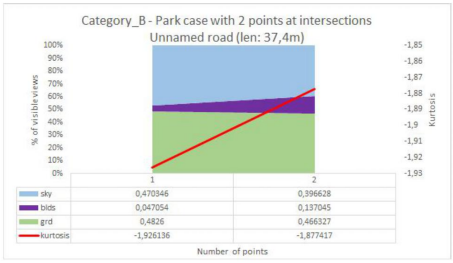

	1	2
sky	0,470346	0,396628
blds	0,047054	0,137045
grd	0,4826	0,466327
kurtosis	-1,926136	-1,877417

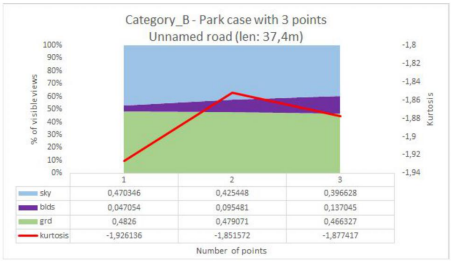

	1	2	3
sky	0,470346	0,425448	0,396628
blds	0,047054	0,095481	0,137045
grd	0,4826	0,479071	0,466327
kurtosis	-1,926136	-1,851572	-1,877417

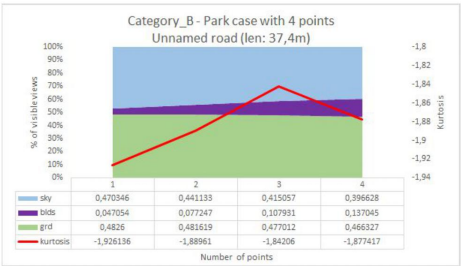

	1	2	3	4
sky	0,470346	0,441133	0,415057	0,396628
blds	0,047054	0,077247	0,107931	0,137045
grd	0,4826	0,481619	0,477012	0,466327
kurtosis	-1,926136	-1,88961	-1,84206	-1,877417

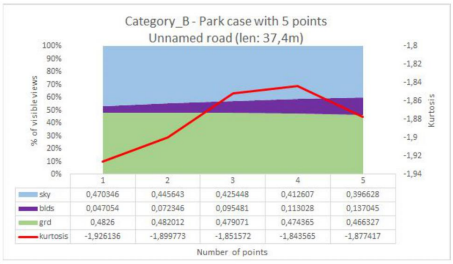

	1	2	3	4	5
sky	0,470346	0,445643	0,425448	0,412607	0,396628
blds	0,047054	0,072346	0,095481	0,113028	0,137045
grd	0,4826	0,482012	0,479071	0,474365	0,466327
kurtosis	-1,926136	-1,899773	-1,851572	-1,843565	-1,877417

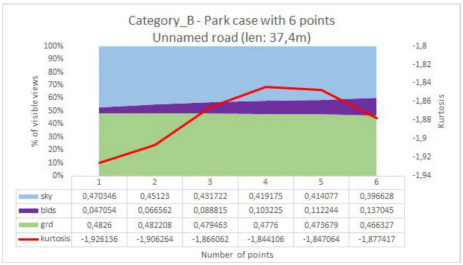

	1	2	3	4	5	6
sky	0,470346	0,45123	0,431722	0,419175	0,414077	0,396628
blds	0,047054	0,066562	0,088815	0,103225	0,112244	0,137045
grd	0,4826	0,482208	0,479463	0,4776	0,473679	0,466327
kurtosis	-1,926136	-1,906264	-1,866062	-1,844106	-1,847064	-1,877417

Water

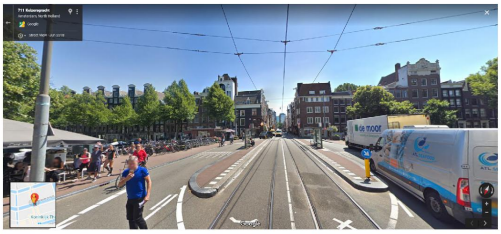

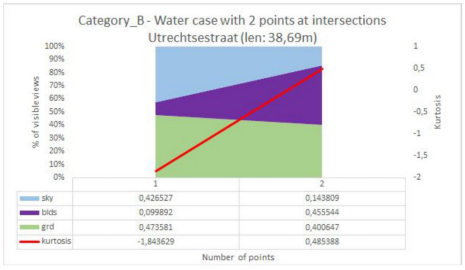

	1	2
sky	0,426527	0,143809
blds	0,099892	0,455544
grd	0,473581	0,400647
kurtosis	-1,843629	0,485388

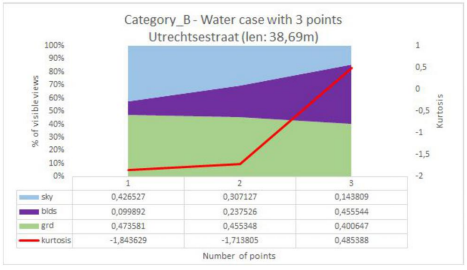

	1	2	3
sky	0,426527	0,307127	0,143809
blds	0,099892	0,237526	0,455544
grd	0,473581	0,455348	0,400647
kurtosis	-1,843629	-1,713805	0,485388

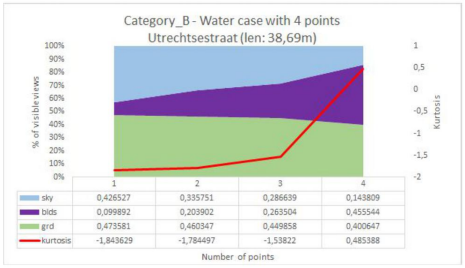

	1	2	3	4
sky	0,426527	0,335751	0,286639	0,143809
blds	0,099892	0,203902	0,263504	0,455544
grd	0,473581	0,460347	0,449858	0,400647
kurtosis	-1,843629	-1,784497	-1,53822	0,485388

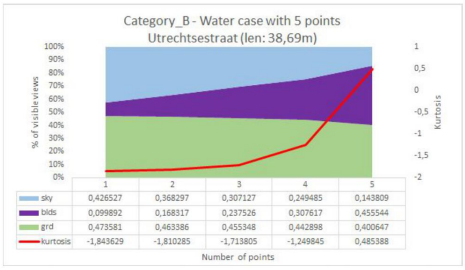

	1	2	3	4	5
sky	0,426527	0,368297	0,307127	0,249485	0,143809
blds	0,099892	0,168317	0,237526	0,307617	0,455544
grd	0,473581	0,463386	0,455348	0,442898	0,400647
kurtosis	-1,843629	-1,810285	-1,713805	-1,249845	0,485388

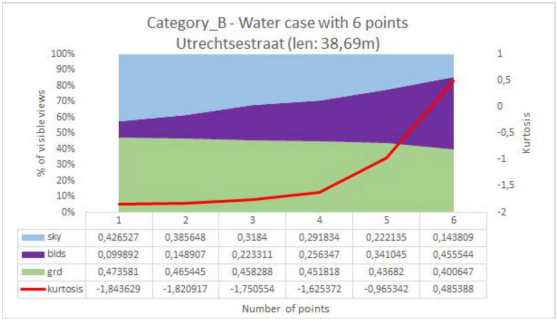

	1	2	3	4	5	6
sky	0,426527	0,385648	0,3184	0,291834	0,222135	0,143809
blds	0,099892	0,148907	0,223311	0,256347	0,341045	0,455544
grd	0,473581	0,465445	0,458288	0,451818	0,43682	0,400647
kurtosis	-1,843629	-1,820917	-1,750554	-1,625372	-0,965342	0,485388

High Density

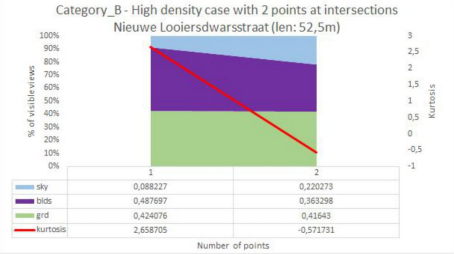

	1	2
sky	0,088227	0,220273
blds	0,487697	0,363298
grd	0,424076	0,41643
kurtosis	2,658705	-0,571731

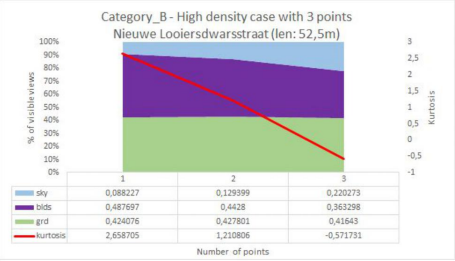

	1	2	3
sky	0,088227	0,129399	0,220273
blds	0,487697	0,4428	0,363298
grd	0,424076	0,427801	0,41643
kurtosis	2,658705	1,210806	-0,571731

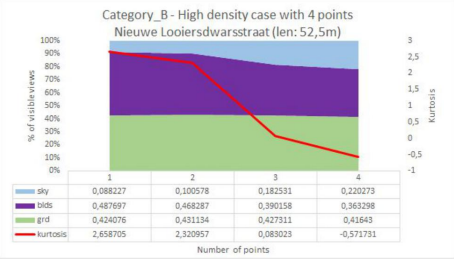

	1	2	3	4
sky	0,088227	0,100578	0,182531	0,220273
blds	0,487697	0,468287	0,390158	0,363298
grd	0,424076	0,431134	0,427311	0,41643
kurtosis	2,658705	2,320957	0,083023	-0,571731

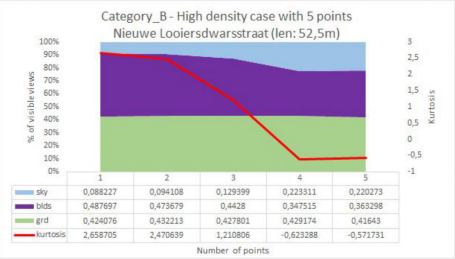

	1	2	3	4	5
sky	0,088227	0,094108	0,129399	0,223311	0,220273
blds	0,487697	0,473679	0,4428	0,347515	0,363298
grd	0,424076	0,432213	0,427801	0,429174	0,41643
kurtosis	2,658705	2,470639	1,210806	-0,623288	-0,571731

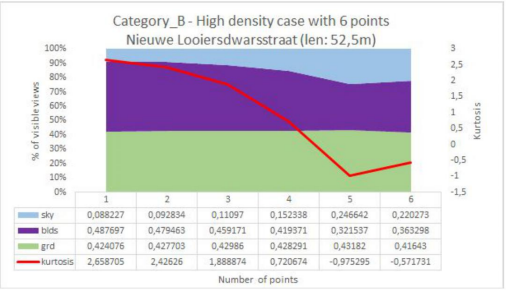

	1	2	3	4	5	6
sky	0,088227	0,092834	0,11097	0,152338	0,246642	0,220273
blds	0,487697	0,479463	0,459171	0,419371	0,321537	0,363298
grd	0,424076	0,427703	0,42986	0,428291	0,43182	0,41643
kurtosis	2,658705	2,42626	1,888874	0,720674	-0,975295	-0,571731

Low Density


Sarphatistraat
Alexanderstraat

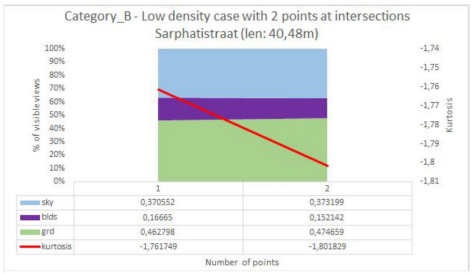
Category_B - Low density case with 2 points at intersections
Sarphatistraat (len: 40,48m)
% of visible views
Kurtosis
Number of points
sky 0,370552 0,373199
blds 0,16665 0,152142
grd 0,462798 0,474659
kurtosis -1,761749 -1,801829

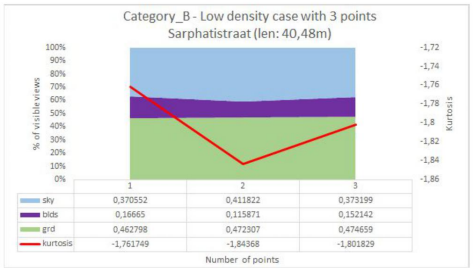
Category_B - Low density case with 3 points
Sarphatistraat (len: 40,48m)
% of visible views
Kurtosis
Number of points
sky 0,370552 0,411822 0,373199
blds 0,16665 0,115871 0,152142
grd 0,462798 0,472307 0,474659
kurtosis -1,761749 -1,84368 -1,801829

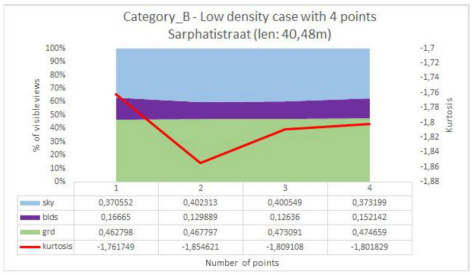
Category_B - Low density case with 4 points
Sarphatistraat (len: 40,48m)
% of visible views
Kurtosis
Number of points
sky 0,370552 0,402313 0,400549 0,373199
blds 0,16665 0,129889 0,12636 0,152142
grd 0,462798 0,467797 0,473091 0,474659
kurtosis -1,761749 -1,854621 -1,809108 -1,801829

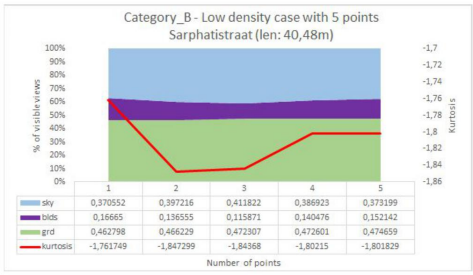
Category_B - Low density case with 5 points
Sarphatistraat (len: 40,48m)
% of visible views
Kurtosis
Number of points
sky 0,370552 0,397216 0,411822 0,386923 0,373199
blds 0,16665 0,136555 0,115871 0,140476 0,152142
grd 0,462798 0,466229 0,472307 0,472601 0,474659
kurtosis -1,761749 -1,847299 -1,84368 -1,80215 -1,801829

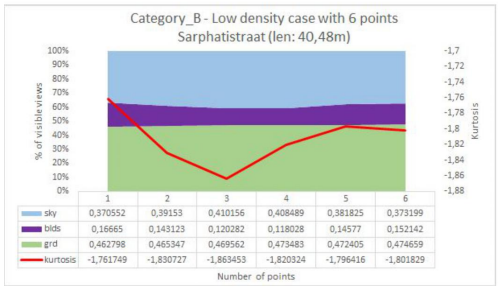
Category_B - Low density case with 6 points
Sarphatistraat (len: 40,48m)
% of visible views
Kurtosis
Number of points
sky 0,370552 0,39153 0,410156 0,408489 0,381825 0,373199
blds 0,16665 0,143123 0,120282 0,118028 0,14577 0,152142
grd 0,462798 0,465347 0,469562 0,473483 0,472405 0,474659
kurtosis -1,761749 -1,830727 -1,863453 -1,820324 -1,796416 -1,801829

Category C - [53m, 73m)

Park

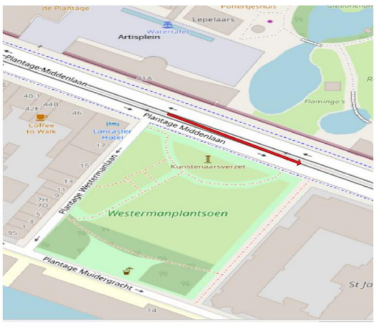

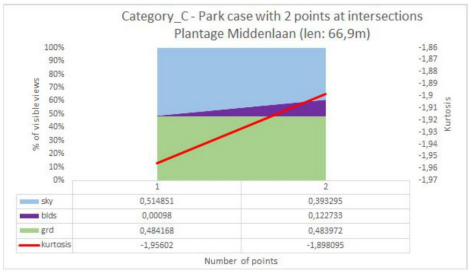

	1	2
sky	0,514851	0,393295
blds	0,00098	0,122733
grd	0,484168	0,483972
kurtosis	-1,95602	-1,898095

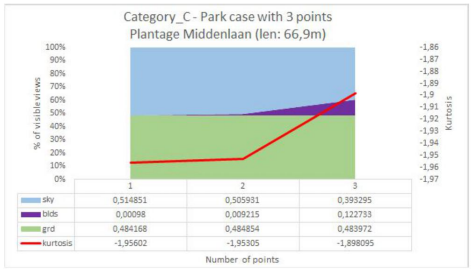

	1	2	3
sky	0,514851	0,505931	0,393295
blds	0,00098	0,009215	0,122733
grd	0,484168	0,484854	0,483972
kurtosis	-1,95602	-1,95305	-1,898095

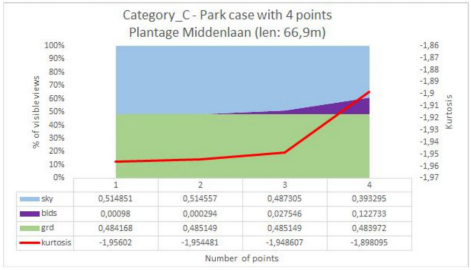

	1	2	3	4
sky	0,514851	0,514557	0,487305	0,393295
blds	0,00098	0,000294	0,027546	0,122733
grd	0,484168	0,485149	0,485149	0,483972
kurtosis	-1,95602	-1,954481	-1,948607	-1,898095

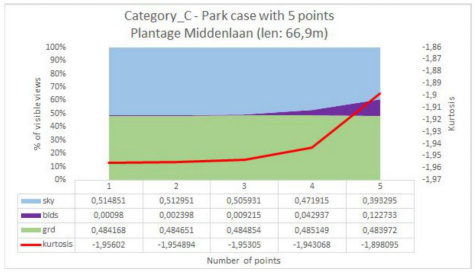

	1	2	3	4	5
sky	0,514851	0,512951	0,505931	0,471915	0,393295
blds	0,00098	0,002398	0,009215	0,042937	0,122733
grd	0,484168	0,484651	0,484854	0,485149	0,483972
kurtosis	-1,95602	-1,954894	-1,95305	-1,943068	-1,898095

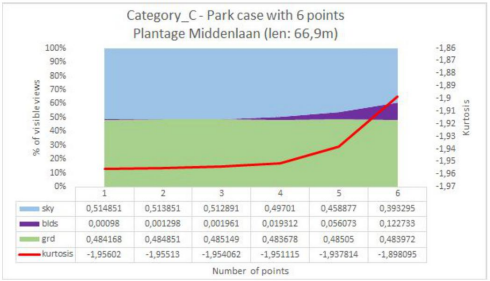

	1	2	3	4	5	6
sky	0,514851	0,513851	0,512891	0,49701	0,458877	0,393295
blds	0,00098	0,001298	0,001961	0,019312	0,056073	0,122733
grd	0,484168	0,484851	0,485149	0,483678	0,48505	0,483972
kurtosis	-1,95602	-1,95513	-1,954062	-1,951115	-1,937814	-1,898095

Water

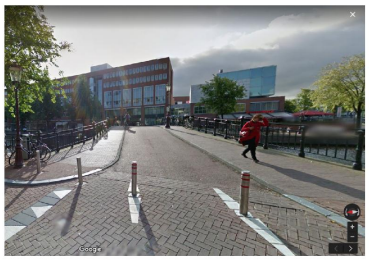

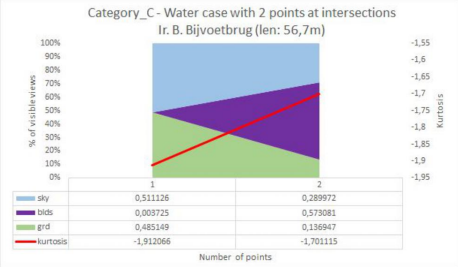

	1	2
sky	0,511126	0,289972
blds	0,003725	0,573081
grd	0,485149	0,136947
kurtosis	-1,912066	-1,701115

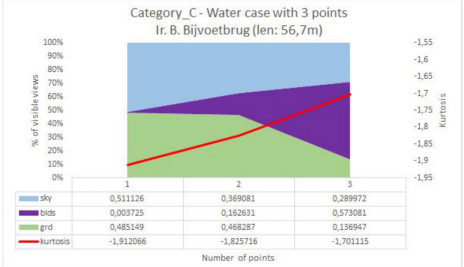

	1	2	3
sky	0,511126	0,369081	0,289972
blds	0,003725	0,162631	0,573081
grd	0,485149	0,468287	0,136947
kurtosis	-1,912066	-1,825716	-1,701115

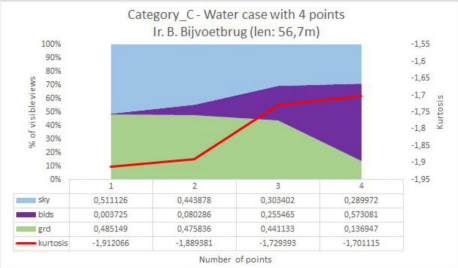

	1	2	3	4
sky	0,511126	0,443878	0,303402	0,289972
blds	0,003725	0,080286	0,255465	0,573081
grd	0,485149	0,475836	0,441133	0,136947
kurtosis	-1,912066	-1,889381	-1,729393	-1,701115

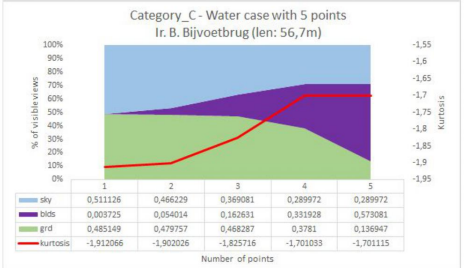

	1	2	3	4	5
sky	0,511126	0,466229	0,369081	0,289972	0,289972
blds	0,003725	0,054014	0,162631	0,331928	0,573081
grd	0,485149	0,479757	0,468287	0,3781	0,136947
kurtosis	-1,912066	-1,902026	-1,825716	-1,701033	-1,701115

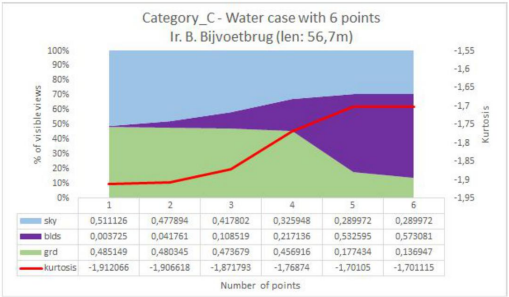

	1	2	3	4	5	6
sky	0,511126	0,477894	0,417802	0,325948	0,289972	0,289972
blds	0,003725	0,041761	0,108519	0,217136	0,532595	0,573081
grd	0,485149	0,480345	0,473679	0,456916	0,177434	0,136947
kurtosis	-1,912066	-1,906618	-1,871793	-1,76874	-1,70105	-1,701115

High Density

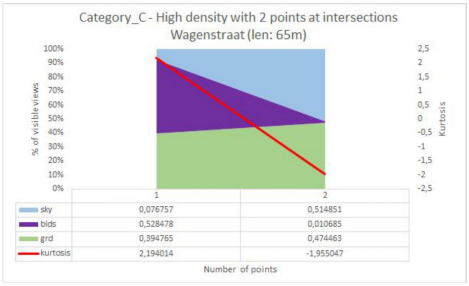

	1	2
sky	0,076757	0,514851
blds	0,528478	0,010685
grd	0,394765	0,474463
kurtosis	2,194014	-1,955047

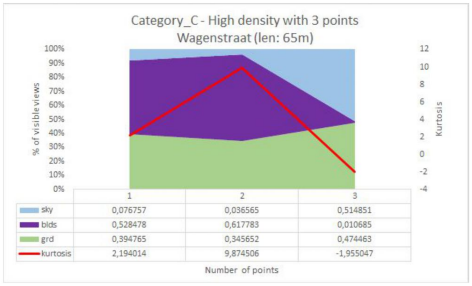

	1	2	3
sky	0,076757	0,036565	0,514851
blds	0,528478	0,617783	0,010685
grd	0,394765	0,345652	0,474463
kurtosis	2,194014	9,874506	-1,955047

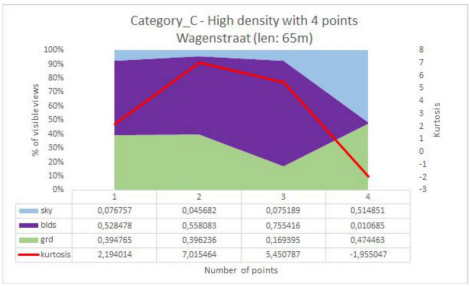

	1	2	3	4
sky	0,076757	0,045682	0,075189	0,514851
blds	0,528478	0,558083	0,755416	0,010685
grd	0,394765	0,396236	0,169395	0,474463
kurtosis	2,194014	7,015464	5,450787	-1,955047

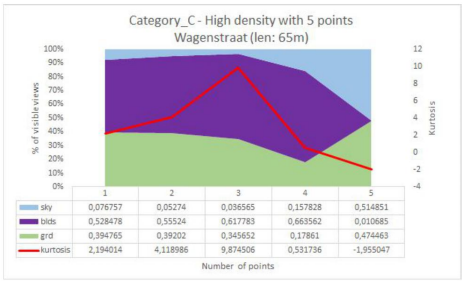

	1	2	3	4	5
sky	0,076757	0,05274	0,036565	0,157828	0,514851
blds	0,528478	0,55524	0,617783	0,663562	0,010685
grd	0,394765	0,39202	0,345652	0,17861	0,474463
kurtosis	2,194014	4,118986	9,874506	0,531736	-1,955047

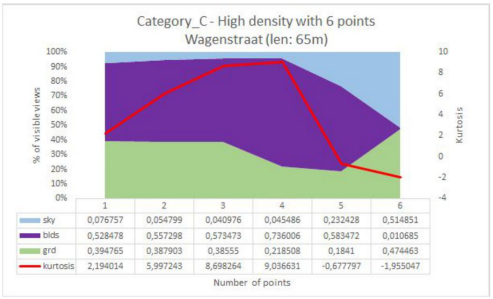

	1	2	3	4	5	6
sky	0,076757	0,054799	0,040976	0,045486	0,232428	0,514851
blds	0,528478	0,557298	0,573473	0,736006	0,583472	0,010685
grd	0,394765	0,387903	0,38555	0,218508	0,1841	0,474463
kurtosis	2,194014	5,997243	8,698264	9,036631	-0,677797	-1,955047

Low Density

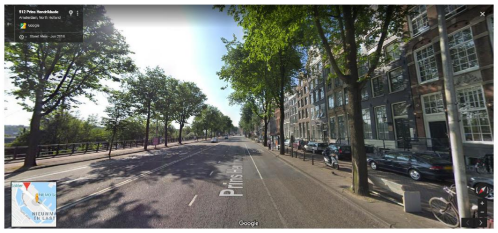

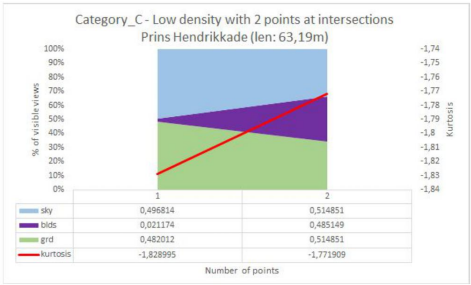

	1	2
sky	0,496814	0,514851
blds	0,021174	0,485149
grd	0,482012	0,514851
kurtosis	-1,828995	-1,771909

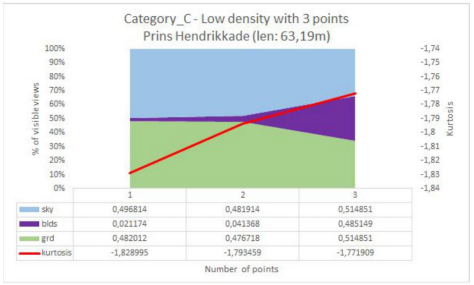

	1	2	3
sky	0,496814	0,481914	0,514851
blds	0,021174	0,041368	0,485149
grd	0,482012	0,476718	0,514851
kurtosis	-1,828995	-1,793459	-1,771909

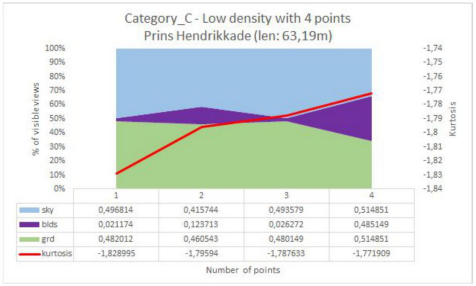

	1	2	3	4
sky	0,496814	0,415744	0,493579	0,514851
blds	0,021174	0,123713	0,026272	0,485149
grd	0,482012	0,460543	0,480149	0,514851
kurtosis	-1,828995	-1,79594	-1,787633	-1,771909

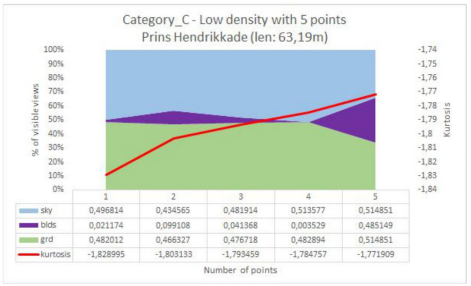

	1	2	3	4	5
sky	0,496814	0,434565	0,481914	0,513577	0,514851
blds	0,021174	0,099108	0,041368	0,003529	0,485149
grd	0,482012	0,466327	0,476718	0,482894	0,514851
kurtosis	-1,828995	-1,803133	-1,793459	-1,784757	-1,771909

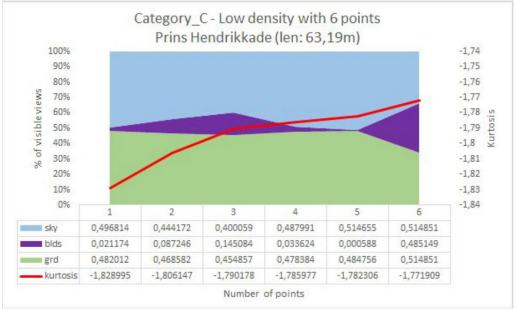

	1	2	3	4	5	6
sky	0,496814	0,444172	0,400059	0,487991	0,514655	0,514851
blds	0,021174	0,087246	0,145084	0,033624	0,000588	0,485149
grd	0,482012	0,468582	0,454857	0,478384	0,484756	0,514851
kurtosis	-1,828995	-1,806147	-1,790178	-1,785977	-1,782306	-1,771909

Category D - [73m, 113m)

Park

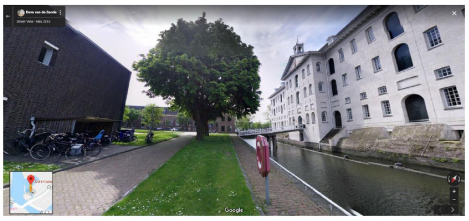

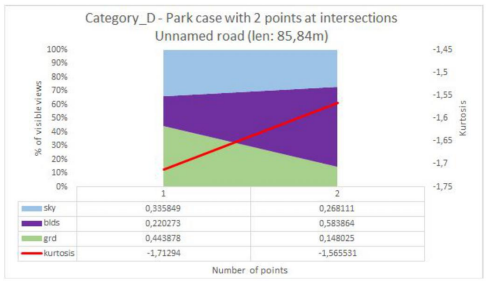

	1	2
sky	0,335849	0,268111
blds	0,220273	0,583864
grd	0,443878	0,148025
kurtosis	-1,71294	-1,565531

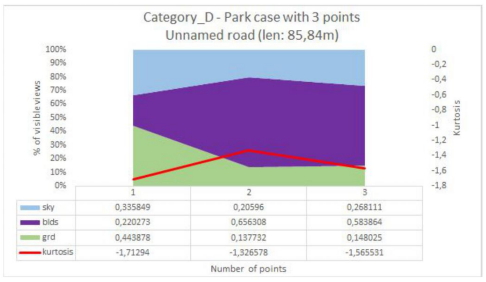

	1	2	3
sky	0,335849	0,20596	0,268111
blds	0,220273	0,656308	0,583864
grd	0,443878	0,137732	0,148025
kurtosis	-1,71294	-1,326578	-1,565531

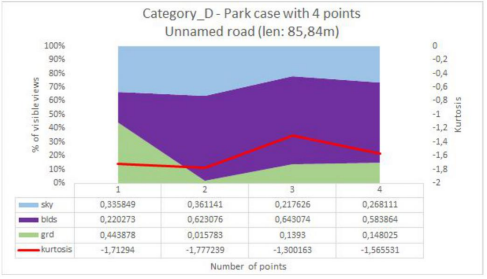

	1	2	3	4
sky	0,335849	0,361141	0,217626	0,268111
blds	0,220273	0,623076	0,643074	0,583864
grd	0,443878	0,015783	0,1393	0,148025
kurtosis	-1,71294	-1,777239	-1,300163	-1,565531

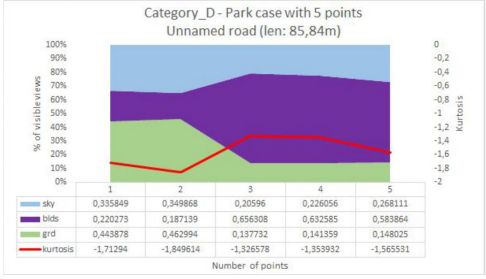

	1	2	3	4	5
sky	0,335849	0,349868	0,20596	0,226056	0,268111
blds	0,220273	0,187139	0,656308	0,632585	0,583864
grd	0,443878	0,462994	0,137732	0,141359	0,148025
kurtosis	-1,71294	-1,849614	-1,326578	-1,353932	-1,565531

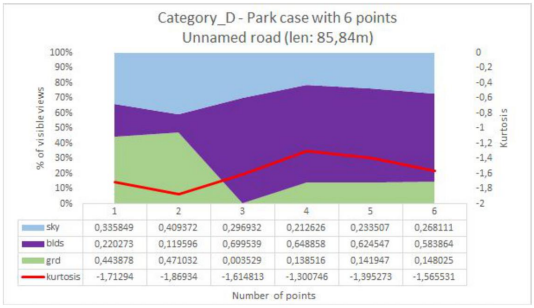

	1	2	3	4	5	6
sky	0,335849	0,409372	0,296932	0,212626	0,233507	0,268111
blds	0,220273	0,119596	0,699539	0,648858	0,624547	0,583864
grd	0,443878	0,471032	0,003529	0,138516	0,141947	0,148025
kurtosis	-1,71294	-1,86934	-1,614813	-1,300746	-1,395273	-1,565531

Water

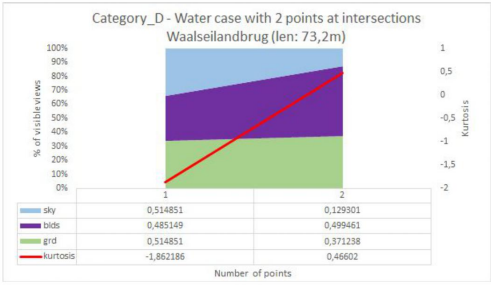

	1	2
sky	0,514851	0,129301
blds	0,485149	0,499461
grd	0,514851	0,371238
kurtosis	-1,862186	0,46602

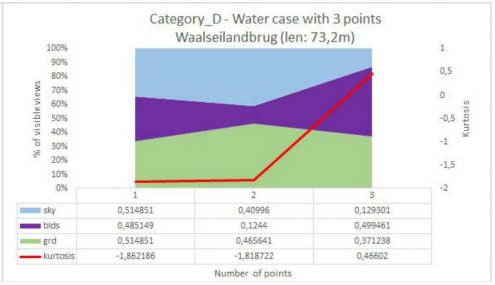

	1	2	3
sky	0,514851	0,40996	0,129301
blds	0,485149	0,1244	0,499461
grd	0,514851	0,465641	0,371238
kurtosis	-1,862186	-1,818722	0,46602

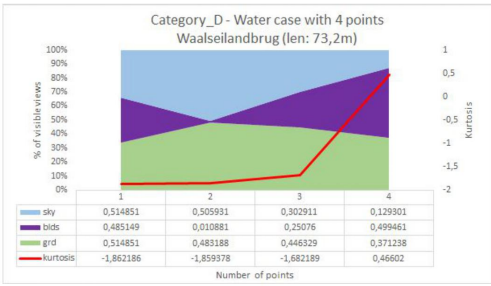

	1	2	3	4
sky	0,514851	0,505931	0,302911	0,129301
blds	0,485149	0,010881	0,25076	0,499461
grd	0,514851	0,483188	0,446329	0,371238
kurtosis	-1,862186	-1,859378	-1,682189	0,46602

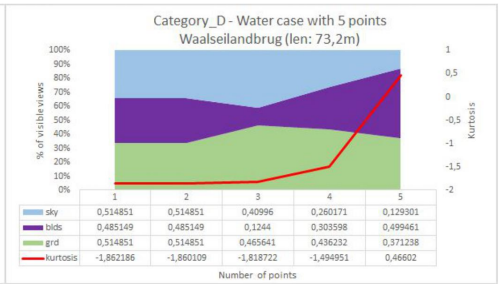

	1	2	3	4	5
sky	0,514851	0,514851	0,40996	0,260171	0,129301
blds	0,485149	0,485149	0,1244	0,303598	0,499461
grd	0,514851	0,514851	0,465641	0,436232	0,371238
kurtosis	-1,862186	-1,860109	-1,818722	-1,494951	0,46602

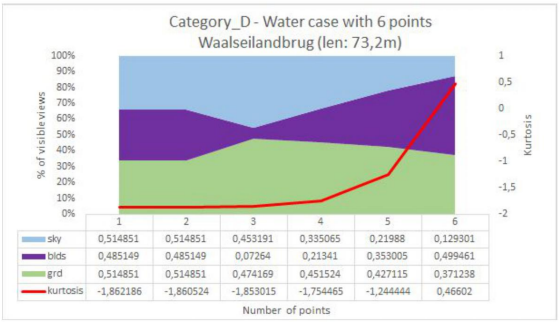

	1	2	3	4	5	6
sky	0,514851	0,514851	0,453191	0,335065	0,21988	0,129301
blds	0,485149	0,485149	0,07264	0,21341	0,353005	0,499461
grd	0,514851	0,514851	0,474169	0,451524	0,427115	0,371238
kurtosis	-1,862186	-1,860524	-1,853015	-1,754465	-1,244444	0,46602

High Density

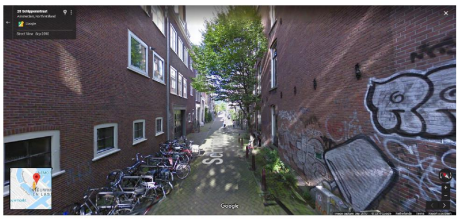

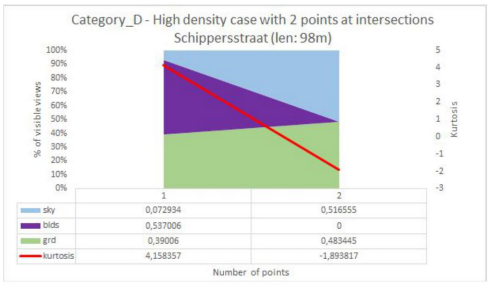

	1	2
sky	0,072934	0,516555
blds	0,537006	0
grd	0,39006	0,483445
kurtosis	4,158357	-1,893817

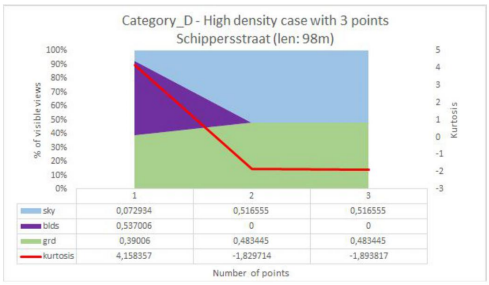

	1	2	3
sky	0,072934	0,516555	0,516555
blds	0,537006	0	0
grd	0,39006	0,483445	0,483445
kurtosis	4,158357	-1,829714	-1,893817

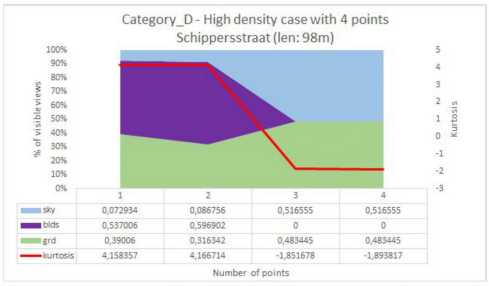

	1	2	3	4
sky	0,072934	0,086756	0,516555	0,516555
blds	0,537006	0,596902	0	0
grd	0,39006	0,316342	0,483445	0,483445
kurtosis	4,158357	4,166714	-1,851678	-1,893817

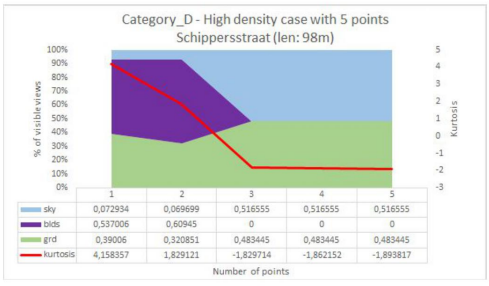

	1	2	3	4	5
sky	0,072934	0,069699	0,516555	0,516555	0,516555
blds	0,537006	0,60945	0	0	0
grd	0,39006	0,320851	0,483445	0,483445	0,483445
kurtosis	4,158357	1,829121	-1,829714	-1,862152	-1,893817

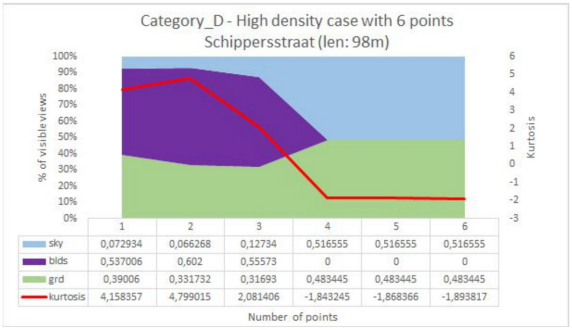

	1	2	3	4	5	6
sky	0,072934	0,066268	0,12734	0,516555	0,516555	0,516555
blds	0,537006	0,602	0,55573	0	0	0
grd	0,39006	0,331732	0,31693	0,483445	0,483445	0,483445
kurtosis	4,158357	4,799015	2,081406	-1,843245	-1,868366	-1,893817

Low Density


Kattenburgerkade
Jacob Bontiusstraat
Bootstraat
Tweede Witte
De Witte Boer

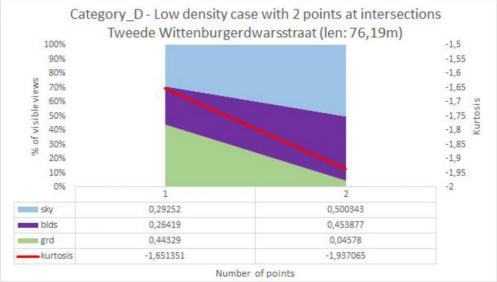
Category_D - Low density case with 2 points at intersections
Tweede Wittenburgerdwarsstraat (len: 76,19m)
% of visible views
Kurtosis
Number of points
sky 0,29252 0,500343
blds 0,26419 0,453877
grd 0,44329 0,04578
kurtosis -1,651351 -1,937065

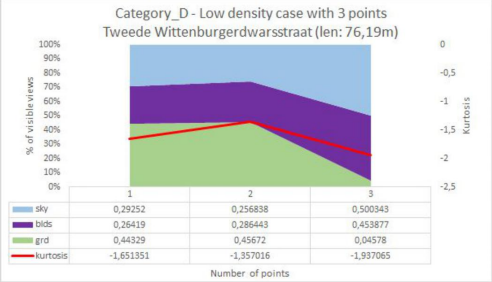
Category_D - Low density case with 3 points
Tweede Wittenburgerdwarsstraat (len: 76,19m)
% of visible views
Kurtosis
Number of points
sky 0,29252 0,256838 0,500343
blds 0,26419 0,286443 0,453877
grd 0,44329 0,45672 0,04578
kurtosis -1,651351 -1,357016 -1,937065

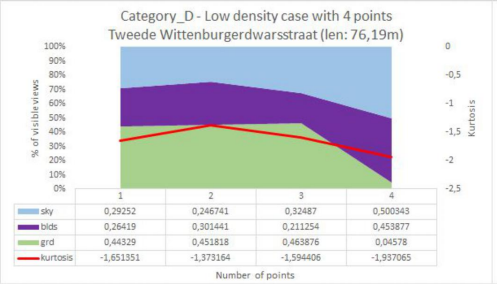
Category_D - Low density case with 4 points
Tweede Wittenburgerdwarsstraat (len: 76,19m)
% of visible views
Kurtosis
Number of points
sky 0,29252 0,246741 0,32487 0,500343
blds 0,26419 0,301441 0,211254 0,453877
grd 0,44329 0,451818 0,463876 0,04578
kurtosis -1,651351 -1,373164 -1,594406 -1,937065

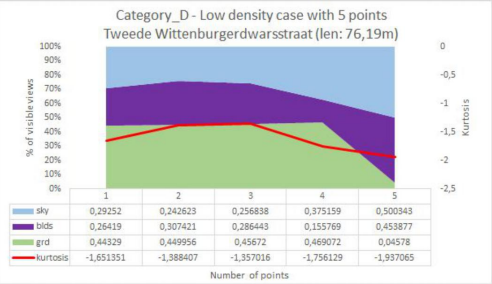
Category_D - Low density case with 5 points
Tweede Wittenburgerdwarsstraat (len: 76,19m)
% of visible views
Kurtosis
Number of points
sky 0,29252 0,242623 0,256838 0,375159 0,500343
blds 0,26419 0,307421 0,286443 0,155769 0,453877
grd 0,44329 0,449956 0,45672 0,469072 0,04578
kurtosis -1,651351 -1,388407 -1,357016 -1,756129 -1,937065

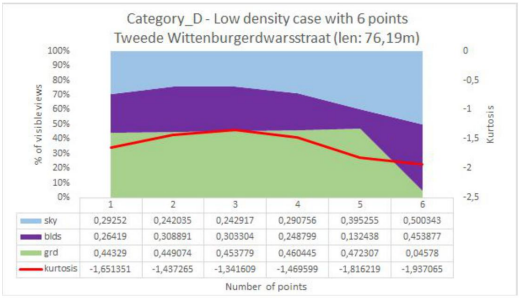
Category_D - Low density case with 6 points
Tweede Wittenburgerdwarsstraat (len: 76,19m)
% of visible views
Kurtosis
Number of points
sky 0,29252 0,242035 0,242917 0,290756 0,395255 0,500343
blds 0,26419 0,308891 0,303304 0,248799 0,132438 0,453877
grd 0,44329 0,449074 0,453779 0,460445 0,472307 0,04578
kurtosis -1,651351 -1,437265 -1,341609 -1,469599 -1,816219 -1,937065

Category E - [113m, 194m)

Park

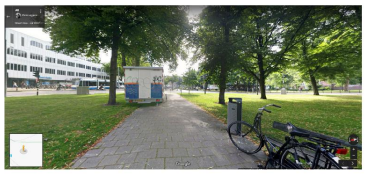

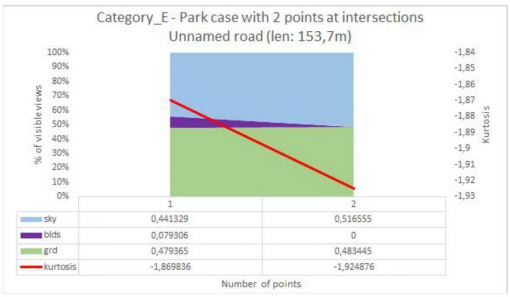

	1	2
sky	0,441329	0,516555
blds	0,079306	0
grd	0,479365	0,483445
kurtosis	-1,869836	-1,924876

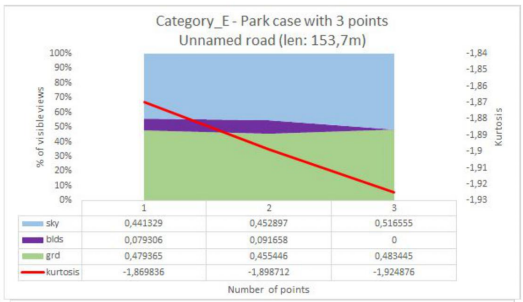

	1	2	3
sky	0,441329	0,452897	0,516555
blds	0,079306	0,091658	0
grd	0,479365	0,455446	0,483445
kurtosis	-1,869836	-1,898712	-1,924876

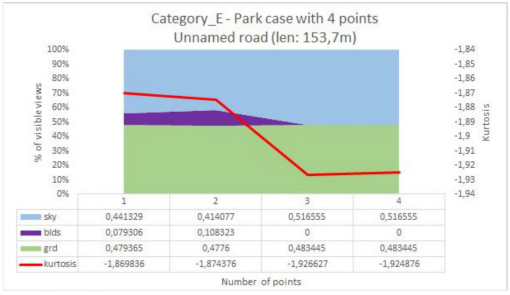

	1	2	3	4
sky	0,441329	0,414077	0,516555	0,516555
blds	0,079306	0,108323	0	0
grd	0,479365	0,4776	0,483445	0,483445
kurtosis	-1,869836	-1,874376	-1,926627	-1,924876

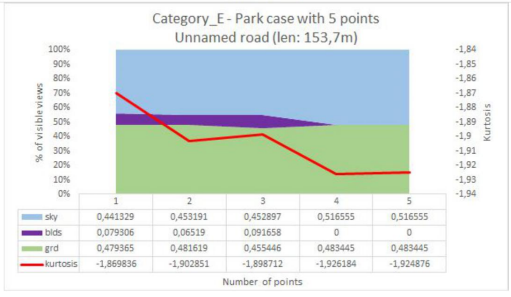

	1	2	3	4	5
sky	0,441329	0,453191	0,452897	0,516555	0,516555
blds	0,079306	0,06519	0,091658	0	0
grd	0,479365	0,481619	0,455446	0,483445	0,483445
kurtosis	-1,869836	-1,902851	-1,898712	-1,926184	-1,924876

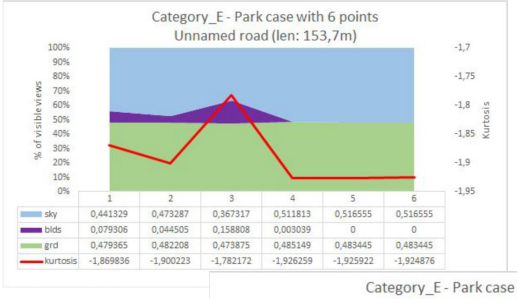

	1	2	3	4	5	6
sky	0,441329	0,473287	0,367317	0,511813	0,516555	0,516555
blds	0,079306	0,044505	0,158808	0,003039	0	0
grd	0,479365	0,482208	0,473875	0,485149	0,483445	0,483445
kurtosis	-1,869836	-1,900223	-1,782172	-1,926259	-1,925922	-1,924876

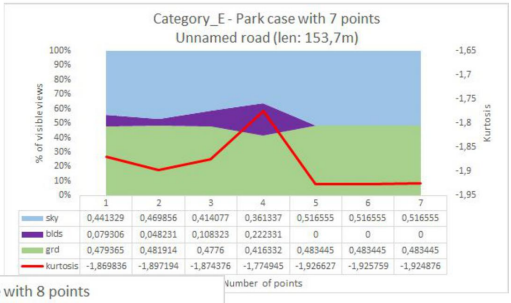

	1	2	3	4	5	6	7
sky	0,441329	0,469856	0,414077	0,361337	0,516555	0,516555	0,516555
blds	0,079306	0,048231	0,108323	0,222331	0	0	0
grd	0,479365	0,481914	0,4776	0,416332	0,483445	0,483445	0,483445
kurtosis	-1,869836	-1,897194	-1,874376	-1,774945	-1,926627	-1,925759	-1,924876

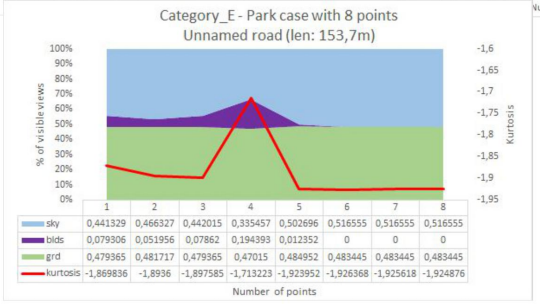

	1	2	3	4	5	6	7	8
sky	0,441329	0,466327	0,442015	0,335457	0,502696	0,516555	0,516555	0,516555
blds	0,079306	0,051956	0,07862	0,194393	0,012352	0	0	0
grd	0,479365	0,481717	0,479365	0,47015	0,484952	0,483445	0,483445	0,483445
kurtosis	-1,869836	-1,8936	-1,897585	-1,713223	-1,923952	-1,926368	-1,925618	-1,924876

Water

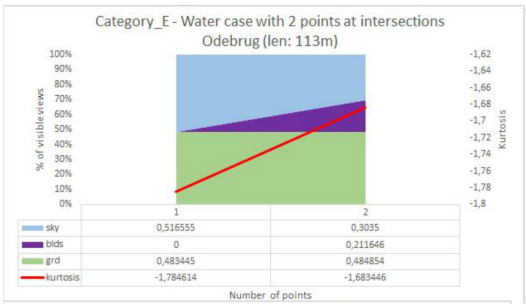

	1	2
sky	0,516555	0,3035
blds	0	0,211646
grd	0,483445	0,484854
kurtosis	-1,784614	-1,683446

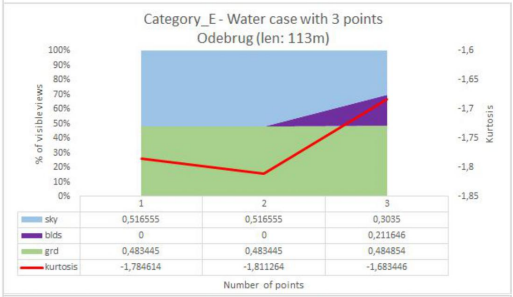

	1	2	3
sky	0,516555	0,516555	0,3035
blds	0	0	0,211646
grd	0,483445	0,483445	0,484854
kurtosis	-1,784614	-1,811264	-1,683446

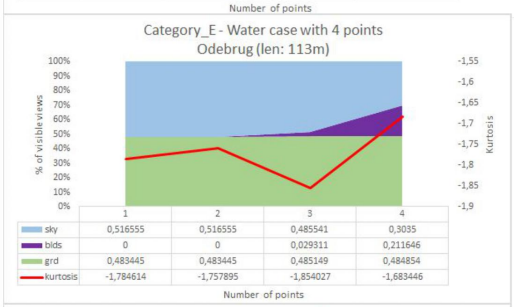

	1	2	3	4
sky	0,516555	0,516555	0,485541	0,3035
blds	0	0	0,029311	0,211646
grd	0,483445	0,483445	0,485149	0,484854
kurtosis	-1,784614	-1,757895	-1,854027	-1,683446

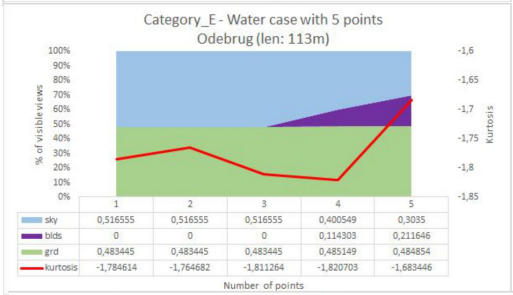

	1	2	3	4	5
sky	0,516555	0,516555	0,516555	0,400549	0,3035
blds	0	0	0	0,114303	0,211646
grd	0,483445	0,483445	0,483445	0,485149	0,484854
kurtosis	-1,784614	-1,764682	-1,811264	-1,820703	-1,683446

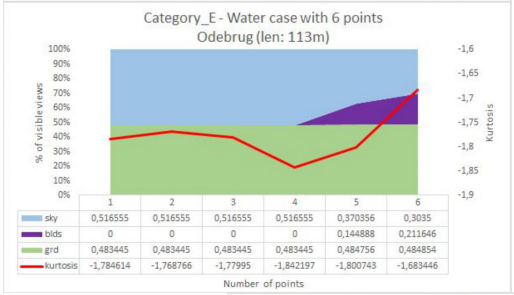

	1	2	3	4	5	6
sky	0,516555	0,516555	0,516555	0,516555	0,370356	0,3035
blds	0	0	0	0	0,144888	0,211646
grd	0,483445	0,483445	0,483445	0,483445	0,484756	0,484854
kurtosis	-1,784614	-1,768766	-1,77995	-1,842197	-1,800743	-1,683446

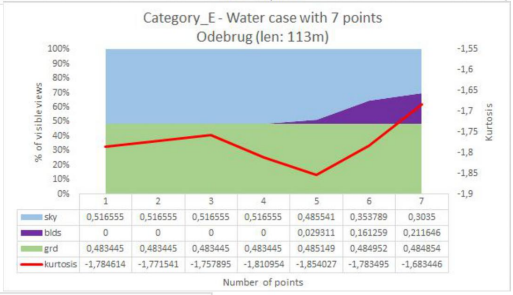

	1	2	3	4	5	6	7
sky	0,516555	0,516555	0,516555	0,516555	0,485541	0,353789	0,3035
blds	0	0	0	0	0,029311	0,161259	0,211646
grd	0,483445	0,483445	0,483445	0,483445	0,485149	0,484952	0,484854
kurtosis	-1,784614	-1,771541	-1,757895	-1,810954	-1,854027	-1,783495	-1,683446

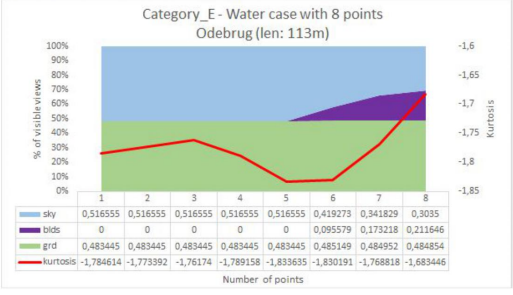

	1	2	3	4	5	6	7	8
sky	0,516555	0,516555	0,516555	0,516555	0,516555	0,419273	0,341829	0,3035
blds	0	0	0	0	0	0,095579	0,173218	0,211646
grd	0,483445	0,483445	0,483445	0,483445	0,483445	0,485149	0,484952	0,484854
kurtosis	-1,784614	-1,773392	-1,76174	-1,789158	-1,833635	-1,830191	-1,768818	-1,683446

High Density

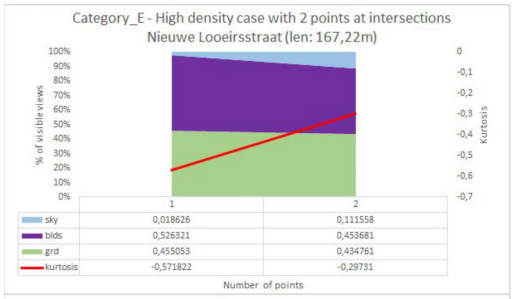

	1	2
sky	0,018626	0,111558
blds	0,526321	0,453681
grd	0,455053	0,434761
kurtosis	-0,571822	-0,29731

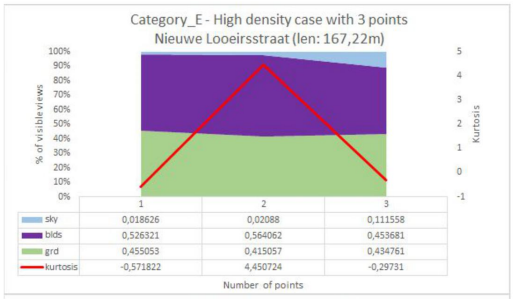

	1	2	3
sky	0,018626	0,02088	0,111558
blds	0,526321	0,564062	0,453681
grd	0,455053	0,415057	0,434761
kurtosis	-0,571822	4,450724	-0,29731

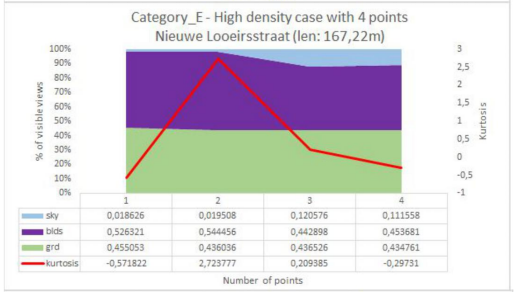

	1	2	3	4
sky	0,018626	0,019508	0,120576	0,111558
blds	0,526321	0,544456	0,442898	0,453681
grd	0,455053	0,436036	0,436526	0,434761
kurtosis	-0,571822	2,723777	0,209385	-0,29731

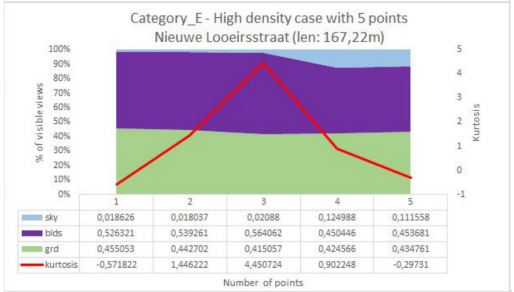

	1	2	3	4	5
sky	0,018626	0,018037	0,02088	0,124988	0,111558
blds	0,526321	0,539261	0,564062	0,450446	0,453681
grd	0,455053	0,442702	0,415057	0,424566	0,434761
kurtosis	-0,571822	1,446222	4,450724	0,902248	-0,29731

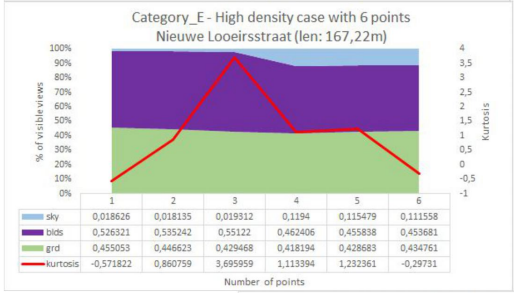

	1	2	3	4	5	6
sky	0,018626	0,018135	0,019312	0,1194	0,115479	0,111558
blds	0,526321	0,535242	0,55122	0,462406	0,455838	0,453681
grd	0,455053	0,446623	0,429468	0,418194	0,428683	0,434761
kurtosis	-0,571822	0,860759	3,695959	1,113394	1,232361	-0,29731

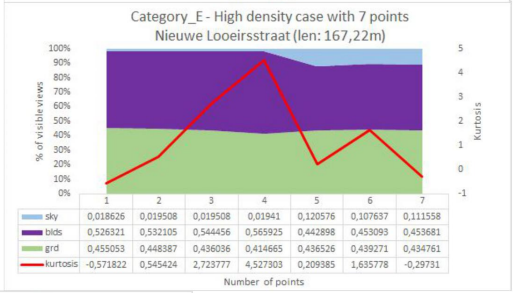

	1	2	3	4	5	6	7
sky	0,018626	0,019508	0,019508	0,01941	0,120576	0,107637	0,111558
blds	0,526321	0,532105	0,544456	0,565925	0,442898	0,453093	0,453681
grd	0,455053	0,448387	0,436036	0,414665	0,436526	0,439271	0,434761
kurtosis	-0,571822	0,545424	2,723777	4,527303	0,209385	1,635778	-0,29731

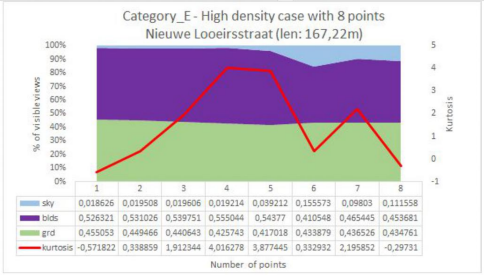

	1	2	3	4	5	6	7	8
sky	0,018626	0,019508	0,019606	0,019214	0,039212	0,155573	0,09803	0,111558
blds	0,526321	0,531026	0,539751	0,555044	0,54377	0,410548	0,465445	0,453681
grd	0,455053	0,449466	0,440643	0,425743	0,417018	0,433879	0,436526	0,434761
kurtosis	-0,571822	0,338859	1,912344	4,016278	3,877445	0,332932	2,195852	-0,29731

Low density


Museumbrug
Weteringschans

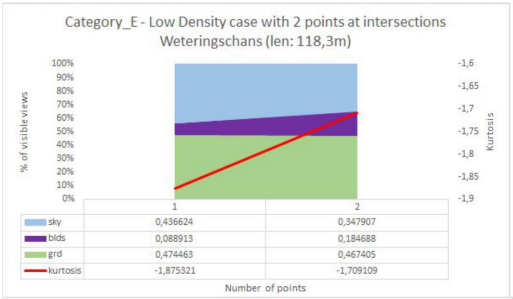
Category_E - Low Density case with 2 points at intersections
Weteringschans (len: 118,3m)
% of visible views
Kurtosis
Number of points
1 2
sky 0,436624 0,347907
blds 0,088913 0,184688
grd 0,474463 0,467405
kurtosis -1,875321 -1,709109

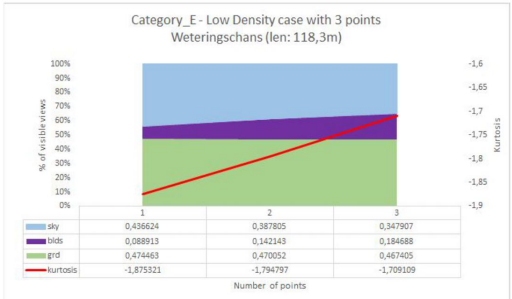
Category_E - Low Density case with 3 points
Weteringschans (len: 118,3m)
% of visible views
Kurtosis
Number of points
1 2 3
sky 0,436624 0,387805 0,347907
blds 0,088913 0,142143 0,184688
grd 0,474463 0,470052 0,467405
kurtosis -1,875321 -1,794797 -1,709109

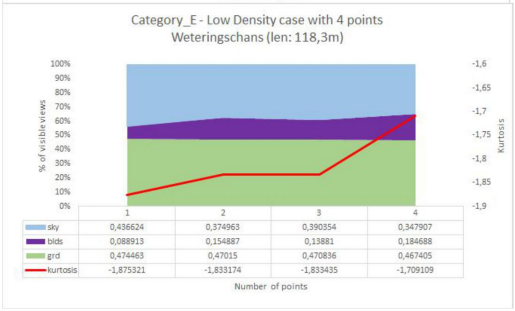
Category_E - Low Density case with 4 points
Weteringschans (len: 118,3m)
% of visible views
Kurtosis
Number of points
1 2 3 4
sky 0,436624 0,374963 0,390354 0,347907
blds 0,088913 0,154887 0,13881 0,184688
grd 0,474463 0,47015 0,470836 0,467405
kurtosis -1,875321 -1,833174 -1,833435 -1,709109

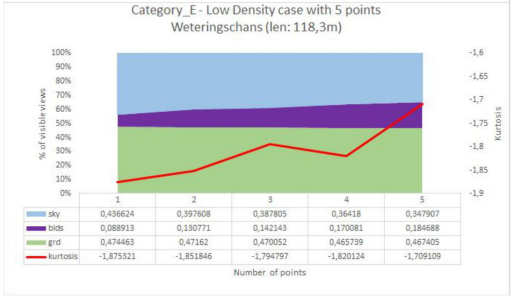
Category_E - Low Density case with 5 points
Weteringschans (len: 118,3m)
% of visible views
Kurtosis
Number of points
1 2 3 4 5
sky 0,436624 0,397608 0,387805 0,36418 0,347907
blds 0,088913 0,130771 0,142143 0,170081 0,184688
grd 0,474463 0,47162 0,470052 0,465739 0,467405
kurtosis -1,875321 -1,851846 -1,794797 -1,820124 -1,709109

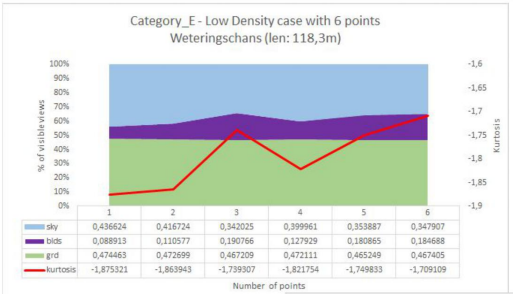
Category_E - Low Density case with 6 points
Weteringschans (len: 118,3m)
% of visible views
Kurtosis
Number of points
1 2 3 4 5 6
sky 0,436624 0,416724 0,342025 0,399961 0,353887 0,347907
blds 0,088913 0,110577 0,190766 0,127929 0,180865 0,184688
grd 0,474463 0,472699 0,467209 0,472111 0,465249 0,467405
kurtosis -1,875321 -1,863943 -1,739307 -1,821754 -1,749833 -1,709109

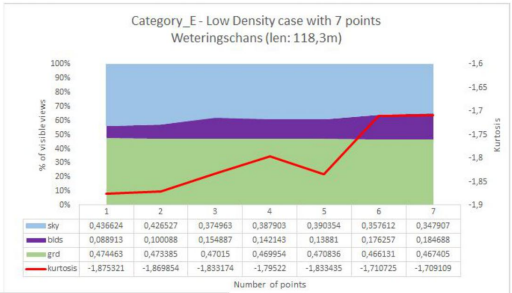
Category_E - Low Density case with 7 points
Weteringschans (len: 118,3m)
% of visible views
Kurtosis
Number of points
1 2 3 4 5 6 7
sky 0,436624 0,426527 0,374963 0,387903 0,390354 0,357612 0,347907
blds 0,088913 0,100088 0,154887 0,142143 0,13881 0,176257 0,184688
grd 0,474463 0,473385 0,47015 0,469954 0,470836 0,466131 0,467405
kurtosis -1,875321 -1,869854 -1,833174 -1,79522 -1,833435 -1,710725 -1,709109

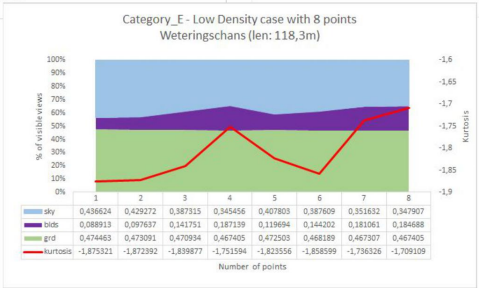
Category_E - Low Density case with 8 points
Weteringschans (len: 118,3m)
% of visible views
Kurtosis
Number of points
1 2 3 4 5 6 7 8
sky 0,436624 0,429272 0,387315 0,345456 0,407803 0,387609 0,351632 0,347907
blds 0,088913 0,097637 0,141751 0,187139 0,119694 0,144202 0,181061 0,184688
grd 0,474463 0,473091 0,470934 0,467405 0,472503 0,468189 0,467307 0,467405
kurtosis -1,875321 -1,872392 -1,839877 -1,751594 -1,823556 -1,858599 -1,736326 -1,709109

Category F [194, 624]

Park

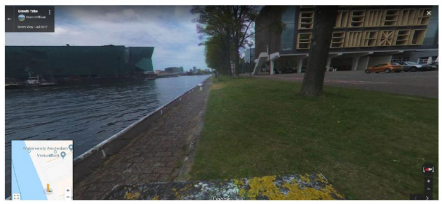

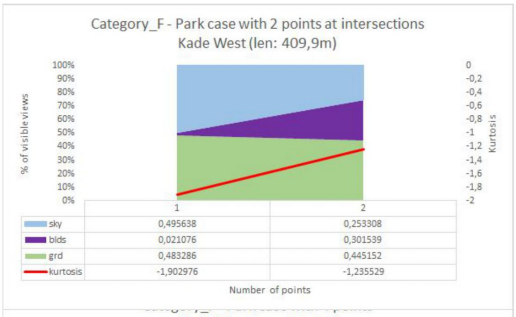

	1	2
sky	0,495638	0,253308
blds	0,021076	0,301539
grd	0,483286	0,445152
kurtosis	-1,902976	-1,235529

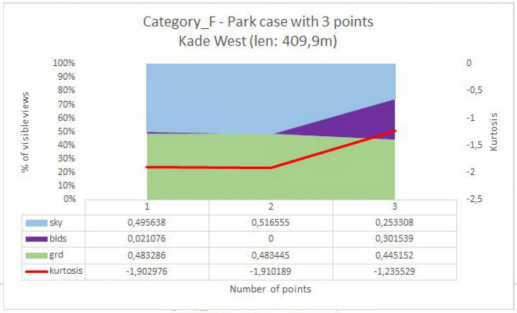

	1	2	3
sky	0,495638	0,516555	0,253308
blds	0,021076	0	0,301539
grd	0,483286	0,483445	0,445152
kurtosis	-1,902976	-1,910189	-1,235529

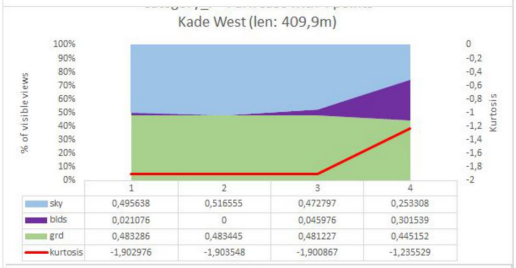

	1	2	3	4
sky	0,495638	0,516555	0,472797	0,253308
blds	0,021076	0	0,045976	0,301539
grd	0,483286	0,483445	0,481227	0,445152
kurtosis	-1,902976	-1,903548	-1,900867	-1,235529

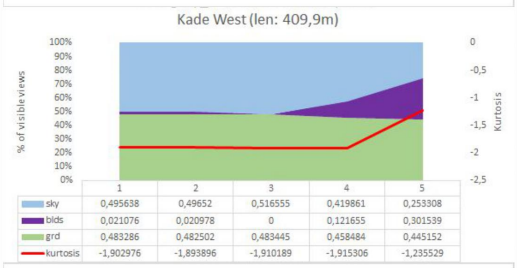

	1	2	3	4	5
sky	0,495638	0,49652	0,516555	0,419861	0,253308
blds	0,021076	0,020978	0	0,121655	0,301539
grd	0,483286	0,482502	0,483445	0,458484	0,445152
kurtosis	-1,902976	-1,893896	-1,910189	-1,915306	-1,235529

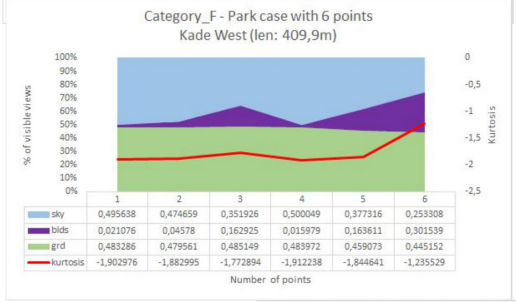

	1	2	3	4	5	6
sky	0,495638	0,474659	0,351926	0,500049	0,377316	0,253308
blds	0,021076	0,04578	0,162925	0,015979	0,163611	0,301539
grd	0,483286	0,479561	0,485149	0,483972	0,459073	0,445152
kurtosis	-1,902976	-1,882995	-1,772894	-1,912238	-1,844641	-1,235529

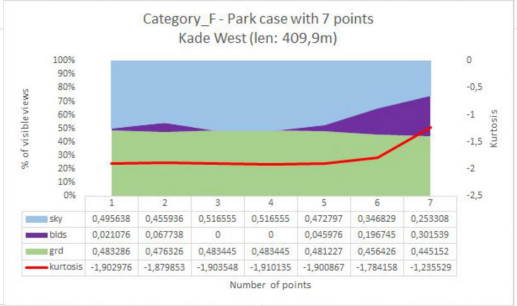

	1	2	3	4	5	6	7
sky	0,495638	0,455936	0,516555	0,516555	0,472797	0,346829	0,253308
blds	0,021076	0,067738	0	0	0,045976	0,196745	0,301539
grd	0,483286	0,476326	0,483445	0,483445	0,481227	0,456426	0,445152
kurtosis	-1,902976	-1,879853	-1,903548	-1,910135	-1,900867	-1,784158	-1,235529

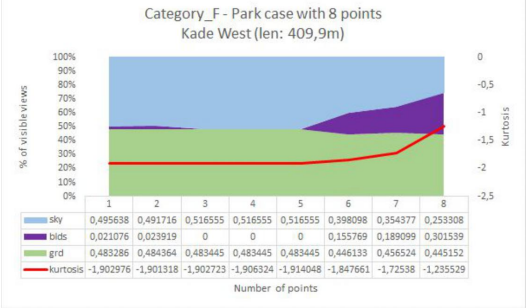

	1	2	3	4	5	6	7	8
sky	0,495638	0,491716	0,516555	0,516555	0,516555	0,398098	0,354377	0,253308
blds	0,021076	0,023919	0	0	0	0,155769	0,189099	0,301539
grd	0,483286	0,484364	0,483445	0,483445	0,483445	0,446133	0,456524	0,445152
kurtosis	-1,902976	-1,901318	-1,902723	-1,906324	-1,914048	-1,847661	-1,72538	-1,235529

Water

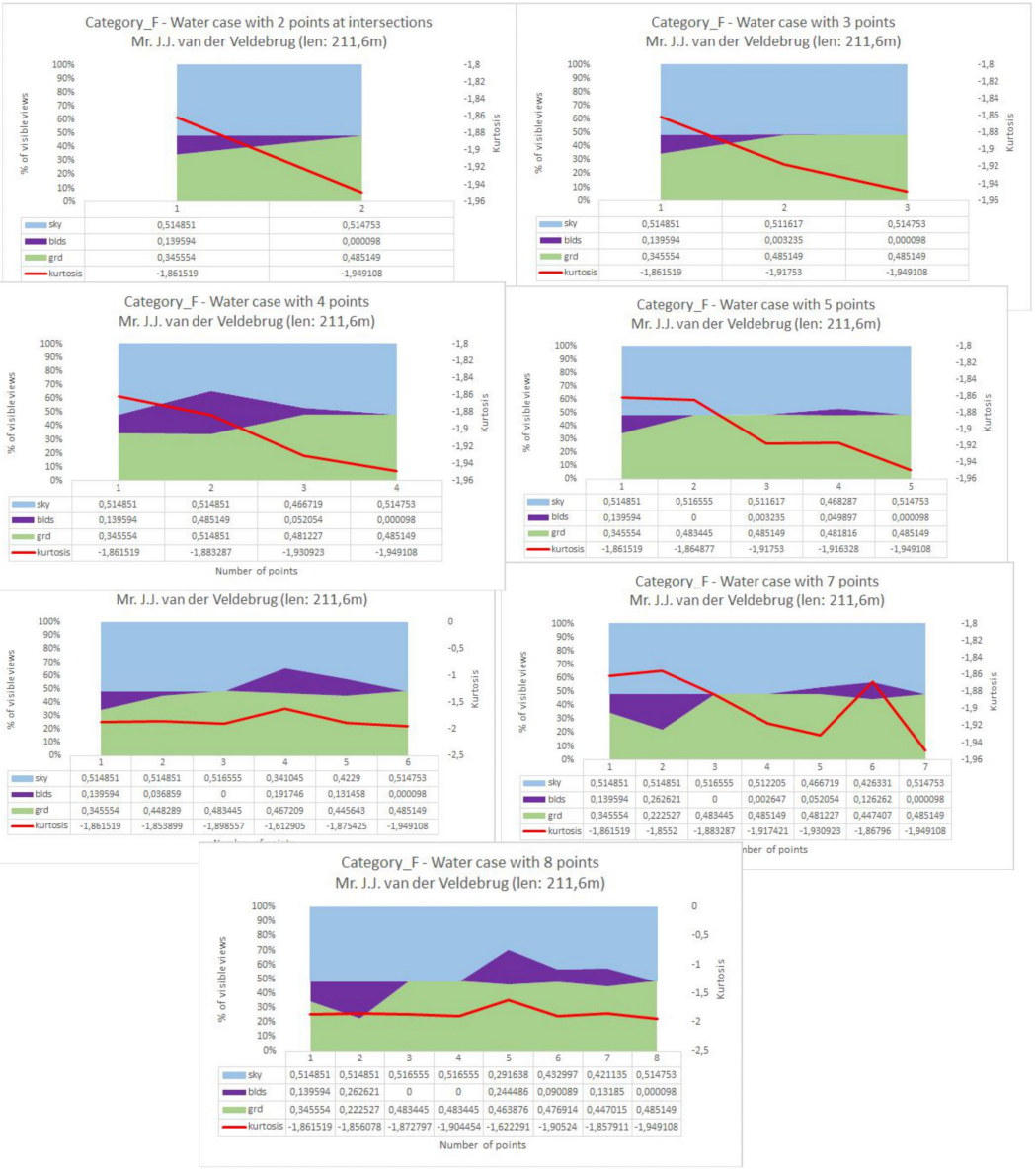
Category_F - Water case with 2 points at intersections
Mr. J.J. van der Veldebrug (len: 211,6m)
% of visible views
Kurtosis
sky 0,514851 0,514753
blds 0,139594 0,000098
grd 0,345554 0,485149
kurtosis -1,861519 -1,949108
Category_F - Water case with 3 points
Mr. J.J. van der Veldebrug (len: 211,6m)
sky 0,514851 0,511617 0,514753
blds 0,139594 0,003235 0,000098
grd 0,345554 0,485149 0,485149
kurtosis -1,861519 -1,91753 -1,949108
Category_F - Water case with 4 points
Mr. J.J. van der Veldebrug (len: 211,6m)
sky 0,514851 0,514851 0,466719 0,514753
blds 0,139594 0,485149 0,052054 0,000098
grd 0,345554 0,514851 0,481227 0,485149
kurtosis -1,861519 -1,883287 -1,930923 -1,949108
Number of points
Category_F - Water case with 5 points
Mr. J.J. van der Veldebrug (len: 211,6m)
sky 0,514851 0,516555 0,511617 0,468287 0,514753
blds 0,139594 0 0,003235 0,049897 0,000098
grd 0,345554 0,483445 0,485149 0,481816 0,485149
kurtosis -1,861519 -1,864877 -1,91753 -1,916328 -1,949108
Mr. J.J. van der Veldebrug (len: 211,6m)
sky 0,514851 0,514851 0,516555 0,341045 0,4229 0,514753
blds 0,139594 0,036859 0 0,191746 0,131458 0,000098
grd 0,345554 0,448289 0,483445 0,467209 0,445643 0,485149
kurtosis -1,861519 -1,853899 -1,898557 -1,612905 -1,875425 -1,949108
Category_F - Water case with 7 points
Mr. J.J. van der Veldebrug (len: 211,6m)
sky 0,514851 0,514851 0,516555 0,512205 0,466719 0,426331 0,514753
blds 0,139594 0,262621 0 0,002647 0,052054 0,126262 0,000098
grd 0,345554 0,222527 0,483445 0,485149 0,481227 0,447407 0,485149
kurtosis -1,861519 -1,8552 -1,883287 -1,917421 -1,930923 -1,86796 -1,949108
Category_F - Water case with 8 points
Mr. J.J. van der Veldebrug (len: 211,6m)
sky 0,514851 0,514851 0,516555 0,516555 0,291638 0,432997 0,421135 0,514753
blds 0,139594 0,262621 0 0 0,244486 0,090089 0,13185 0,000098
grd 0,345554 0,222527 0,483445 0,483445 0,463876 0,476914 0,447015 0,485149
kurtosis -1,861519 -1,856078 -1,872797 -1,904454 -1,622291 -1,90524 -1,857911 -1,949108
Number of points

High Density

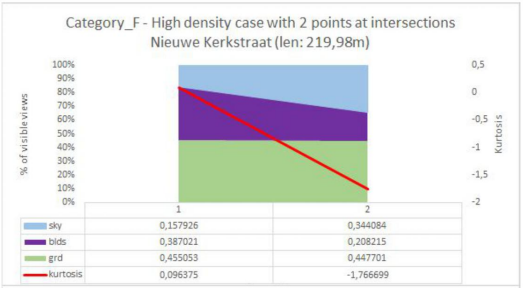

	1	2
sky	0,157926	0,344084
blds	0,387021	0,208215
grd	0,455053	0,447701
kurtosis	0,096375	-1,766699

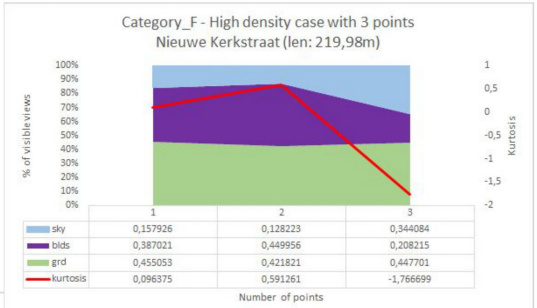

	1	2	3
sky	0,157926	0,128223	0,344084
blds	0,387021	0,449956	0,208215
grd	0,455053	0,421821	0,447701
kurtosis	0,096375	0,591261	-1,766699

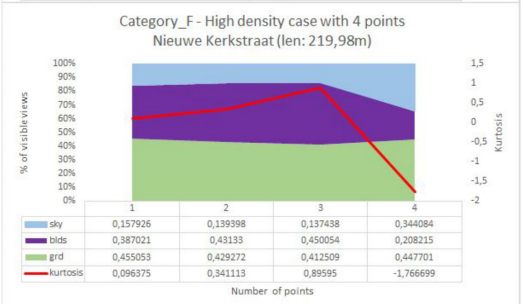

	1	2	3	4
sky	0,157926	0,139398	0,137438	0,344084
blds	0,387021	0,43133	0,450054	0,208215
grd	0,455053	0,429272	0,412509	0,447701
kurtosis	0,096375	0,341113	0,89595	-1,766699

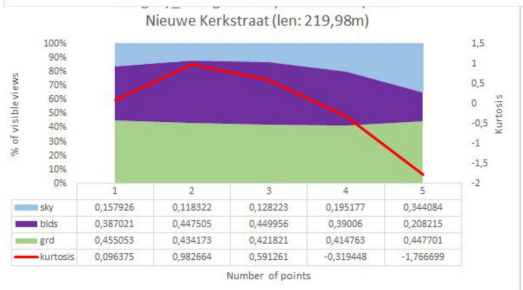

	1	2	3	4	5
sky	0,157926	0,118322	0,128223	0,195177	0,344084
blds	0,387021	0,447505	0,449956	0,39006	0,208215
grd	0,455053	0,434173	0,421821	0,414763	0,447701
kurtosis	0,096375	0,982664	0,591261	-0,319448	-1,766699

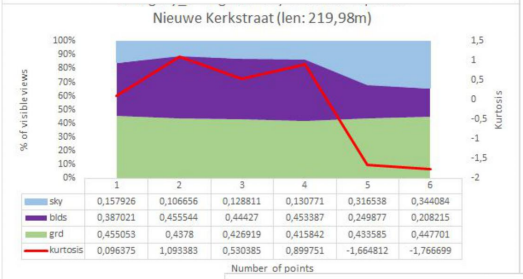

	1	2	3	4	5	6
sky	0,157926	0,106656	0,128811	0,130771	0,316538	0,344084
blds	0,387021	0,455544	0,44427	0,453387	0,249877	0,208215
grd	0,455053	0,4378	0,426919	0,415842	0,433585	0,447701
kurtosis	0,096375	1,093383	0,530385	0,899751	-1,664812	-1,766699

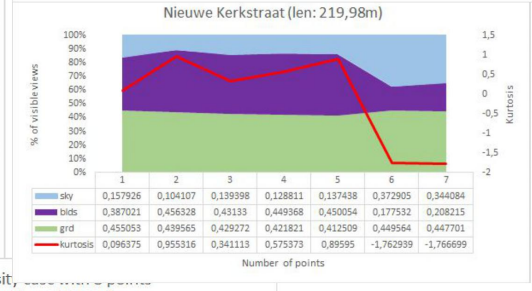

	1	2	3	4	5	6	7
sky	0,157926	0,104107	0,139398	0,128811	0,137438	0,372905	0,344084
blds	0,387021	0,456328	0,43133	0,449368	0,450054	0,177532	0,208215
grd	0,455053	0,439565	0,429272	0,421821	0,412509	0,449564	0,447701
kurtosis	0,096375	0,955316	0,341113	0,575373	0,89595	-1,762939	-1,766699

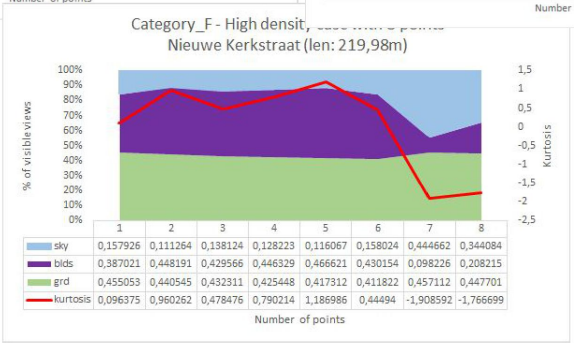

	1	2	3	4	5	6	7	8
sky	0,157926	0,111264	0,138124	0,128223	0,116067	0,158024	0,444662	0,344084
blds	0,387021	0,448191	0,429566	0,446329	0,466621	0,430154	0,098226	0,208215
grd	0,455053	0,440545	0,432311	0,425448	0,417312	0,411822	0,457112	0,447701
kurtosis	0,096375	0,960262	0,478476	0,790214	1,186986	0,44494	-1,908592	-1,766699

Low Density

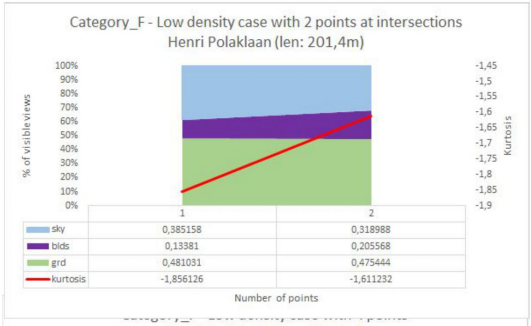

	1	2
sky	0,385158	0,318988
blds	0,13381	0,205568
grd	0,481031	0,475444
kurtosis	-1,856126	-1,611232

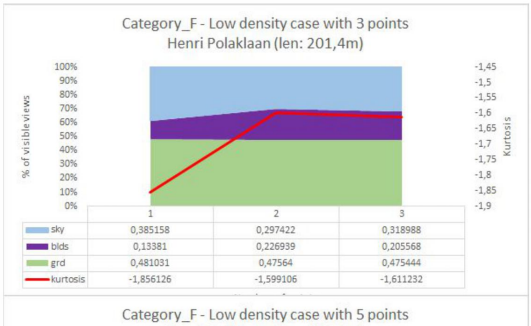

	1	2	3
sky	0,385158	0,297422	0,318988
blds	0,13381	0,226939	0,205568
grd	0,481031	0,47564	0,475444
kurtosis	-1,856126	-1,599106	-1,611232

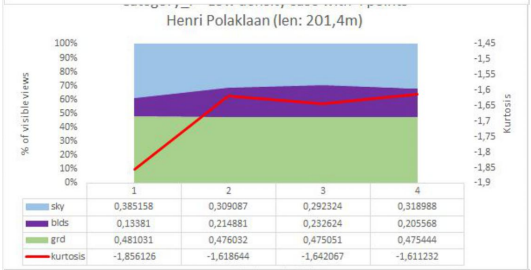

	1	2	3	4
sky	0,385158	0,309087	0,292324	0,318988
blds	0,13381	0,214881	0,232624	0,205568
grd	0,481031	0,476032	0,475051	0,475444
kurtosis	-1,856126	-1,618644	-1,642067	-1,611232

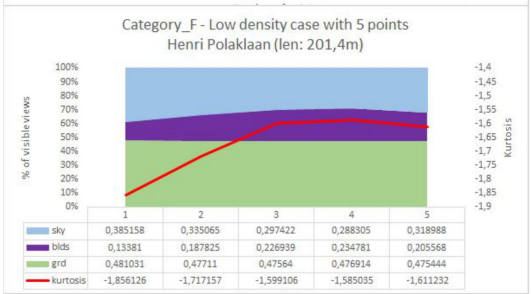

	1	2	3	4	5
sky	0,385158	0,335065	0,297422	0,288305	0,318988
blds	0,13381	0,187825	0,226939	0,234781	0,205568
grd	0,481031	0,47711	0,47564	0,476914	0,475444
kurtosis	-1,856126	-1,717157	-1,599106	-1,585035	-1,611232

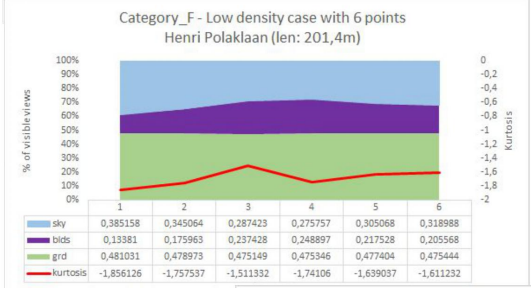

	1	2	3	4	5	6
sky	0,385158	0,345064	0,287423	0,275757	0,305068	0,318988
blds	0,13381	0,175963	0,237428	0,248897	0,217528	0,205568
grd	0,481031	0,478973	0,475149	0,475346	0,477404	0,475444
kurtosis	-1,856126	-1,757537	-1,511332	-1,74106	-1,639037	-1,611232

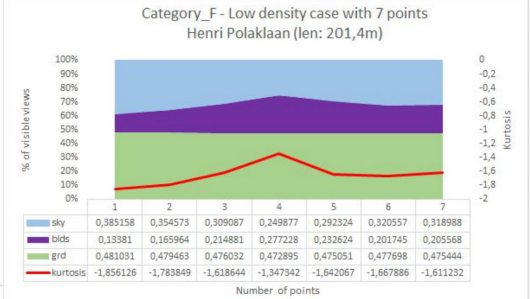

	1	2	3	4	5	6	7
sky	0,385158	0,354573	0,309087	0,249877	0,292324	0,320557	0,318988
blds	0,13381	0,165964	0,214881	0,277228	0,232624	0,201745	0,205568
grd	0,481031	0,479463	0,476032	0,472895	0,475051	0,477698	0,475444
kurtosis	-1,856126	-1,783849	-1,618644	-1,347342	-1,642067	-1,667886	-1,611232

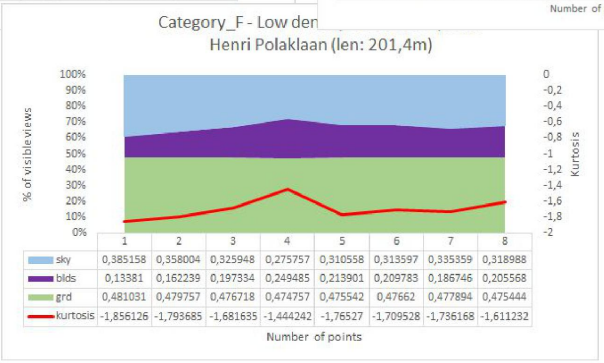

	1	2	3	4	5	6	7	8
sky	0,385158	0,358004	0,325948	0,275757	0,310558	0,313597	0,335359	0,318988
blds	0,13381	0,162239	0,197334	0,249485	0,213901	0,209783	0,186746	0,205568
grd	0,481031	0,479757	0,476718	0,474757	0,475542	0,47662	0,477894	0,475444
kurtosis	-1,856126	-1,793685	-1,681635	-1,444242	-1,76527	-1,709528	-1,736168	-1,611232

B AGGREGATION OF THE METRICS ON THE STREET NETWORK OF AMSTERDAM CENTRUM

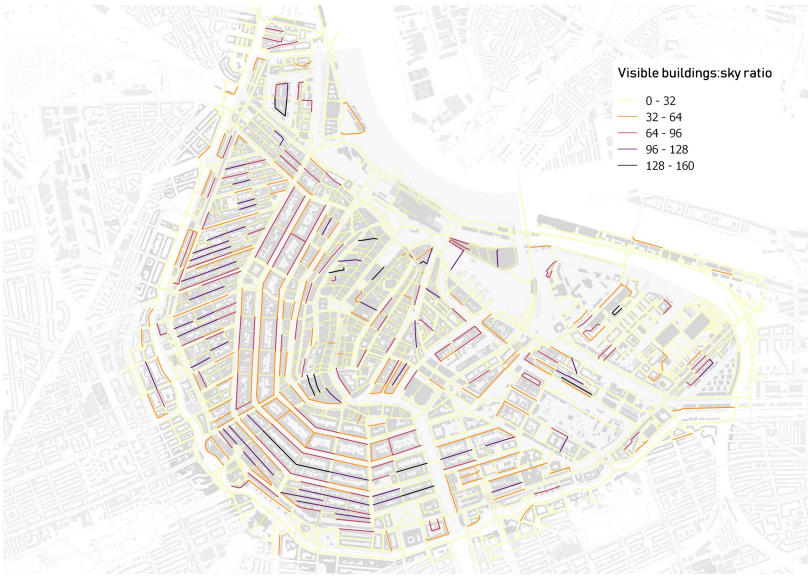

Figure B.1: The ratio of the visible buildings and the visible sky in Amsterdam Centrum.

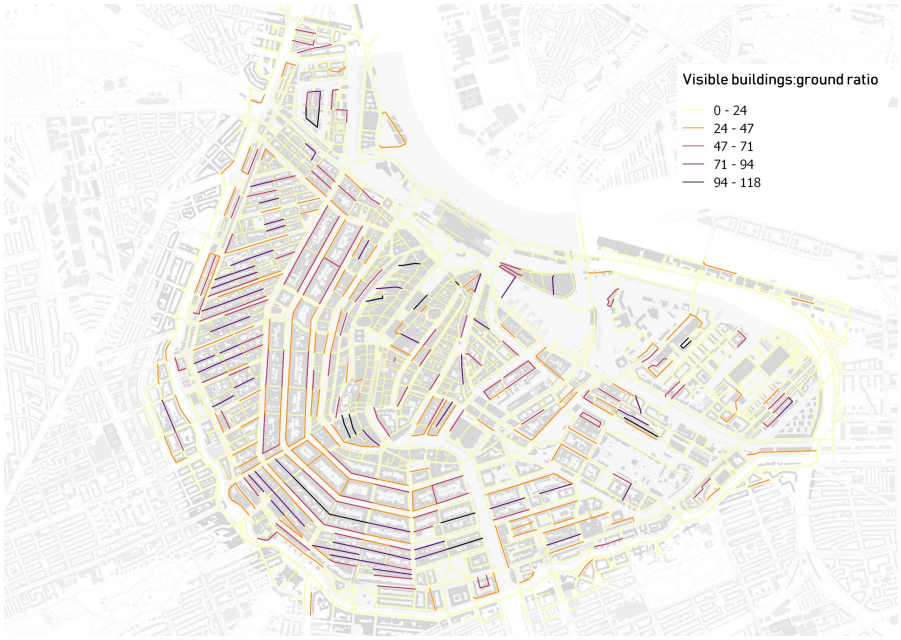

Figure B.2: The ratio of the visible buildings and the visible ground in Amsterdam Centrum.

Figure B.3: The ratio of the visible sky and the visible ground in Amsterdam Centrum.

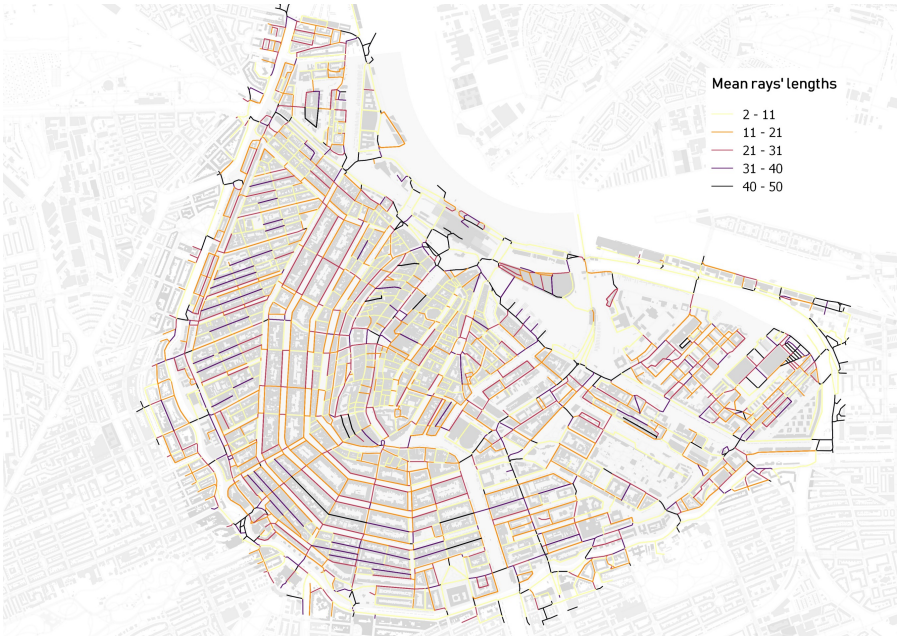

Figure B.4: The mean lengths of the rays in Amsterdam Centrum.

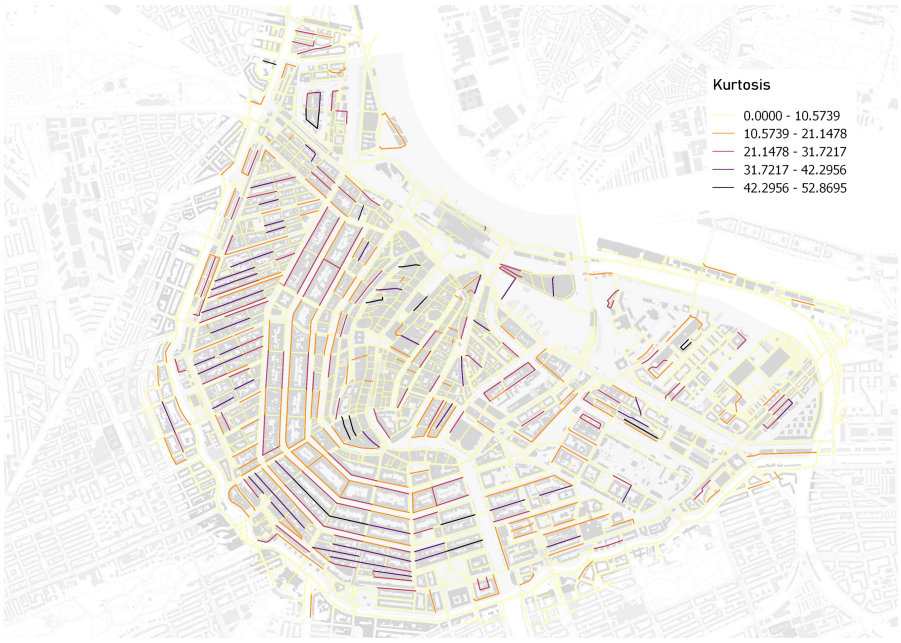

Figure B.5: The kurtosis values of the lengths of the rays in Amsterdam Centrum.

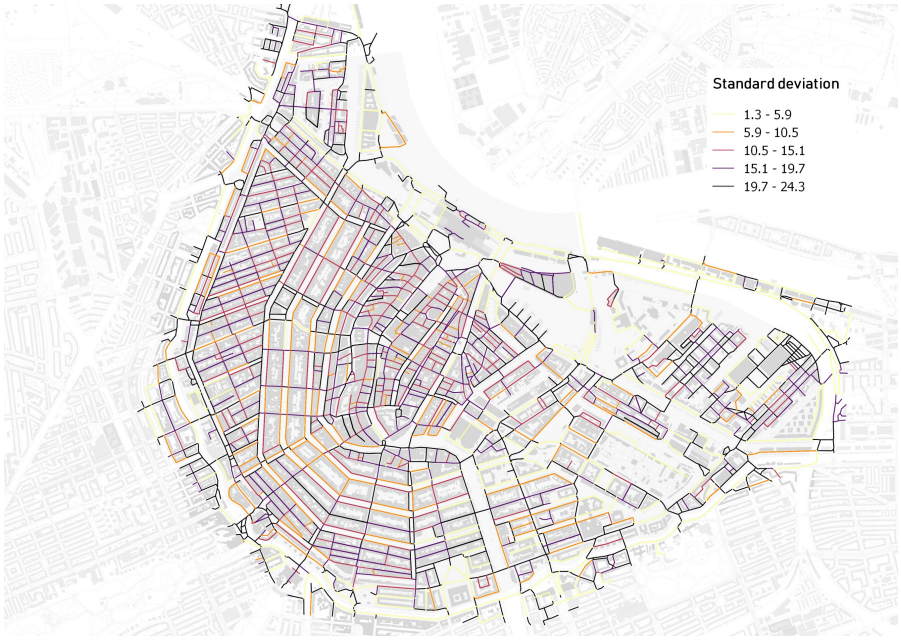

Figure B.6: The standard deviation of the lengths of the rays in Amsterdam Centrum.

COLOPHON

This document was typeset using LaTeX. The document layout was generated using the `arsclassica` package by Lorenzo Pantieri, which is an adaption of the original `classicthesis` package from André Miede.